UNIVERSITÀ DEGLI STUDI DI SALERNO
DIPARTIMENTO DI FISICA "E. R. CAIANIELLO" E DIPARTIMENTO DI MATEMATICA

UNIVERSITÀ DEGLI STUDI DELLA CAMPANIA "LUIGI VANVITELLI"
DIPARTIMENTO DI MATEMATICA E FISICA

PhD in "Mathematics, Physics and Applications"
XXIX Cycle
Curriculum Physics

PhD thesis in

Quantum Information Theory in Condensed Matter Physics

Giuseppe Zonzo

Coordinator
Prof. Sandro Pace

Supervisor
Prof. Fabrizio Illuminati
Prof. Federico Corberi

A. A. 2015-2016

Abstract

In the "standard" Gizburg-Landau approach, a phase transition is intimately connected to a local order parameter, that spontaneously breaks some symmetries. In addition to the "traditional" symmetry-breaking ordered phases, a complex quantum system exhibits exotic phases, without classical counterpart, that can be described, for example, by introducing non-local order parameters that preserve symmetries.

In this scenario, this thesis aims to shed light on open problems, such as the local distinguishability between ground states of a symmetry-breaking ordered phase and the classification of one dimensional quantum orders, in terms of entanglement measures, in systems for which the Gizburg-Landau approach fails.

In particular, I briefly introduce the basic tools that allow to understand the nature of entangled states and to quantify non-classical correlations. Therefore, I analyze the conjecture for which the maximally symmetry-breaking ground states (MSBGSs) are the most classical ones, and thus the only ones selected in real-world situations, among all the ground states of a symmetry-breaking ordered phase. I make the conjecture quantitatively precise, by proving that the MSBGSs are the only ones that: i) minimize pairwise quantum correlations, as measured by the quantum discord; ii) are always local convertible, by only applying LOCC transformations; iii) minimize the residual tangle, satisfying at its minimum the monogamy of entanglement.

Moreover, I analyze how evolves the distinguishability, after a sudden change of the Hamiltonian parameters. I introduce a quantitative measure of distinguishability, in terms of the trace distance between two reduced density matrices. Therefore, in the framework of two integrable models that falls in two different classes of symmetries, i.e. XY models in a transverse magnetic field and the N-cluster Ising models, I prove that the maximum of the distinguishability shows a time-exponential decay. Hence, in the limit of diverging time, all the informations about the particular initial ground state disappear, even if a system is integrable.

Far away from the Gizburg-Landau scenario, I analyze a family of fully-analytical solvable one dimensional spin-1/2 models, named the N-cluster models in a transverse magnetic field. Regardless of the cluster size $N + 2$, these models exhibit a quantum phase transition, that separates a paramagnetic phase

from a cluster one. The cluster phase coresponds to a nematic ordered phase or a symmetry-protected topological ordered one, for even or odd N respectively. Using the Jordan-Wigner transformations, it is possible to diagonalize these models and derive all their spin correlation functions, with which reconstruct their entanglement properties. In particular, I prove that these models have only a non-vanishing bipartite entanglement, as measured by the concurrence, between spins at the endpoints of the cluster, for a magnetic field strong enough.

Moreover, I introduce the minimal set of nonlinear ground-states functionals to detect all 1-D quantum orders for systems of spin-1/2 and fermions. I show that the von Neumann entanglement entropy distinguishes a critical system from a non critical one, because of the logarithmic divergence at a quantum critical point. The Schmidt gap detect the disorder of a system , because it saturates to a constant value in a paramagnetic phase and goes to zero otherwise. The mutual information, between two subsystems macroscopically separated, identifies the symmetry-breaking ordered phases, because of its dependence on the order parameters. The topological order phases, instead, via their deeply non-locality, can be characterized by analyzing all three functionals.

There is a way to escape the inference of superluminal speeds and spooky-action at a distance. But it involves absolute determinism in the universe, the complete absence of free will. Suppose the world is super-deterministic, with not just inanimate nature running on behind-the-scenes clockwork, but with our behavior, including our belief that we are free to choose to do one experiment rather than another, absolutely predetermined, including the "decision" by the experimenter to carry out one set of measurements rather than another, the difficulty disappears. There is no need for a faster-than-light signal to tell particle A what measurement has been carried out on particle B, because the universe, including particle A, already "knows" what that measurement, and its outcome, will be.

J. B.
BBC radio interview, 1985

Contents

Introduction

It is well known that, following the Gizburg-Landau approach, the appearance of an ordered phase in a classical system is associated to the rising of a local order parameter, with a support on a single site of the system, that spontaneously breaks some symmetries of the Hamiltonian [53]. In the study of ordered phases, associated to a spontaneous symmetry-breaking, a key concept is played by the existence of locally inequivalent ground states, that are not eigenstates of one or more symmetry operators for the corresponding Hamiltonian [113]. Counter-intuitively, among all these energetically equiprobable and equally accessible ground states, the maximally symmetry-breaking ground states are always selected. In complete analogy with the case of classical phase transitions driven by temperature, the pedagogical explanation of this phenomenon invokes the unavoidable presence of some local small perturbing external field, that selects one of the maximally symmetry-breaking ground states, among all the elements of the quantum ground space. The implicit assumption hidden in this type of reasoning is that the maximally symmetry-breaking ground states are the most classical ones, thus selected in real-world situations. Efforts have been devoted to the investigation of the physical mechanism that, in the thermodynamic limit, selects the symmetry-breaking ground states. However, the complete understanding of this distinguishability remains an open problem [16, 8].

It is therefore also natural to wonder how evolves the distinguishability between different ground states of a symmetry-breaking ordered phase. There are several ways to prepare a system away from the equilibrium. An important role is played by the one associated to a sudden quench of the Hamiltonian parameters. The system is initially prepared in an equilibrium state, typically the ground state. Then the Hamiltonian parameters are suddenly changed and the system starts to evolve under the action of a new Hamiltonian [54, 79, 111, 112, 24, 129]. For several models and initial conditions, the local physical quantities equilibrate exponentially in time, i.e the time evolution produce a steady state that looks locally thermal [11, 106, 105, 103, 85, 52]. This implies that the local physical quantities lose any information about the initial state, with the exception of the effective temperature induced by the quench

[106, 108, 67]. However, not all models have complex quantum dynamics and not all models thermalize when placed away from the equilibrium. The discovery that the integrability of a model avoids the thermalization, triggers an intense discussion on the general relation between integrability and thermalization in the long-time dynamics of strongly interacting complex quantum systems [68, 19, 25, 107, 11, 106, 38]. The lack of thermalization in solvable systems, implies that the steady state preserve informations about the initial Hamiltonian parameters [107].

The lack of thermalization also suggest that the image of an integrable system, that starts in one of the distinguishable ground states of a symmetry-breaking ordered phase, continues to preserve memory of the particular initial ground state.

Far away from the symmetry-breaking ordered phases, a complex quantum system exhibits certain kinds of orders that are unsuitable to be described in terms of the standard Gizburg-Landau scenario. A paradigmatic example is a translation invariant spin-1/2 chain, for which the ground states correspond to the so called valence bond states, i.e. states made by tensor products of Bell states [5, 6]. Notable examples arise also in the presence of deconfined criticality, like at the transition semimetal-insulator on the graphene or in the Haldane-Shastry model [117, 14], or in long range interacting systems [87]. In such cases, any possible local operator shows a vanishing expectation value and, hence, there is no order parameter, as defined in the Gizburg-Landau picture. Nevertheless, it is well known that these systems show an order, that can be highlighted by properly defining a non local order parameter. A similarly challenging situation realizes in materials for which the phase diagram is not known at all, as for some high-Tc superconductors or for various lattice tight-binding models [89]. Therefore, in recent years, efforts have been devoted to the understanding of quantum phase transitions with alternative approaches, based on methods and techniques, originally developed in the field of quantum information theory [4, 124]. For example, various types of quantum phase transitions have been characterized by identifying the singular points in the derivative of different measures of bipartite [99, 97] and multipartite [45, 46] entanglement.

Among these non trivial orders, nematic and topological phases are attracting an increasing interest. Nematic phases [7, 78] occur if it is possible to define a ground state that: a) It breaks at least one symmetry of the Hamiltonian; b) It is characterized by an order parameter with a support on a finite set of sites, with a dimension strictly greater than one single site. In this sense, the nematic order can be seen as a generalization of the ferromagnetic/antiferromagnetic order. On the opposite limit, the topological ordered phases are characterized by string order parameters, i.e. non vanishing expectation value of operators

which support extends on the whole system. [88, 35].

Such novel phases have a theoretical deeply importance. In fact, topological ordered phases are associated to the robustness of ground state degeneracies [127], show quantized non-Abelian geometric phases [126] or possess peculiar patterns of long-range quantum entanglement [26]. Moreover, these phases have interesting applications. The topological ordered phases, in fact, play a fundamental role in the spin liquids [69, 130] and in non-Abelian fractional Hall systems [83] and are predicted to play a key role in the future development of fault-tolerant quantum computers [76]. The nematic order is usually found in materials commercially used in the liquid crystal technology [120], such as LCDs (liquid crystal display).

Due to the great interest on these novel phases, scientists are trying to provide models in which they can be founded. For what concern the one dimensional system, it is known that frustrated one dimensional ferromagnetic spin-1/2 chain in an external magnetic field shows a nematic ordered phase [28, 60] and the one dimensional cluster-Ising model exhibits a symmetry protected topological ordered phase [118, 92, 46]. More recently, in Ref. [47], it has been analyzed a very extensive set of exactly solvable models, that can be simulated via Floquet interactions in atomic systems [81] and that show a quantum phase transition between an antiferromagnetic phase and a nematic or topological one.

Following this line of research, this thesis aims to shed light on the problem of distinguishability between different ground states, associated to the same set of Hamiltonian parameters, in a symmetry-breaking ordered phase and on the exotic quantum phases, far away from the Gizburg-Landau scenario, for which an approach in terms of entanglement measures needs. The thesis is organized as follows.

In Chapter (1), I make a review on the entanglement, a keypoint of quantum mechanics with no classical counterpart. In Sec. (1.1), I introduce the notion of entangled and separable states, in Sec. (1.2) I review the criteria to detect entangled states and in Sec. (1.3) I present measures to quantify the amount of entanglement in a quantum state.

In Chapter (2), I review the properties of the one dimensional quantum spin-1/2 models, that can be solved via Jordan Wigner transformations. In Sec. (2.1), I diagonalize these models and derive the exact ground states, with which I reconstruct all the spin correlation functions (Sec. (2.2)) and the reduced density matrices (Sec. (2.3)). In Sec. (2.4), I extend the analysis to the time-dependence induced by a sudden quench of the Hamiltonian parameters.

In Chapter (3), I analyze the nature of spontaneous symmetry-breaking associated to an ordered phase, by investigating the conjecture for which the max-

imally symmetry-breaking ground states (MSBGSs) are the most classical ones. I make this argument quantitatively precise by proving that the MSBGS are the only ones that: i) minimize pairwise quantum correlations as measured by the quantum discord (Sec. (3.1)); ii) are always locally convertible, i.e. can be obtained from all other ground states by only applying LOCC transformations, while the reverse is impossible; iii) minimize the residual tangle between a dynamical variable and the rest of the system, satisfying the monogamy of entanglement at its minimum (Sec. (3.2)).

In Chapter (4), I analyze how distinguishability between different ground states of a symmetry-breaking ordered phase evolves after a sudden quench of the Hamiltonian parameters. In Sec. (4.1), I define a quantitative approach to the local distinguishability, in terms of the trace distance between two reduced density matrices. In the framework of the XY model (Sec. (4.2)) and the N-cluster Ising model (Sec. (4.3)), I prove that the maximum of the local distinguishability shows an exponential decay in time. Hence, in the limit of diverging time, all the informations about the particular initial ground state disappear, even if the systems are integrable.

In Chapter (5), I analyze a family of fully analytical solvable models, named the N-cluster models in a transverse magnetic field. In Sec. (5.1), I diagonalize the models and show that exhibit a quantum phase transition between a cluster phase, that is a nematic or topological phase, depending on N, and a paramagnetic one. In Sec. (5.2), I derive all the spin correlation functions, with which I reconstruct the order parameters (Sec. (5.3)) and all the entanglement properties (Sec. (5.4)), by proving that these systems have only bipartite entanglement, as measured by the concurrence, between two endpoints spins.

In Chapter (6), I introduce the minimal set of nonlinear ground-states functionals to detect 1-D quantum orders. In Sec. (6.1), I briefly review the models of spin-1/2 and fermions that span all possible phases in 1-D. In Sec. (6.1), I show that von Neumann entanglement entropy characterizes the criticality of a system, because of the logarithmic divergence at a quantum critical point. In Sec. (6.2), I show that the Schmidt gap captures the disorder of a system, because it saturates to a constant value in a paramagnetic phase and goes rapidly to zero otherwise. In Sec. (6.3), I prove that the mutual information identifies symmetry-breaking ordered phases, because of its dependence on the order parameters. The topological order, via its deeply non locality, can be described by analyzing all three functionals.

In Chapter (7), I draw my conclusions.

The results discussed in the thesis are collected in four papers:

Classical nature of ordered quantum phases and origin of spontaneous symmetry breaking
M. CIANCIARUSO, S. M. GIAMPAOLO, L. FERRO, W. ROGA, G. ZONZO, M. BLASONE, F. ILLUMINATI
arXiv: 1604.06403, submitted to Phys. Rev. A

Quench of a symmetry broken ground state
S. M. GIAMPAOLO, G. ZONZO
Phys. Rev. A 95, 012121 (2017)

N-cluster models in a transverse magnetic field
G. ZONZO, S. M. GIAMPAOLO, F. ILLUMINATI
In preparation

Minimal set of nonlinear ground-states functionals to detect 1*-D quantum orders*
G. ZONZO, S. M. GIAMPAOLO, M. DALMONTE, F. ILLUMINATI
In preparation

1
Entangled states: basic concepts

Quantum systems show properties with no classical counterpart, such as the superposition of quantum states, interference or tunneling. These are effects that can be observed in quantum systems composed of a single particle. Further and more evident differences between arise when one treats composite quantum systems, i.e. systems that decompose into two or more subsystems. It is the correlations between these subsystems that give additional distinctions between classical and quantum objects. Whereas classical systems exhibit classical correlations, described in terms of classical probabilities, this is not always true in quantum systems. Such non-classical correlations lead to apparent paradoxes, like the famous Einstein-Podolsky-Rosen paradox (EPR) [39], that might suggest, on the first glance, a remote action in quantum mechanics.

In 1935 Einstein, Podolsky and Rosen designed a thought experiment that, with the assumption of the principles of *locality* and *reality* as a requirements for a completeness of a physical theory, demonstrated the incompleteness of quantum mechanics. The logic of the experiment of Einstein, Podolsky and Rosen was as follows. If one considers a system of two particles in a state $|\phi_-\rangle = (|01\rangle - |10\rangle)/\sqrt{2}$, then the measurement made on the first particle has an impact to the outcome of the second particle. Suppose that the particles are separated from each other in millions of light years. After the measurement on the first subsystem, the first particle is in state $|0\rangle$ or $|1\rangle$ with probability $1/2$. The same results are obtained for the second particle. If the measurement on the first particle obtaines the state $|0\rangle$, then it is known that second one is in the state $|1\rangle$. It looks like the knowledge of the state of the second particle come to the first particle observer faster than the speed of light, in contradiction with the principle of local realism. Einstein, Podolsky and Rosen came to the conclusion that some quantum effects propagated faster than light, in contradiction with the theory of relativity. Thus, the quantum mechanics could not be complete and needed for "hidden variables". As a response to the EPR paradox, Irish physicist John Stewart Bell performed a thought experiment, showing that at least one of the quantum mechanics assumptions must be false [66]. Bell in-

troduced inequalities that satisfied the assumptions of local realism, and then showed that, for certain quantum states, they are violated. Experimental violation of Bell's inequalities was repeatedly confirmed by some quantum systems [95, 123].

EPR paradox introduce states that display non-classical correlations, i.e. *entangled* states, and the aim of this chapter is to introduce the basic tools that allow to understand the nature of such states, to distinguish them from the classically correlated ones, and to quantify these non-classical correlations.

1.1 What is entanglement?

Quantum states are described by operators ρ, acting on the state space $\mathcal{B}(\mathcal{H})$, i.e. the Hilbert space of bounded operators acting on $\mathcal{H}$. Such operators are called density matrices or density operators. Any density operator can be written through a non-uniquely convex combinations of one-dimensional projectors

$$\rho = \sum_i p_i \, |\psi_i\rangle\langle\psi_i| \tag{1.1}$$

where $\{p_i\}$ is a probability distribution such that $p_i \geq 0, \forall i$ and $\sum_i p_i = 1$. It can be demostrated that

- $\mathrm{Tr}(\rho) = 1$ (unity trace)
- ρ is semi-definite positive, i.e. all the eigenvalues of ρ are non-negative
- $\mathrm{Tr}(\rho^2) \leq 1$

A special case is represented by *pure* states, i.e. $p_i = 1$ for some i, for which the density operator is described by a unidimensional projector

$$\rho = |\psi_i\rangle\langle\psi_i| \tag{1.2}$$

such that $\mathrm{Tr}(\rho^2) = 1$. Pure states are the extreme point of the set of quantum states and then represent those systems for which the most complete informations are available.

Composite or *multipartite* quantum systems, i.e. systems that naturally decompose into two or more quantum subsystems $A, B, \cdots, N$, usually characterized by mutual distances larger than the size of the subsystems, are also represented by density operators. Formally, the Hilbert space $\mathcal{H}$ of a composite quantum system is given by the tensor product of the Hilbert spaces $\mathcal{H}_i$ $(i = A, B, \cdots, N)$ of each subsystem

$$\mathcal{H} = \mathcal{H}_A \otimes \cdots \otimes \mathcal{H}_N \tag{1.3}$$

The notion of "entanglement" appears in these composite quantum spaces, in terms of correlators that have no classical counterpart. Consider a *bipartite* quantum system $(A|B)$, i.e. a system composed of two distinct subsystems, described by the Hilbert space $\mathcal{H} = \mathcal{H}_A \otimes \mathcal{H}_B$. It follows

Definition 1 (Bipartite separability)**.** *A quantum state is called biseparable if it can be written as a convex combination of tensor products of density matrices, i.e.* $\rho \in \mathcal{B}(\mathcal{H}_A \otimes \mathcal{H}_B)$ *is bi-separable if*

$$\rho = \sum_i p_i \, \rho_i^A \otimes \rho_i^B \tag{1.4}$$

Alternatively, states that cannot be written in this form are called entangled.

An example of entangled state, in $\mathcal{H} = \mathcal{H}_A \otimes \mathcal{H}_B$, is the Bell state

$$|\phi_+\rangle = \frac{(|00\rangle + |11\rangle)}{\sqrt{2}} \tag{1.5}$$

Let $|\phi_A\rangle = \alpha\,|0\rangle + \beta\,|1\rangle$ in $\mathcal{H}_A$ and $|\phi_B\rangle = \gamma\,|0\rangle + \delta\,|1\rangle$ in $\mathcal{H}_B$, with the normalization conditions $|\alpha|^2 + |\beta|^2 = 1$ and $|\gamma|^2 + |\delta|^2 = 1$. Suppose that $|\phi_+\rangle$ is separable, thus it can be written in the form

$$|\phi_+\rangle = |\phi_A\rangle \otimes |\phi_B\rangle = (\alpha\,|0\rangle + \beta\,|1\rangle) \otimes (\gamma\,|0\rangle + \delta\,|1\rangle) \tag{1.6}$$

Hence

$$\frac{(|00\rangle + |11\rangle)}{\sqrt{2}} = \alpha\gamma\,|00\rangle + \alpha\delta\,|01\rangle + \beta\gamma\,|10\rangle + \beta\delta\,|11\rangle \tag{1.7}$$

but there are no values of α,β,γ and δ such that $\alpha\gamma = 1/\sqrt{2} = \beta\delta$ and $\alpha\delta = 0 = \beta\gamma$. Thus one obtains that $|\phi_+\rangle \neq |\phi_A\rangle \otimes |\phi_B\rangle$, i.e $|\phi_+\rangle$ is entangled.

For bipartite systems, one need just to make a distinction between separable and entangled states. When multiple parts are involved it may happen that a state contains entanglement among some parts which, at the same time, are not entangled with others. An example is the state

$$\frac{(|00\rangle + |11\rangle)}{\sqrt{2}} \otimes \frac{(|00\rangle + |11\rangle)}{\sqrt{2}} \tag{1.8}$$

which contains entanglement between the first two and between the last two subsystems, but not between these two subgroups. In this context, it is

necessary to introduce the notion of k-separability [37, 36, 1]. Consider a k-partite quantum system $(A_1|A_2|\cdots|A_k)$, i.e. a system composed of k distinct subsystems, describe by the Hilbert space $\mathcal{H} = \mathcal{H}_{\mathcal{A}_1} \otimes \cdots \otimes \mathcal{H}_{\mathcal{A}_k}$. It follows

Definition 2 (k-separability). *A quantum state is called k-separable if it can be written as a convex combination of k-tensor products of density matrices (as a generalization of Eq. (1.4))*

$$\rho = \sum_i p_i \, \rho_i^{A_1} \otimes \rho_i^{A_2} \otimes \cdots \otimes \rho_i^{A_k} \tag{1.9}$$

1.2 How to detect entanglement?

The question spontaneously arises is: given a general quantum state ρ, how to determine if it is entangled or not? In principle, one could think to check whether the quantum state ρ could be written as a tensor product as in Eq. (1.4). However, as ρ can be represented in infinitely many convex combinations, it is amazing difficult to find one of these forms that reads like Eq. (1.4) [55, 66]. Following this reasoning, several *entanglement criteria* have been developed in the last years [121].

1.2.1 Schmidt decomposition

Any pure state $|\psi\rangle$ of a bipartite quantum system $(A|B)$ in $\mathcal{H}_A \otimes \mathcal{H}_B$ can be written as

$$|\psi\rangle = \sum_{j=1}^{m} \sqrt{\lambda_j} \, |j_A\rangle \otimes |j_B\rangle \tag{1.10}$$

where $m = \min[\dim(\mathcal{H}_A), \dim(\mathcal{H}_B)]$, $\{|j_A\rangle, j_A = 1, \cdots, m\}$ and $\{|j_B\rangle, j_B = 1, \cdots, m\}$) are orthonormal basis in $\mathcal{H}_A$ and $\mathcal{H}_B$ respectively, and $\lambda_i > 0$ with $\sum_{j=1}^{m} \lambda_j = 1$ [115, 40, 94]. The decomposition expressed in Eq. (1.10) is called the *Schmidt decomposition* and the coefficients λ_j are called the *Schmidt coefficients* of $|\psi\rangle$.

If $|\psi\rangle$ has only one non-vanishing Schmidt coefficient, it is clearly separable, and it is entangled if more than one Schmidt coefficient are different from zero

$$\begin{aligned} \lambda_j \neq 0 \quad &\text{for one } j \quad \Longrightarrow \text{ separable} \\ \lambda_j \neq 0 \quad &\text{for several } j \quad \Longrightarrow \text{ entangled} \end{aligned} \tag{1.11}$$

In this way, the Schmidt decomposition completely characterizes separability for *bipartite pure* states.

The reduced density matrices are particularly helpful to determine the Schmidt coefficients. The reduced density matrix of the subsystem A (or equivalently B), in terms of the Schmidt decomposition, reads

$$\begin{aligned}\rho_A &= \mathrm{Tr}_B\left(|\psi\rangle\langle\psi|\right) \\ &= \mathrm{Tr}_B\left(\sum_{ij}\sqrt{\lambda_i\lambda_j}\,|i_A\rangle\langle j_A|\otimes|i_B\rangle\langle j_B|\right) \\ &= \sum_i \lambda_i\,|i_A\rangle\langle i_A|\end{aligned} \tag{1.12}$$

Thus, the Schmidt coefficients are given by the eigenvalues of the reduced density matrix ρ_A (or equivalently ρ_B, that has the same eigenvalues). Since separability for bipartite pure states requires that exactly one Schmidt coefficient is different from zero, it can be restate in terms of the reduced density matrix as

$$\begin{aligned}\mathrm{Tr}(\rho_r^2) = 1 \implies \rho_r \text{ is pure} \implies |\psi\rangle \text{ is separable} \\ \mathrm{Tr}(\rho_r^2) < 1 \implies \rho_r \text{ is mixed} \implies |\psi\rangle \text{ is entangled}\end{aligned} \tag{1.13}$$

where r refers to one of the two subsystems.

1.2.2 Peres-Horodecki criterion

Although the Schmidt decomposition is a very powerful and useful entanglement criterion, it can be applied only to pure states. The first entanglement criterion for mixed states was proposed by A. Peres (and Horodecki) and uses the notion of partial transposition [101]. The Peres-Horodecki criterion, also called *positive partial transposition* (**PPT**), is a necessary condition for separability of mixed states. Let ρ be a state from the $M \times N$ Hilbert space $\mathcal{H} = \mathcal{H}_A \otimes \mathcal{H}_B$ with $\dim(\mathcal{H}_A) = M$ and $\dim(\mathcal{H}_B) = N$

$$\rho_{m\mu,n\nu} = \langle m\mu|\rho|n\nu\rangle \tag{1.14}$$

where the Latin letters describe the first subsystem and the Greek letters refer to the second subsystem. The partial transposition of the density operator ρ is defined in Ref. [17, 13] as

$$\rho^{T_A}_{m\mu,n\nu} = \rho_{n\mu,m\nu} \quad \text{and} \quad \rho^{T_B}_{m\mu,n\nu} = \rho_{m\nu,n\mu} \tag{1.15}$$

Hence, for any separable state $\rho = \rho_A \otimes \rho_B$, one can write

$$\rho^{T_A} = (\rho_A)^T \otimes \rho_B \quad \text{and} \quad \rho^{T_B} = \rho_A \otimes (\rho_B)^T \tag{1.16}$$

The Peres-Hodorecki criterion states that

- *If a state ρ is separable, then ρ^{T_A} and ρ^{T_B} are positive operators* (Peres);
- *Composite states of dimension 2×2 and 2×3 are separable if and only if ρ^{T_A} and ρ^{T_B} are positive operators* (Horodecki).

For 2×2 and 3×3 dimensional states, the **PPT** criterion is also sufficient condition for separability [17].

1.2.3 Entanglement and positive maps

Let $\mathcal{B}(\mathcal{H}_A)$ and $\mathcal{B}(\mathcal{H}_B)$ be the spaces of the bounded operators on the Hilbert spaces $\mathcal{H}_A$ and $\mathcal{H}_B$ respectively. Let $\mathcal{L}\left(\mathcal{B}(\mathcal{H}_A), \mathcal{B}(\mathcal{H}_B)\right)$ be the space of the linear maps from $\mathcal{B}(\mathcal{H}_A)$ to $\mathcal{B}(\mathcal{H}_B)$. Let $\Lambda \in \mathcal{L}\left(\mathcal{B}(\mathcal{H}_A), \mathcal{B}(\mathcal{H}_B)\right)$ be a *positive map*, i.e. $\rho \geq 0$ implies $\Lambda(\rho) \geq 0$. Λ is completely positive (CP), if the extended map $\mathbb{I} \otimes \Lambda : \mathcal{B}(\mathbb{M} \otimes \mathcal{H}_A) \rightarrow \mathcal{B}(\mathbb{M} \otimes \mathcal{H}_B)$ is positive for any space $\mathbb{M}$. The separability criterion in terms of positive maps states that

- *Let $\rho = \rho_A \otimes \rho_B$ be a density operator acting on Hilbert space $\mathcal{H} = \mathcal{H}_A \otimes \mathcal{H}_B$. Then ρ is separable if and only if, for any positive map $\Lambda \in \mathcal{L}\left(\mathcal{B}(\mathcal{H}_A), \mathcal{B}(\mathcal{H}_B)\right)$, the operator $\mathbb{I} \otimes \Lambda(\rho) : \rho_A \otimes \rho_B \rightarrow \rho_A \otimes \Lambda(\rho_B)$ is positive.*

This criterion reduces to **PPT** criterion if Λ is the transposition operator, i.e. $\mathbb{I} \otimes \Lambda(\rho) = \rho^{T_B}$ for any $\Lambda(\sigma) = \sigma^T$, with σ an arbitrary state.

1.2.4 Entanglement witness

Entanglement witness is a separability criterion based on the Hahn-Banach theorem, that follows directly from the Def. (2) of k-separable states. The Hahn-Banach theorem states that

Denote by S a convex, compact set in a finite dimensional Banach space. Let ρ be a point in the space with $\rho \notin S$. Then there exist a hyperplane that separates ρ from S.

In Fig. (1.1) it is shown a geometric interpretation of the Hahn-Banach theorem. Hyperplane, separating the set S from the point ρ, is identified by the orthonormal vector W, which is selected from outside the set S. Each point ρ

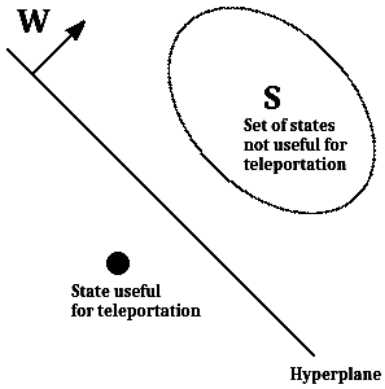

Figure 1.1: Geometric interpretaion of the Hahn-Banach theorem

may be characterized by the signum of the scalar product $\mathrm{Tr}(W\rho)$. Since the separable states form a convex, compact set, hence the Hahn-Banach theorem can be used in terms of entanglement detection. It follows that

- *A density operator ρ is entangled if and only if there exist a Hermitian operator W with $Tr(W\rho) < 0$. On the contrary, $Tr(W\sigma) > 0$ for any separable state σ.*

The operator W is called *entanglement witness*.

Between positive maps and entangled witness it exists a close relationship [101]. For any entanglement operator W, it can be defined a positive map Λ such that

$$W = (\mathbb{I} \otimes \Lambda)(P_+) \tag{1.17}$$

where P_+ is the projector operator onto the mawimally entangled state

$$P_+ = \frac{1}{m} \sum_{i,j=1}^{m} |i_A i_B\rangle \langle j_A j_B| \tag{1.18}$$

Each entangled state can be detected by some W [102, 114, 115], but in general entanglement witness cannot be used because there is no a general method to construct it.

1.2.5 Majorization

The majorization criterion, proposed by Nielsen and Kempe [95], is necessary but not sufficient condition for separability. From the definition of majorization

Definition 3. *Let $X = \{x_1, \cdots, x_n\}$ and $Y = \{y_1, \cdots, y_n\}$ be non-increasing sequences such that $x_1 \geq x_2 \geq \cdots \geq x_n$ and $y_1 \geq y_2 \geq \cdots \geq y_n$. X majorizes Y $(X \prec Y)$ if*

$$\sum_{i=1}^{k} x_i \geq \sum_{i=1}^{k} y_i \tag{1.19}$$

for each $k = 1, 2, \cdots, n$

it follows that

- *Let $(A|B)$ be a composite quantum system, and let ρ_A, ρ_B and ρ_{AB} be the density operators of the systems A, B and AB, with a non-increasing sequences of eigenvalues $\lambda(\rho_A)$, $\lambda(\rho_B)$ and $\lambda(\rho_{AB})$ respectively. If the state ρ_{AB} is separable, then*

$$\lambda(\rho_{AB}) \prec \lambda(\rho_A) \quad \text{and} \quad \lambda(\rho_{AB}) \prec \lambda(\rho_B) \tag{1.20}$$

Note that sequences $\lambda(\rho_A)$ and $\lambda(\rho_B)$ are shorter than $\lambda(\rho_{AB})$, thus they are equalized by appending zeros.

1.3 How to quantify entanglement?

Entanglement criteria are helpful to detect if a state is entangled or not, but they do not give a quantitative information on how much a state is entangled. With the development of the Quantum Information Theory, the entanglement has been considered as a resource. Hence, it became fundamental to know and to measure how much of this resource is available in each state.

Even if it is still being discussed on the conditions to be fulfilled, a good measure of entanglement should satisfy the following requirements [31]

- *Semi-definite positivity*, i.e. a measure of entanglement E is a function which assigns non-negative value for each state ρ;
- *LOCC monotonicity*, i.e. a measure of entanglement E cannot increase under *LOCC* operations.

  LOCC (*Local Operations and Classical Communications*) are an important class of maps, necessary to define measures of entanglement. The class of *LOCC* operations includes all quantum operations, also measurements, characterized by two properties:

  - all operations are performed locally on the respective subsystem (*Local Operations*). An example of local operation is the trace operation, which can be performed locally on each subsystem A or B of a composite quantum system $(A|B)$;
  - the information between subsystems is exchanged by means of classical communication channels (*Classical Communication*);

- *Normalization*, i.e. for every arbitrary state σ we have $E(\sigma) < E(\rho)$, where ρ is the maximally entangled state;
- *Convexity*, i.e. $E(\lambda\rho + (1-\lambda)\sigma) \leq \lambda E(\rho) + (1-\lambda)E(\sigma)$, for any arbitrary states ρ and σ;
- *Continuity*, i.e. let ρ_n and σ_n be a sequences of states acting on the composite Hilbert spaces $(\mathcal{H}_A \otimes \mathcal{H}_B)^{\otimes n}$. If $\lim_{n\to\infty} ||\rho_n - \sigma_n||_1 = 0$, then

$$\lim_{n\to\infty} \frac{E(\rho_n) - E(\sigma_n)}{n \ln(dim(\mathcal{H}_A \otimes \mathcal{H}_B))} = 0$$

- Depending on the requirements of measurement functions, the *additivity* condition can be formulated in several ways
  - *Additivity*, i.e. $E(\rho \otimes \sigma) = E(\rho) + E(\sigma)$, for any arbitrary states ρ and σ;
  - *Subadditivity*, i.e. $E(\rho \otimes \sigma) \leq E(\rho) + E(\sigma)$, for any arbitrary states ρ and σ;
  - *Weak additivity*, i.e. $E(\rho) = \frac{E(\rho^{\otimes N})}{N}$, for any arbitrary state ρ;
  - *Existence of regularization*, i.e. $E(\rho) = \lim_{N\to\infty} \frac{E(\rho^{\otimes N})}{N}$.

Examples of quantifiers of entanglement can be found in references [4]. I limit my analysis to the most useful ones.

1.3.1 Von Neumann entropy

For bipartite pure states $(A|B)$ in the Hilbert space $\mathcal{H} = \mathcal{H}_A \otimes \mathcal{H}_B$, there exist only one entanglement measure, the von Neumann entropy of the reduced density operator ρ [31], given by

$$E(\rho) = S(\rho_A) = -\mathrm{Tr}\,(\rho_a \log \rho_A) \tag{1.21}$$

where $\rho_A = \mathrm{Tr}_B(\rho)$ and the default logarithm base equals to 2. Using spectral decomposition, the von Neumann entropy can be written in terms of the eigenvalues $\{\lambda_j\}$ of the reduced density operator ρ_A

$$S(\rho_A) = -\sum_j \lambda_j \log \lambda_j \tag{1.22}$$

On the contrary, for mixed states there exist a lot of measures of entanglement. In the following, I analyze the most important ones.

1.3.2 Entanglement cost

The *entanglement cost* is an entanglement measure that quantifies how many ebits (unit of bipartite entanglement, i.e. the amount of entanglement contained in a maximally entangled two-qubit state) are required to prepare a copy of a state, only using *LOCC* operations. Many copies of a state can be prepared at the same time and the entanglement cost, therefore, quantifies how many ebits are required per copy.

Let P_+ be the projector onto a Bell state $|\Phi^+\rangle = (|00\rangle + |11\rangle)/\sqrt{2}$

$$P_+ := |\Phi^+\rangle\langle\Phi^+| \tag{1.23}$$

The entanglement cost aims to quantify the rate m/n at which it is possible to convert $P_+^{\otimes m}$ into $\rho^{\otimes n}$ with a *LOCC* operation Λ. It is usually impossible to perform this exactly, then one makes an approximation $\Lambda(P_+^{\otimes m}) \approx \rho^{\otimes n}$, which quality can be quantified by a distance measure $D(\Lambda(P_+^{\otimes m}), \rho^{\otimes n})$, that can be either the Bures, the trace or another suitable distance. The entanglement cost E_C is then the infimum of all possible rates m/n at which the approximation can be made arbitrarily good, by choosing m and n sufficiently large. Mathematically, it can be formulated as

$$E_C(\rho) = \inf\{E \mid \forall \epsilon, \delta > 0, \exists m, n, \Lambda, |E - \frac{m}{n}| \leq \delta \text{ and } D(\Lambda(P_+^{\otimes m}), \rho^{\otimes n}) \leq \epsilon\} \tag{1.24}$$

1.3.3 Distillable entanglement

The Bell state $|\phi_+\rangle = (|00\rangle + |11\rangle)/\sqrt{2}$ is, in general, the optimal state to perform quantum information tasks. Suppose that two observers, Alice (A) and Bob (B), separated by arbitrarily large distance, would like to perform one of these tasks but they do not share $|\phi_+\rangle$. Instead, they are supplied with as many

mixed states ρ_{AB} as they want. Can they use these states ρ_{AB} to establish $|\phi_+\rangle$ states between them, by only using LOCC?

The *distillable entanglement* answers to this question, and determines how many m pairs of $|\phi_+\rangle$ can be extracted (or distilled) out of n pairs of the state ρ_{AB}, by only using LOCC strategies Λ, in the limit of $n \to \infty$. In mathematical words the distillable entanglement of ρ_{AB} is given by

$$E_D(\rho_{AB}) = \sup_{\Lambda} \lim_{n\to\infty} \frac{m}{n} \tag{1.25}$$

The main difficulty of the distillable entanglement is the optimization over all possible LOCC protocols it contains, that, in general, makes this quantifier extremely hard to compute. Moreover, not all entangled states are distillable [65], such as the bound entangled states, for which there is no LOCC protocol able to get maximally entangled states out of them, even if many copies are available.

1.3.4 Entanglement of formation

For each pure state of a composite quantum system $(A|B)$, the entanglement of formation is defined as the von Neumann entropy of either of the two subsystems A and B. The entanglement of formation E_F of a mixed state ρ, is then defined as the average entanglement of the pure states of the decomposition, minimized over all possible decomposition of ρ

$$E_F(\rho) = \min \left\{ \sum_i p_i E(\psi_i) \right\} \tag{1.26}$$

It is possible to express the Eq. (1.26) as an explicit funtion of ρ, thanks to the "spin flip" transformation. For a mixed state ρ of two qubits, the spin flipped state is given by

$$\tilde{\rho} = (\sigma_y \otimes \sigma_y)\rho^*(\sigma_y \otimes \sigma_y) \tag{1.27}$$

where ρ^* is the complex conjugate of ρ and σ_y is the Pauli matrix. It has been demonstrated [128] that

$$E_F(\rho) = \mathcal{E}(C(\rho)) \tag{1.28}$$

where $\mathcal{E}$ is a funtion monotonically increasing from 0 to 1, given by

$$\mathcal{E}(C) = -\frac{1+\sqrt{1-C^2}}{2}\log_2\frac{1+\sqrt{1-C^2}}{2} - \frac{1-\sqrt{1-C^2}}{2}\log_2\frac{1-\sqrt{1-C^2}}{2} \tag{1.29}$$

and $C(\rho)$ is the concurrence, equal to

$$C(\rho) = \max\{0, \lambda_1 - \lambda_2 - \lambda_3 - \lambda_4\} \tag{1.30}$$

where $\{\lambda_j\}$ are the eigenvalues, in decreasing order, of the Hermitian matrix $R = \sqrt{\sqrt{\rho}\tilde{\rho}\sqrt{\rho}}$, or alternatively the square root of the eigenvalues of the non-Hermitian matrix $\rho\tilde{\rho}$

The equation (1.28) is very useful, because it works for all density matrices and give an explicit formulation of the entanglement of formation in terms of the reduced density operators.

This measure of entanglement is close to entanglement cost. In fact, this last is equal to the regularization of the entanglement of formation

$$E_C(\rho) = \lim_{n\to\infty} \frac{1}{n} E_F(\rho^{\otimes n}) \tag{1.31}$$

1.3.5 Relative entropy of entanglement

As with many other objects in Quantum Information Theory, the relative entropy of entanglement is defined by extending the classical definition from probability distributions to density matrices. Let S be a set of separable states. The relative entropy of entanglement E_R for a state ρ is defined as

$$E_R(\rho) = \inf_{\sigma\in S}\{S(\rho||\sigma)\} = \inf_{\sigma\in S}\{\mathrm{Tr}\,(\rho\log\rho - \rho\log\sigma)\} \tag{1.32}$$

where S is the von Neumann entropy for the state ρ. The relative entropy of entanglement is a measure of similarity between two quantum states, i.e. it gives the distance between ρ and the nearest separable state.

For pure states, the above-mentioned measures coincide with the von Neumann entropy. The situation is quite different for mixed states, for which there exist many entanglement measures. It can be shown that, for a given density operator ρ, it holds a relation [27] between the different entanglement measures

$$E_D(\rho) \leq E(\rho) \leq E_C(\rho) \tag{1.33}$$

Thus, the distillable entanglement E_D and the entanglement cost E_C are the lower and upper limits of any entanglement measures.

2
Mathematical framework and techniques

In this chapter, I review some results on the exact diagonalization of one dimensional spin-1/2 models. I consider systems described by a translational invariant Hamiltonian $H_{\{\lambda\}}$ that depends on a set of parameters $\{\lambda\}$. By knowing the analitical expression of the ground states, I extract all the spin correlation functions with which I reconstruct the reduced density matrices and the entanglement properties of each model. I extend the analysis to the time dependence induced by a sudden quench of the Hamiltonian parameters.

2.1 Exact diagonalization via Jordan Wigner transformations

The one dimensional spin-1/2 models under invetigation are the XY models in a transverse magnetic field, the N-cluster Ising models and the N-cluster models in a transverse magnetic field, which Hamiltonians respectively read:

$$H^{XY}_{\{\gamma,h\}} = -\frac{1+\gamma}{2}\sum_j \sigma^x_j \sigma^x_{j+1} - \frac{1-\gamma}{2}\sum_j \sigma^y_j \sigma^y_{j+1} - h\sum_j \sigma^z_j \tag{2.1}$$

$$H^{cI}_{\{\phi,N\}} = -\cos(\phi)\sum_j \sigma^x_j Z^N_j \sigma^x_{j+N+1} + \sin(\phi)\sum_j \sigma^y_j \sigma^y_{j+1} \tag{2.2}$$

$$H^{ch}_{\{\phi,N\}} = -\cos(\phi)\sum_j \sigma^x_j Z^N_j \sigma^x_{j+N+1} + \sin(\phi)\sum_j \sigma^z_j \tag{2.3}$$

where γ, h and ϕ are respectively the anisotropy parameter, the magnetic field and the phase parameter that control the relative weight of the interacting terms, the operator Z^N_j stands for

$$Z_j^N = \bigotimes_{k=1}^{N} \sigma_{j+k}^z$$

and the spin operators are defined in terms of the Pauli matrices

$$\sigma^x = \begin{pmatrix} 0 & 1 \\ 1 & 0 \end{pmatrix} \quad \sigma^y = \begin{pmatrix} 0 & -\imath \\ \imath & 0 \end{pmatrix} \quad \sigma^z = \begin{pmatrix} 1 & 0 \\ 0 & -1 \end{pmatrix}$$

I introduce the ladder operators

$$\sigma_j^+ = \frac{\sigma_j^x + \imath\sigma_j^y}{2} \qquad \sigma_j^- = \frac{\sigma_j^x - \imath\sigma_j^y}{2} \tag{2.4}$$

in terms of which the Pauli matrices read

$$\sigma_j^x = \sigma_j^- + \sigma_j^+ \qquad \sigma_j^y = \imath(\sigma_j^- - \sigma_j^+) \qquad \sigma_j^z = 2\sigma_j^+\sigma_j^- - 1 \tag{2.5}$$

The ladder operators have either a Fermi part

$$\{\sigma_j^-, \sigma_j^+\} = 1 \qquad (\sigma_j^-)^2 = (\sigma_j^+)^2 = 0 \tag{2.6}$$

and a Bose part

$$[\sigma_j^+, \sigma_k^-] = [\sigma_j^+, \sigma_k^+] = [\sigma_j^-, \sigma_k^-] = 0 \quad j \neq k \tag{2.7}$$

The Hamiltonian in terms of the ladder operators cannot be diagonalized, because a canonical transformation does not preserve the set of canonical rules. However, one can introduce a new set of strictly fermionic operators, by performing a Jordan-Wigner (JW) transformation [73]

$$c_j = \prod_{k=1}^{j-1} (\sigma_k^z)\, \sigma_j^- \qquad c_j^\dagger = \prod_{k=1}^{j-1} (\sigma_k^z)\, \sigma_j^+ \tag{2.8}$$

with which the spin-1/2 systems can be mapped into models of non-interacting fermions, moving freely along the chain, only obeying Pauli's exclusion principle. Here, c_j and $c_j^\dagger$ stand respectively for the annihilation and creation fermionic operators on the j-th site, with strictly fermionic commutation rules

$$\{c_j, c_k^\dagger\} = \delta_{jk} \quad \{c_j, c_k\} = \{c_j^\dagger, c_k^\dagger\} = 0 \tag{2.9}$$

The Hamiltonians of Eqs. (2.1), (2.2) and (2.3) can be rewritten into a quadratic form, in terms of fermionic operators

$$H^{XY}_{\{\gamma,h\}} = \sum_j \left(c_j^\dagger c_{j+1}^\dagger + \gamma c_j^\dagger c_{j+1} + h.c. \right) - h \sum_j \left(2 c_j^\dagger c_j - 1 \right) \tag{2.10}$$

$$\begin{aligned} H^{cI}_{\{\phi,N\}} = & \cos(\phi) \sum_j \left(c_j^\dagger c_{j+N+1}^\dagger + c_j^\dagger c_{j+N+1} + h.c. \right) \\ & + \sin(\phi) \sum_j \left(c_j^\dagger c_{j+1}^\dagger - c_j^\dagger c_{j+1} + h.c. \right) \end{aligned} \tag{2.11}$$

$$\begin{aligned} H^{ch}_{\{\phi,N\}} = & \cos(\phi) \sum_j \left(c_j^\dagger c_{j+N+1}^\dagger + c_j^\dagger c_{j+N+1} + h.c. \right) \\ & + \sin(\phi) \sum_j \left(2 c_j^\dagger c_j - 1 \right) \end{aligned} \tag{2.12}$$

Note that I consider the thermodynamic limit, in which the boundary terms are negligible. In terms of fermionic operators, the cluster interaction of the Hamiltonians of Eqs. (2.2) and (2.3) is reduced from a $N+2$ interaction to a two-body interaction between sites at distance $N+1$.

The fermionic problem can hence be diagonalized using a Fourier transform

$$b_k = \frac{1}{\sqrt{N}} \sum_j c_j e^{-\imath k j} \qquad b_k^\dagger = \frac{1}{\sqrt{N}} \sum_j c_j^\dagger e^{\imath k j} \tag{2.13}$$

where the wave number k is given by $k = 2\pi l / M$ and l is an integer index that runs from -$M/2$ to $M/2$, where M is the total number of spins in the chain. The Hamiltonians can be expressed as

$$H_{\{\lambda\}} = \sum_{k>0} \tilde{H}_{\{\lambda\},k} \tag{2.14}$$

where λ is a set of parameters on which the Hamiltonian depends and $\tilde{H}_{\{\lambda\},k}$ is a term acting only on fermions with momentum equal to k or $-k$. This local Hamiltonian, in the momentum space, is equal to

$$\tilde{H}_{\{\lambda\},k} = 2\varepsilon_{\{\lambda\},k} (b_k^\dagger b_k + b_{-k}^\dagger b_{-k} - 1) + 2\imath \delta_{\{\lambda\},k} (b_k^\dagger b_{-k}^\dagger - b_{-k} b_k) \tag{2.15}$$

where $\varepsilon_{\{\lambda\},k}$ and $\delta_{\{\lambda\},k}$ depend on the model analyzed. In the XY model ($\{\lambda\} = \{\gamma, h\}$), they are equal to

$$\begin{cases} \varepsilon_{\{\gamma,h\},k} = \cos(k) - h \\ \delta_{\{\gamma,h\},k} = \gamma \sin(k) \end{cases} \tag{2.16}$$

for the N-cluster Ising model ($\{\lambda\} = \{\phi, N\}$), they are equal to

$$\begin{cases} \varepsilon_{\{\phi,N\},k} = \cos((N+1)k)\cos\varphi - \cos(k)\sin(\varphi) \\ \delta_{\{\phi,N\},k} = \sin((N+1)k)\cos\varphi - \sin(k)\sin(\varphi) \end{cases} \tag{2.17}$$

and for the N-cluster model in a transverse magnetic field ($\{\lambda\} = \{\phi, N\}$), they correspond to

$$\begin{cases} \varepsilon_{\{\phi,N\},k} = \cos((N+1)k)\cos(\phi) + \sin(\phi) \\ \delta_{\{\phi,N\},k} = \sin((N+1)k)\cos(\phi) \end{cases} \tag{2.18}$$

Defining the occupation number basis $|1_k, 1_{-k}\rangle$, $|0_k, 0_{-k}\rangle$, $|1_k, 0_{-k}\rangle$, $|0_k, 1_{-k}\rangle$, each $\tilde{H}_{\{\lambda\},k}$ corresponds to a four-level system described by a 4×4 matrix

$$\tilde{H}_{\{\lambda\},k} = \begin{pmatrix} 2\varepsilon_{\{\lambda\},k} & 2\imath\delta_{\{\lambda\},k} & 0 & 0 \\ -2\imath\delta_{\{\lambda\},k} & -2\varepsilon_{\{\lambda\},k} & 0 & 0 \\ 0 & 0 & 0 & 0 \\ 0 & 0 & 0 & 0 \end{pmatrix} \tag{2.19}$$

From this expression of $\tilde{H}_{\{\lambda\},k}$, it is easy to evaluate the ground state energy, that results to be

$$\omega_{\{\lambda\},k} = -2\sqrt{\varepsilon^2_{\{\lambda\},k} + \delta^2_{\{\lambda\},k}} \tag{2.20}$$

The associated ground state $|\psi_{\{\lambda\},k}\rangle$ is a superposition of $|1_k, 1_{-k}\rangle$ and $|0_k, 0_{-k}\rangle$

$$|\psi_{\{\lambda\},k}\rangle = \alpha_{\{\lambda\},k}\,|1_k, 1_{-k}\rangle + \beta_{\{\lambda\},k}\,|0_k, 0_{-k}\rangle \tag{2.21}$$

with superposition parameters given by

$$\begin{aligned} \alpha_{\{\lambda\},k} &= \imath \frac{\varepsilon_{\{\lambda\},k} - \sqrt{\varepsilon^2_{\{\lambda\},k} + \delta^2_{\{\lambda\},k}}}{\sqrt{\delta^2_{\{\lambda\},k} + \left(\varepsilon_{\{\lambda\},k} - \sqrt{\varepsilon^2_{\{\lambda\},k} + \delta^2_{\{\lambda\},k}}\right)^2}} \\ \beta_{\{\lambda\},k} &= \frac{\delta_{\{\lambda\},k}}{\sqrt{\delta^2_{\{\lambda\},k} + \left(\varepsilon_{\{\lambda\},k} - \sqrt{\varepsilon^2_{\{\lambda\},k} + \delta^2_{\{\lambda\},k}}\right)^2}} \end{aligned} \tag{2.22}$$

Since the Hamiltonian is the sum of the non-interacting terms $\tilde{H}_{\{\lambda\},k}$, each one of them acting on a different Hilbert space, the ground state of the total Hamiltonian is the tensor product of all $|\psi_{\{\lambda\},k}\rangle$

$$|\psi_{\{\lambda\}}\rangle = \bigotimes_k |\psi_{\{\lambda\},k}\rangle \tag{2.23}$$

and the associated density energy, in the thermodynamic limit, is equal to

$$\Omega_{\{\lambda\}} = \frac{1}{\pi}\int_0^\pi \omega_{\{\lambda\},k}\ dk \tag{2.24}$$

It is worth to note that the ground state holds a well defined parity, that depends on the particular set of parameters taken into account [15]. However, going towards the thermodynamic limit, the energy gap between the even and the odd sectors tends to vanish and, when the number of spins diverges, the system shows a perfect degeneracy, below the quantum critical point, between even and odd ground states [10, 113].

2.2 Correlation functions

By having the expression of the exact ground state in Eq. (2.23), all the spin correlation functions can be reconstructed. However, the state is not expressed neither in terms of spins nor in terms of fermionic operators in real space, but in terms of fermionic variables in the momentum space. For this reason, in order to determine the spin correlation functions, one must, at first, transform all the spin operators in fermionic operators, thanks to the Jordan Wigner transformations of Eq. (2.8). To simplify such process it was shown [84, 10] that all the spin operators can be mapped into ordered products of 2 types of Majorana fermionic operators, indicated with A_j and B_j respectively

$$A_j = c_j + c_j^\dagger \qquad\qquad B_j = c_j - c_j^\dagger \tag{2.25}$$

where j is an index that runs on all the spins of the system. In general, after this process, one obtains a fermionic operator made by a large number of fermionic terms, that can be evaluated by applying the Wick's theorem.

Having two types of fermionic operators, it is enough to evaluate five expectation values, that possess all the ingredients to determine each spin correlation functions. From the expression of the ground state $|\psi_{\{\lambda\}}\rangle$ in Eq. (2.21), it immediately follows that both $\langle A_j\rangle$ and $\langle B_j\rangle$ vanish ($\langle O\rangle$ is used as a shortcut for $\langle\psi_{\{\lambda\}}|\, O\, |\psi_{\{\lambda\}}\rangle$). In fact, adding or removing a single fermion from $|\psi_{\{\lambda\}}\rangle$, the state is driven in an orthogonal subspace, that implies

$$\begin{aligned}\langle A_j\rangle &= 0\\ \langle B_j\rangle &= 0\end{aligned} \tag{2.26}$$

As a consequence, if a spin operator is mapped into a fermionic operator made by an odd number of components, its expectation value on $|\psi_{\{\lambda\}}\rangle$ vanishes.

On the contrary, the other three basic elements can be non zero

$$\begin{aligned} \langle A_i A_k \rangle &= f_{i,k}(\{\lambda\}) \\ \langle B_i A_k \rangle &= g_{i,k}(\{\lambda\}) \\ \langle B_i B_k \rangle &= h_{i,k}(\{\lambda\}) \end{aligned} \tag{2.27}$$

and must be evaluated to obtain the explicit value of a generic spin correlation function. Because the models are invariant under spatial translation, also these functions hold the same property and hence they have not to depend on the particular choice of the spin i and k but only on their relative distance $r = i - k$. Therefore, $f_{i,k}(\{\lambda\}) \equiv f_r(\{\lambda\})$, $g_{i,k}(\{\lambda\}) \equiv g_r(\{\lambda\})$ and $h_{i,k}(\{\lambda\}) \equiv h_r(\{\lambda\})$. By substituting the expression of A_i and B_i given in Eq. (2.25), it follows

$$\begin{aligned} g_r(\{\lambda\}) &= \langle B_r A_0 \rangle = \langle \psi_{\{\lambda\}} | \, (c_r - c_r^+)(c_0 + c_0^+) \, | \psi_{\{\lambda\}} \rangle \\ f_r(\{\lambda\}) &= \langle A_r A_0 \rangle = \langle \psi_{\{\lambda\}} | \, (c_r + c_r^+)(c_0 + c_0^+) \, | \psi_{\{\lambda\}} \rangle \\ h_r(\{\lambda\}) &= \langle B_r B_0 \rangle = \langle \psi_{\{\lambda\}} | \, (c_r - c_r^+)(c_0 - c_0^+) \, | \psi_{\{\lambda\}} \rangle \end{aligned} \tag{2.28}$$

With a straightforward calculations, one obtains, in the thermodynamic limit, that

$$g_r(\{\lambda\}) = \frac{1}{\pi} \int_0^\pi \left[(|\tilde{\beta}_{\{\lambda\},k}|^2 - |\tilde{\alpha}_{\{\lambda\},k}|^2) \cos(kr) + \imath (\tilde{\alpha}^*_{\{\lambda\},k} \tilde{\beta}_{\{\lambda\},k} - \tilde{\alpha}_{\{\lambda\},k} \tilde{\beta}^*_{\{\lambda\},k}) \sin(kr) \right] dk \tag{2.29}$$

$$\begin{aligned} f_r(\{\lambda\}) &= \delta_{r,0} + \frac{\imath}{\pi} \int_0^\pi (\tilde{\alpha}^*_{\{\lambda\},k} \tilde{\beta}_{\{\lambda\},k} + \tilde{\alpha}_{\{\lambda\},k} \tilde{\beta}^*_{\{\lambda\},k}) \sin(kr) dk \\ h_r(\{\lambda\}) &= -\delta_{r,0} + \frac{\imath}{\pi} \int_0^\pi (\tilde{\alpha}^*_{\{\lambda\},k} \tilde{\beta}_{\{\lambda\},k} + \tilde{\alpha}_{\{\lambda\},k} \tilde{\beta}^*_{\{\lambda\},k}) \sin(kr) dk \end{aligned} \tag{2.30}$$

where $\delta_{r,0}$ is the Kronecker delta that is different from zero only for $r = 0$.

In all the models analyzed, $\alpha_{\{\lambda\},k}$ is an imaginary number while $\beta_{\{\lambda\},k}$ is real, as one can see in Eq. (2.22). Therefore, in the static case, the integrals in the definition of both $f_r(\{\lambda\})$ and $h_r(\{\lambda\})$ are all zero and $f_r(\{\lambda\}) = -h_r(\{\lambda\}) = \delta_{r,0}$. On the contrary, the functions $g_r(\{\lambda\})$ are all reals.

With the knowledge of $g_r(\{\lambda\})$, $f_r(\{\lambda\})$ and $h_r(\{\lambda\})$, one can evaluate all the spin correlation functions. However, the approach to the evaluation is different, depending on the fact that the spin operators commute or anti-commute with the parity $P_z = \otimes_{i=1}^{M} \sigma_i^z$.

In the case of operators that commutes with P_z, the correlation functions can be evaluated directly. In the following, I just limit to describe the characteristic examples of the symmetric spin correlation functions that enter in the reduced density matrix of two spin at a generic distance r. With some algebra, it is easy to show that

$$\langle \sigma_i^z \rangle = -g_0(\{\lambda\}) \tag{2.31}$$

$$\langle \sigma_i^z \sigma_{i+r}^z \rangle = g_0(\{\lambda\})^2 - g_r(\{\lambda\}) g_{-r}(\{\lambda\}) \tag{2.32}$$

$$\langle \sigma_i^x \sigma_{i+r}^x \rangle = \begin{vmatrix} g_{-1}(\{\lambda\}) & g_{-2}(\{\lambda\}) & \cdots & g_{-r}(\{\lambda\}) \\ g_0(\{\lambda\}) & g_{-1}(\{\lambda\}) & \cdots & g_{1-r}(\{\lambda\}) \\ \vdots & \vdots & \ddots & \vdots \\ g_{r-2}(\{\lambda\}) & g_{r-3}(\{\lambda\}) & \cdots & g_{-1}(\{\lambda\}) \end{vmatrix} \tag{2.33}$$

$$\langle \sigma_i^y \sigma_{i+r}^y \rangle = \begin{vmatrix} g_1(\{\lambda\}) & g_2(\{\lambda\}) & \cdots & g_r(\{\lambda\}) \\ g_0(\{\lambda\}) & g_1(\{\lambda\}) & \cdots & g_{r-1}(\{\lambda\}) \\ \vdots & \vdots & \ddots & \vdots \\ g_{2-r}(\{\lambda\}) & g_{3-r}(\{\lambda\}) & \cdots & g_1(\{\lambda\}) \end{vmatrix} \tag{2.34}$$

Unfortunately, the way to obtain the spin correlation functions associated to operators that do not commute with the parity P_z is much more complex. In the next section, I illustrate in details the trick used to the evaluation.

2.3 Symmetry-breaking ground states

The Hamiltonians under analysis $H_{\{\lambda\}}$, all satisfy the parity symmetry respect to a spin direction, regardeless the values of the Hamiltonian parameters $\{\lambda\}$. This means that $H_{\{\lambda\}}$ commutes with the parity operator

$$P_\nu = \bigotimes_{i=1}^{M} \sigma_i^\nu \tag{2.35}$$

where M is the total number of spins in the system. For sake of simplicity and without loosing of generality, one can fix $\nu = z$. Because $[H_{\{\lambda\}}, P_z] = 0$, the Hamiltonian and the parity operator admit a complete set of eigenstates in

common. However, in the case in which the Hamiltonian shows degenerated spectrum, there exist eigenstates of the Hamiltonian that are not eigenstates of the parity. When this happens at the level of the ground state, the phenomenon is known as a spontaneous symmetry breaking, of which the magnetically ordered phases are the most known examples.

In the magnetically ordered phases of one dimensional spin-1/2 systems, the Hamiltonian admits a twofold degenerated ground states [113, 110], between the infinite number of ground states, that are also eigenstates of the parity operator P_z with opposite eigenvalues. These two symmetric ground states, usually named the even $|e_{\{\lambda\}}\rangle$ ($P_z |e_{\{\lambda\}}\rangle = |e_{\{\lambda\}}\rangle$) and the odd $|o_{\{\lambda\}}\rangle$ ($P_z |o_{\{\lambda\}}\rangle = -|o_{\{\lambda\}}\rangle$) ground states, form a complete orthonormal base for the ground space. Therefore, a generic ground state of the Hamiltonian $H_{\{\lambda\}}$ can be written as

$$|g_{\{\lambda\}}(u,v)\rangle = u\,|e_{\{\lambda\}}\rangle + v\,|o_{\{\lambda\}}\rangle \tag{2.36}$$

where u and v are complex superposition amplitudes that satisfy the normalization condition $|u|^2 + |v|^2 = 1$.

Consider an arbitrary bipartition $(S|R)$ of the system, such that the subsystem $S = \{i_1, \cdots, i_L\}$ is any subset made by L spins, and subsystem R is the remainder. The projection of the state $|g_{\{\lambda\}}(u,v)\rangle$ into S is represented by the reduced density matrix $\rho(u,v,S)$, obtained tracing out all the degrees of freedom that fall outside S. The reduced density matrix $\rho(u,v,S)$ can be expressed in terms of the L-points spin correlation functions [97] as

$$\rho(u,v,S) = \frac{1}{2^L} \sum_{\{\mu_i\}} \langle g_{\{\lambda\}}(u,v)|\hat{O}_S^{\{\mu_i\}}|g_{\{\lambda\}}(u,v)\rangle \hat{O}_S^{\{\mu_i\}} \tag{2.37}$$

In the above equation, $\hat{O}_S^{\{\mu_i\}} = \sigma_{i_1}^{\mu_1} \otimes \sigma_{i_2}^{\mu_2} \otimes \ldots \otimes \sigma_{i_L}^{\mu_L}$ is the tensor product of Pauli operators defined on the spins in S, $\{\mu_i\}$ is a set of L variables where any single element ranges across $\mu_i = 0, x, y, z$, the sum runs on all possible $\{\mu_i\}$ and σ_i^0 stands for the identity operator on the i-th spin.

With respect to the parity operator $P_z = \bigotimes_{i=1}^N \sigma_i^z$, any operator $\hat{O}_S^{\{\mu_i\}}$ can be classified in two different families: the operators that commute or anti-commute with P_z. It is well known that, in the thermodynamic limit, the expectation value of an operator that commutes with the parity is the same on even $|e_{\{\gamma\}}\rangle$ or on odd $|o_{\{\gamma\}}\rangle$ ground state [113, 110]. As a consequence, the two symmetric ground states are always locally indistinguishable. On the contrary, any operator $\hat{O}_S^{\{\mu_i\}}$ that anti-commutes with P_z drives even states in odd ones and, hence, its expectation value on a symmetric ground state vanishes.

With these considerations, the reduced density matrix $\rho(u, v, S)$ of Eq. (2.37) can be rewritten as

$$\rho(u, v, S) = \rho^{sym}(S) + \chi(u, v, S) \tag{2.38}$$

The density matrix $\rho^{sym}(S)$ is obtained projecting one of the two symmetric ground states into S, and it is equal to

$$\rho^{sym}(S) = \frac{1}{2^L} \sum_{\{\mu_i\}} \langle \hat{O}_S^{\{\mu_i\}} \rangle \hat{O}_S^{\{\mu_i\}} \tag{2.39}$$

where the sum extends over all the operators $\hat{O}_S^{\{\mu_i\}}$ that commute with P_z.

Vice versa $\chi(u, v, S)$ is an Hermitian traceless matrix that depends on the superposition parameters and is made by the contributions of all the operators $\hat{O}_S^{\{\mu_i\}}$ that anti-commute with P_z. To evaluate $\chi(u, v, S)$, I introduce, for a generic spin operator $\hat{O}_S^{\{\mu_i\}}$ defined on S and that anti-commutes with P_z, the operator $\hat{W}_{S\cup S+R}^{\{\mu_i\}} = \hat{O}_S^{\{\mu_i\}} \otimes \hat{O}_{S+R}^{\{\mu_i\}}$, with $\hat{O}_{S+R}^{\{\mu_i\}} = \sigma_{i_1+R}^{\mu_1} \otimes \sigma_{i_2+R}^{\mu_2} \otimes \ldots \otimes \sigma_{i_l+R}^{\mu_l}$, defined on a new subset $S + R$, obtained from S by a rigid spatial translation of R. Because both $\hat{O}_S^{\{\mu_i\}}$ and $\hat{O}_{S+R}^{\{\mu_i\}}$ anti-commutes with P_z, $\hat{W}_{S\cup S+R}^{\{\mu_i\}}$ commute with the parity operator and hence its expectation value on a symmetric ground state can be different from zero. Hence, the expectation value of a generic operator $\hat{O}_S^{\{\mu_i\}}$ that anti-commutes with P_z and the spin correlation function associated, is recovered exploiting the property of asymptotic factorization of two local operators separated by an infinite distance, that yields to

$$\langle \hat{O}_S^{\{\mu_i\}} \rangle = \sqrt{\lim_{R\to\infty} \langle \hat{W}_{S\cup S+R}^{\{\mu_i\}} \rangle} \tag{2.40}$$

Starting from this state independent expression of the $\langle \hat{O}_S^{\{\mu_i\}} \rangle$, the Eq. (2.38) can be written as

$$\rho(u, v, S) = \rho^{sym}(S) + (u^* v + v^* u)\tilde{\chi}(S) \tag{2.41}$$

where

$$\tilde{\chi}(S) = \frac{1}{2^l} \sum_{\{\mu_i\}} \langle \hat{O}_S^{\{\mu_i\}} \rangle \hat{O}_S^{\{\mu_i\}} \tag{2.42}$$

and the sum is restricted to all the operators $\hat{O}_S^{\{\mu_i\}}$ that anti-commute with P_z.

2.4 Time evolution induced by a sudden quench

In this section, I illustrate in details the method used to evaluate the time-dependent spin correlation functions. Such approach can be used for all models that can be solved using Jordan-Wigner transformations and for all time-dependences that preserve the parity symmetry of the Hamiltonians.

I consider the following quench protocol. At time $t < 0$ the system is prepared in one of the possible ground state $|g_{\{\lambda_0\}}(u,v)\rangle$ of the Hamiltonian $H_{\{\lambda_0\}}$. At time $t = 0$, the set of the Hamiltonian parameters are suddenly changed from $\{\lambda_0\}$ to $\{\lambda_1\}$ and the state starts to evolve under the action of the new Hamiltonian $H_{\{\lambda_1\}}$.

Such approach

2.4.1 Time evolution of the ground state

After a sudden change of the Hamiltonian parameters from $\{\lambda_0\}$ to $\{\lambda_1\}$, the dynamics of the system, for any time $t \geq 0$, is described by the state

$$|\psi_{\{\lambda_0,\lambda_1\}}(t)\rangle = U(\{\lambda_1\},t)\,|\psi_{\{\lambda_0\}}\rangle \tag{2.43}$$

where $U(\{\lambda_1\},t) = e^{-iH_{\{\lambda_1\}}t}$ is the time evolution unitary operator and $|\psi_{\{\lambda_0\}}\rangle$ is the ground state at $t < 0$ (initial state). Taken into account that:

1. Eq. (2.14) is still valid even for $\{\lambda\} = \{\lambda_1\}$,
2. the wave number k does not depends on the set of the Hamiltonian parameters $\{\lambda\}$,
3. the initial state $|\psi_{\{\lambda_0\}}\rangle$ can be written as a tensor product of states defined on each single $k > 0$ (eq. (2.23)),

it follows that

$$|\psi_{\{\lambda_0,\lambda_1\}}(t)\rangle = \bigotimes_k |\psi_{\{\lambda_0,\lambda_1\},k}(t)\rangle = \bigotimes_k U_k(\{\lambda_1\},t)\,|\psi_{\{\lambda_0\},k}\rangle \tag{2.44}$$

where $U_k(\{\lambda_1\},t)$ is a time evolution unitary operator that acts on a single k. The explicit expression of $U_k(\{\lambda_1\},t)$ can be determined by the solution of the Heisenberg equation

$$\imath\frac{d}{dt}U_k(\{\lambda_1\},t) = \tilde{H}_{\{\lambda_1\},k}U_k(\{\lambda_1\},t) \tag{2.45}$$

that in matrix form reads

$$\imath\frac{d}{dt}\begin{pmatrix} U_{11,k}(t) & U_{12,k}(t) \\ U_{21,k}(t) & U_{22,k}(t) \end{pmatrix} = \begin{pmatrix} 2\varepsilon_{\{\lambda_1\},k} & 2\imath\delta_{\{\lambda_1\},k} \\ -2\imath\delta_{\{\lambda_1\},k} & -2\varepsilon_{\{\lambda_1\},k} \end{pmatrix} \begin{pmatrix} U_{11,k}(t) & U_{12,k}(t) \\ U_{21,k}(t) & U_{22,k}(t) \end{pmatrix} \tag{2.46}$$

From Eq. (2.46), one obtains two non trivial systems of first order coupled differential equations with constant coefficients. The first is given by

$$\begin{cases} \imath\dot{U}_{11,k}(t) = 2\varepsilon_{\{\lambda_1\},k}U_{11,k}(t) + 2\imath\delta_{\{\lambda_1\},k}U_{21,k}(t) \\ \imath\dot{U}_{21,k}(t) = -2\imath\delta_{\{\lambda_1\},k}U_{11,k}(t) - 2\varepsilon_{\{\lambda_1\},k}U_{21,k}(t) \end{cases}$$

while the second is

$$\begin{cases} \imath\dot{U}_{12,k}(t) = 2\varepsilon_{\{\lambda_1\},k}U_{12,k}(t) + 2\imath\delta_{\{\lambda_1\},k}U_{22,k}(t) \\ \imath\dot{U}_{22,k}(t) = -2\imath\delta_{\{\lambda_1\},k}U_{12,k}(t) - 2\varepsilon_{\{\lambda_1\},k}U_{22,k}(t) \end{cases}$$

These two systems can be solved by decoupling them into four second order differential equations, with constant coefficients and opportune boundary conditions.

It follows for $U_{11,k}$

$$\begin{cases} \ddot{U}_{11,k}(t) + \omega^2_{\{\lambda_1\},k}U_{11,k}(t) = 0 \\ U_{11,k}(0) = 1 \\ \dot{U}_{11,k}(0) = -2\imath\varepsilon_{\{\lambda_1\},k} \end{cases} \tag{2.47}$$

for $U_{12,k}$

$$\begin{cases} \ddot{U}_{12,k}(t) + \omega^2_{\{\lambda_1\},k}U_{12,k}(t) = 0 \\ U_{12,k}(0) = 0 \\ \dot{U}_{12,k}(0) = 2\imath\delta_{\{\lambda_1\},k} \end{cases} \tag{2.48}$$

for $U_{21,k}$

$$\begin{cases} \ddot{U}_{21,k}(t) + \omega^2_{\{\lambda_1\},k}U_{21,k}(t) = 0 \\ U_{21,k}(0) = 0 \\ \dot{U}_{21,k}(0) = -2\imath\delta_{\{\lambda_1\},k} \end{cases} \tag{2.49}$$

and, at the end, for $U_{22,k}$

$$\begin{cases} \ddot{U}_{22,k}(t) + \omega^2_{\{\lambda_1\},k}U_{22,k}(t) = 0 \\ U_{22,k}(0) = 1 \\ \dot{U}_{22,k}(0) = 2\imath\varepsilon_{\{\lambda_1\},k} \end{cases} \tag{2.50}$$

The matrix elements of the time evolution unitary operator can be derived by solving the above differential equations

$$\begin{aligned} U_{11,k}(t) &= \cos(\omega_{\{\lambda_1\},k}t) - \imath\frac{\varepsilon_{\{\lambda_1\},k}}{\omega_{\{\lambda_1\},k}}\sin(\omega_{\{\lambda_1\},k}t) \\ U_{12,k}(t) &= \imath\frac{\delta_{\{\lambda_1\},k}}{\omega_{\{\lambda_1\},k}}\sin(\omega_{\{\lambda_1\},k}t) \\ U_{21,k}(t) &= -\imath\frac{\delta_{\{\lambda_1\},k}}{\omega_{\{\lambda_1\},k}}\sin(\omega_{\{\lambda_1\},k}t) \\ U_{22,k}(t) &= \cos(\omega\{\lambda_1\},kt) + \imath\frac{\varepsilon_{\{\lambda_1\},k}}{\omega_{\{\lambda_1\},k}}\sin(\omega_{\{\lambda_1\},k}t) \end{aligned} \tag{2.51}$$

With the explicit expression of the elements of time-evolution unitary operator $U_k(\{\lambda_1\},t)$, one can obtain the image of the initial state $|\psi_{\{\lambda_0\},k}\rangle$, at a generic time t and for any wave number k

$$|\psi_{\{\lambda_0,\lambda_1\},k}(t)\rangle = \tilde{\alpha}_{\{\lambda_0,\lambda_1\},k}(t)\,|1_k,1_{-k}\rangle + \tilde{\beta}_{\{\lambda_0,\lambda_1\},k}(t)\,|0_k,0_{-k}\rangle \tag{2.52}$$

where

$$\begin{aligned} \tilde{\alpha}_{\{\lambda_0,\lambda_1\},k}(t) &= \alpha_{\{\lambda_0\},k}\cos(\omega_{\{\lambda_1\},k}t) - \imath\frac{\varepsilon_{\{\lambda_1\},k}\alpha_{\{\lambda_0\},k} - \delta_{\{\lambda_1\},k}\beta_{\{\lambda_0\},k}}{\omega_{\{\lambda_1\},k}}\sin(\omega_{\{\lambda_1\},k}t) \\ \tilde{\beta}_{\{\lambda_0,\lambda_1\},k}(t) &= \beta_{\{\lambda_0\},k}\cos(\omega_{\{\lambda_1\},k}t) - \imath\frac{\delta_{\{\lambda_1\},k}\alpha_{\{\lambda_0\},k} - \varepsilon_{\{\lambda_1\},k}\beta_{\{\lambda_0\},k}}{\omega_{\{\lambda_1\},k}}\sin(\omega_{\{\lambda_1\},k}t) \end{aligned} \tag{2.53}$$

In complete analogy with the stationary case, it follows from Eq. (2.44) that the global ground state is the tensor product $|\psi_{\{\lambda_0,\lambda_1\}}(t)\rangle = \bigotimes_k |\psi_{\{\lambda_0,\lambda_1\},k}(t)\rangle$.

2.4.2 Time-dependent fermionic correlation functions

The method illustrated in Sec. (2.2), for the stationary case, can be used to obtain the expression of the time-dependent fermionic correlation functions. In completely analogy, one have to evaluate five expectation values, that possess all the ingredients to determine each time-dependent spin correlation function. In completely analogy, it follows that

$$\begin{aligned}\langle A_j\rangle_t &= 0\\ \langle B_j\rangle_t &= 0\end{aligned} \tag{2.54}$$

and

$$\begin{aligned}\langle A_iA_k\rangle_t &= f_{i,k}(\{\lambda_0,\lambda_1\},t)\equiv f_r(\{\lambda_0,\lambda_1\},t)\\ \langle B_iA_k\rangle_t &= g_{i,k}(\{\lambda_0,\lambda_1\},t)\equiv g_r(\{\lambda_0,\lambda_1\},t)\\ \langle B_iB_k\rangle_t &= h_{i,k}(\{\lambda_0,\lambda_1\},t)\equiv h_r(\{\lambda_0,\lambda_1\},t)\end{aligned} \tag{2.55}$$

where $\langle O\rangle_t$ is a shortcut for $\langle\psi_{\{\lambda_0,\lambda_1\}}(t)|\,O\,|\psi_{\{\lambda_0,\lambda_1\}}(t)\rangle$.

The analytical expression of the three non-trivially zero time-dependent correlation functions can be obtained, with a straightforward calculation, by using the definition of Majorana fermions of Eq. (2.25) and the time-dependent aplitudes of Eq. (2.53). In the thermodynamic limit one obtains that

$$\begin{aligned}g_r(\{\lambda_0,\lambda_1\},t) &= \frac{1}{\pi}\int_0^\pi\Big[\left(|\tilde\beta_{\{\lambda_0,\lambda_1\},k}(t)|^2-|\tilde\alpha_{\{\lambda_0,\lambda_1\},k}(t)|^2\right)\cos(kr)\\ &\quad+\imath\left(\tilde\alpha^*_{\{\lambda_0,\lambda_1\},k}(t)\tilde\beta_{\{\lambda_0,\lambda_1\},k}(t)-\tilde\alpha_{\{\lambda_0,\lambda_1\},k}(t)\tilde\beta^*_{\{\lambda_0,\lambda_1\},k}(t)\right)\sin(kr)\Big]dk\\ f_r(\{\lambda_0,\lambda_1\},t) &= \delta_{r,0}+\frac{\imath}{\pi}\int_0^\pi\left(\tilde\alpha^*_{\{\lambda_0,\lambda_1\},k}\tilde\beta_{\{\lambda_0,\lambda_1\},k}+\tilde\alpha_{\{\lambda_0,\lambda_1\},k}\tilde\beta^*_{\{\lambda_0,\lambda_1\},k}\right)\sin(kr)dk\\ h_r(\{\lambda_0,\lambda_1\},t) &= -\delta_{r,0}+\frac{\imath}{\pi}\int_0^\pi\left(\tilde\alpha^*_{\{\lambda_0,\lambda_1\},k}\tilde\beta_{\{\lambda_0,\lambda_1\},k}+\tilde\alpha_{\{\lambda_0,\lambda_1\},k}\tilde\beta^*_{\{\lambda_0,\lambda_1\},k}\right)\sin(kr)dk\end{aligned} \tag{2.56}$$

where $\delta_{r,0}$ is the Kronecker delta that is different from zero only when $r=0$.

By using Eq. (2.53), for example, one can obtain the explicit expression of $g_r(\{\lambda_0,\lambda_1\},t)$, $f_r(\{\lambda_0,\lambda_1\},t)$ and $h_r(\{\lambda_0,\lambda_1\},t)$ in terms of the Hamiltonian parameters before $\{\lambda_0\}=\{\gamma,h_0\}$ and after $\{\lambda_1\}=\{\gamma,h_1\}$ the quench, for the XY model

$$\begin{aligned}g_r(\gamma,h_0,h_1,t) &= \frac{1}{\pi}\int_0^\pi\frac{\left((\cos(k)-h_0)(\cos(k)-h_1)+\gamma^2\sin(k)^2\right)\left((\cos(k)-h_1)\cos(kr)-\gamma\sin(k)\sin(kr)\right)}{\Lambda(\gamma,h_1,k)^2\Lambda(\gamma,h_0,k)}dk\\ &\quad+\frac{\gamma(h_1-h_0)}{\pi}\int_0^\pi\frac{\cos\left(4t\Lambda(\gamma,h_1,k)\right)\sin(k)\left(\gamma\cos(kr)\sin(k)+(\cos(k)-h_1)\sin(kr)\right)}{\Lambda(\gamma,h_1,k)^2\Lambda(\gamma,h_0,k)}dk\end{aligned}$$

and

$$f_r(\gamma,h_0,h_1,t)=\delta(r)+\frac{i\gamma(h_0-h_1)}{\pi}\int_0^\pi \frac{\sin(k)\sin(kr)\sin\left(4t\Lambda(\gamma,h_1,k)\right)}{\Lambda(\gamma,h_0,k)\Lambda(\gamma,h_1,k)}dk$$
$$h_r(\gamma,h_0,h_1,t)=-\delta(r)+\frac{i\gamma(h_0-h_1)}{\pi}\int_0^\pi \frac{\sin(k)\sin(kr)\sin\left(4t\Lambda(\gamma,h_1,k)\right)}{\Lambda(\gamma,h_0,k)\Lambda(\gamma,h_1,k)}dk \tag{2.57}$$

where it has been defined

$$\Lambda(\gamma,h,k)=\sqrt{(h-\cos(k))^2+\gamma^2\sin(k)^2} \tag{2.58}$$

To recover the well known static expression of the fermionic correlation functions, it is enough to take $h_1=h_0$ or $t=0$ equivalently. On the other hand, in the limit of diverging time, the time dependent integrals becomes integrals of rapidly oscillating functions that slowly go to zero. Therefore, in the limit $t\to\infty$, the functions $g_r(\gamma,h_0,h_1,\infty)$, $f_r(\gamma,h_0,h_1,\infty)$ and $h_r(\gamma,h_0,h_1,\infty)$ retrieve the same symmetries of the stationary case. In particular, $f_r(\gamma,h_0,h_1,\infty)=-h_r(\gamma,h_0,h_1,\infty)=\delta_{r,0}$, while $g_r(\gamma,h_0,h_1,\infty)$ becomes

$$\begin{aligned}g_r(\gamma,h_0,h_1,\infty)=&\frac{1}{\pi}\int_0^\pi \frac{\left((\cos(k)-h_0)(\cos(k)-h_1)+\gamma^2\sin(k)^2\right)(\cos(k)-h_1)\cos(kr)}{\Lambda(\gamma,h_1,k)^2\Lambda(\gamma,h_0,k)}dk\\&-\frac{\gamma}{\pi}\int_0^\pi \frac{\left((\cos(k)-h_0)(\cos(k)-h_1)+\gamma^2\sin(k)^2\right)\sin(k)\sin(kr)}{\Lambda(\gamma,h_1,k)^2\Lambda(\gamma,h_0,k)}dk\end{aligned} \tag{2.59}$$

Unfortunately, the analogous analytical expressions for the time-dependent correlation functions for the N-clusters Ising models and the N-cluster models in a transverse magnetic field are longer and more cumbersome to write. In any case, they can be recovered from Eq. (2.53) and Eqs.(2.17), (2.18), with $\{\lambda_0\}=\{\phi_0,N\}$ and $\{\lambda_1\}=\{\phi_1,N\}$. In complete analogy with the XY model, also in the N-cluster models, the $g_r(\phi_0,\phi_1,\infty)$, $f_r(\phi_0,\phi_1,\infty)$ and $h_r(\phi_0,\phi_1,\infty)$ functions have the same symmetries of the static function $g_r(\phi_0)$, $f_r(\phi_0)$ and $h_r(\phi_0)$. Therefore, it follows that $f_r(\phi_0,\phi_1,\infty)=-h_r(\phi_0,\phi_1,\infty)=\delta_{r,0}$ while $g_r(\phi_0,\phi_1,\infty)\neq 0$ only for $r=a(N+2)+1$ or $r=a(N+1)$ (a is an integer) respectively for the N-cluster Ising models and N-cluster models in a transverse magnetic field [47, 118].

2.4.3 Time-dependent spin correlation functions

With the knowledge of $g_r(\{\lambda_0,\lambda_1\},t)$, $f_r(\{\lambda_0,\lambda_1\},t)$ and $h_r(\{\lambda_0,\lambda_1\},t)$, one can recover all the time-dependent spin correlation functions at any time. In com-

pletely analogy with the stationary case, the evaluation of the time-dependent spin correlation functions depends on the fact that the spin operators commute or anti-commute with parity operator P_z.

The time-dependent spin correlation function that commute with P_z can be evaluated directly. I just limit the description to the characteristic examples of the time-dependent spin correlation functions that enter in the reduced density matrix of two spin at a distance $r = 1$

$$\begin{aligned}
\langle \sigma_i^z \rangle_t &= -g_0(\{\lambda_0, \lambda_1\}, t) \\
\langle \sigma_i^z \sigma_{i+1}^z \rangle_t &= g_0(\{\lambda_0, \lambda_1\}, t)^2 - f_{-1}(\{\lambda_0, \lambda_1\}, t)^2 \\
&- g_{-1}(\{\lambda_0, \lambda_1\}, t)\, g_1(\{\lambda_0, \lambda_1\}, t) \\
\langle \sigma_i^x \sigma_{i+1}^y \rangle_t &= i\, f_{-1}(\{\lambda_0, \lambda_1\}, t) \\
\langle \sigma_i^x \sigma_{i+1}^x \rangle_t &= g_{-1}(\{\lambda_0, \lambda_1\}, t) \\
\langle \sigma_i^y \sigma_{i+1}^y \rangle_t &= g_1(\{\lambda_0, \lambda_1\}, t)
\end{aligned} \tag{2.60}$$

Fermionic correlation functions that are identically zero in the stationary case become different from zero for $t > 0$. In Eq. (2.60), it is pointed out the case of $\langle \sigma_i^x \sigma_{i+1}^y \rangle_t$, and the fact that in the expression of $\langle \sigma_i^z \sigma_{i+1}^z \rangle_t$ appears the term $f_{-1}(\{\lambda_0, \lambda_1\}, t)$, identically zero in the stationary case.

Unfortunately, to evaluate the time-dependent correlation functions associated to spin operators $\hat{O}_S^{\{\mu_i\}}$ that do not commute with P_z, one needs to use the same trick discussed in Sec. (2.2), for which

$$\langle \hat{O}_S^{\{\mu_i\}} \rangle_t = \sqrt{\lim_{R \to \infty} \langle W_{S \cup S+R}^{\{\mu_i\}} \rangle_t} \tag{2.61}$$

The expectation value in the r.h.s. of Eq. (2.61) can be evaluated by making use of the Pfaffians, that at $t = 0$ and $t \to \infty$ reduce to the standard determinant [10]. Usually, with the exception of some particular case at $t = 0$ or $t \to \infty$, in which one can use the Szegö theorem ([119]), it is not possible to evaluate analytically the limit of diverging R of the Pfaffians and one is forced to make use of numerical evaluation.

3
Classical nature of ordered phases and origin of spontaneous symmetry breaking

In this chapter, I test the conjecture for which, among the locally inequivalent ground states of the symmetry-breaking ordered phases, the maximally symmetry-breaking ground states (MSBGSs) are the most classical ones, thus selected in real-world situations. I make the conjecture quantitatively precise by proving that the MSBGSs are the most classical ones with respect to three criteria of classicality:

- *Quantum correlations* – For all pairs of dynamical variables (e.g. spins) the MSBGSs are the only ground states that minimize pairwise quantum correlations, as measured by the quantum discord. Moreover, they are the only ground states whose pairwise quantum discord vanishes asymptotically as a function of the intra-pair distance;

- *Local convertibility* – All ground states are locally convertible into MSBGSs via local operations and classical communication (LOCC), while the reverse transformation is impossible;

- *Entanglement distribution* – The MSBGSs are the only ground states that minimize the residual tangle between a dynamical variable and the rest of the system, i.e. the only ground states that satisfy monogamy of entanglement, a quantum constraint on distributed correlations with no classical counterpart, at its minimum.

These three features imply that the mechanism of the spontaneous symmetry-breaking selects the most classical ground states associated to ordered phases of quantum matter.

As standard prototype, I investigate the XY models in a transverse magnetic field [113, 10], which Hamiltonian $H^{XY}_{\{\gamma,h\}}$ I analized in chapter (2), obtaining

results of general validity for all systems that belong in the same universality class.

3.1 Pairwise quantum correlations

In this section, I analyze the behavior of one-way discord-type correlations and entanglement between any two spins, for symmetry-preserving and maximally symmetry-breaking ground states. Operationally, one-way discord-type correlations are defined in terms of the distance with respect to the *classical-quantum states*, i.e. quantum states that are invariant under the action of non trivial local unitary operations. In geometric terms, a *bona fide* measure of quantum correlations must quantify how much a quantum state *discords* from classical-quantum states and must be invariant under the action of all local unitary operations. A computable and operationally well defined geometric measure of quantum correlations is the *discord of response* [109, 50]. The pairwise discord of response Q_r for a two-spin reduced density matrix is defined as:

$$Q_r(\rho_{ij}^{(r)}(u,v)) \equiv \frac{1}{2}\min_{U_i} d_x\left(\rho_{ij}^{(r)}(u,v), \tilde{\rho}_{ij}^{(r)}(u,v)\right)^2, \tag{3.1}$$

where $\rho_{ij}^{(r)}(u,v)$ is the state of two spins i and j at a distance r, with arbitrary amplitudes as pointed out in Sec. (2.3), $\tilde{\rho}_{ij}^{(r)}(u,v) \equiv U_i \rho_{ij}^{(r)}(u,v) U_i^\dagger$ is the two-spin state transformed under the action of a local unitary operation U_i acting on spin i, and d_x is any well-behaved, contractive distance (e.g. Bures, trace, Hellinger) of $\rho_{ij}^{(r)}$ from the set of locally unitarily perturbed states, realized by the least-perturbing operation in the set. The trivial case of the identity is excluded by considering only unitary operations with *harmonic* spectrum, i.e. the fully non-degenerate spectrum on the unit circle with equispaced eigenvalues.

For pure states the discord of response reduces to an entanglement monotone, whose convex-roof extension to mixed states is the so-called *entanglement of response* E_r [48, 91, 41]. Therefore, the entanglement and the discord of response quantify different aspects of bipartite quantum correlations, via two different uses of local unitary operations. The discord of response arises by applying local unitaries directly to the generally mixed state, while the entanglement of response stems from the application of local unitaries to pure states. By virtue of their common origin, it is thus possible to perform a direct comparison between these two quantities.

In terms of the trace distance, which will be relevant in the following, the two-body entanglement of response is simply given by the squared concurrence [128, 109], whereas the two-body discord of response relates nicely to the trace

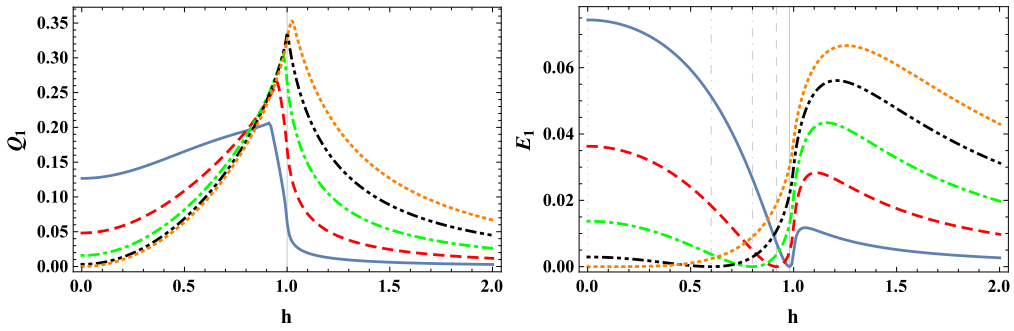

Figure 3.1: (Color online) Behavior of the nearest-neighbor trace distance-based discord of response Q_1 (left panel) and nearest-neighbor trace distance-based entanglement of response E_1 (right panel) for symmetry-preserving ground states, as functions of the external field h, and for different values of the anisotropy γ. Solid blue curve: $\gamma = 0.2$; dashed red curve: $\gamma = 0.4$; dot-dashed green curve: $\gamma = 0.6$; double-dot-dashed black curve: $\gamma = 0.8$; dotted orange curve: $\gamma = 1$. In the right panel, to each curve, there corresponds a vertical line denoting the associated factorizing field h_f. In the left panel, the solid vertical line denotes the critical field $h_c = 1$.

distance-based geometric discord [93], whose closed formula is known only for a particular class of two-body states [29], although it can be computed for a more general class of two-qubit states through a very efficient numerical optimization.

3.1.1 Symmetry-preserving ground states

I first compare the two-body entanglement of response E_r and the two-body discord of response Q_r in symmetry-preserving ground states. In Fig. (3.1) I plot these two quantities, for two neighboring spins ($r = 1$), as functions of the external field h and for different values of the anisotropy γ. By fixing an intermediate value of γ, E_1 and Q_1 exhibit very different behaviors. E_1 features two maxima at $h = 0$ and a $h > h_c$ and two minima at $h = h_c$ (factorization point) and $h \to \infty$ (saturation). On the contrary, Q_1 always features a single maximum, that can be either in the ordered phase ($h < h_c$) or in the paramagnetic one ($h > h_c$), depending on γ, and disappears for $h \to \infty$. Indeed, at the factorizing field $h = h_f$ and for any $\gamma \neq 0, 1$, the symmetry-preserving ground state is not completely factorized but rather is a coherent superposition of the two completely factorized symmetry-breaking ground states. Consequently, while the two-body entanglement of response must vanish in accordance with the convex roof extension, the two-body discord of response remains always finite.

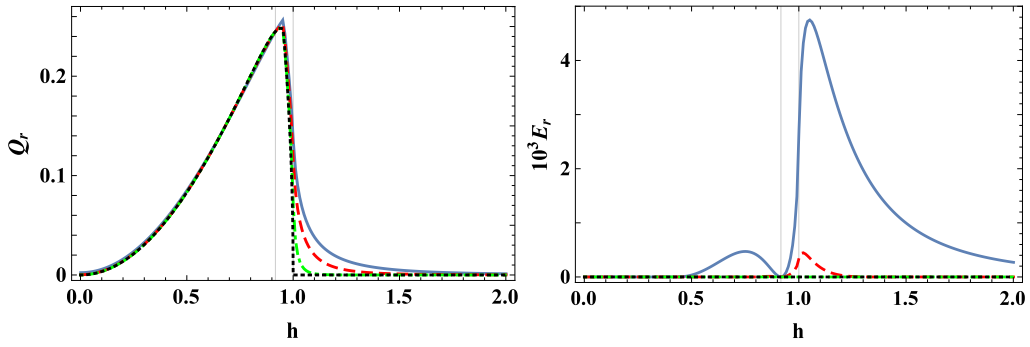

Figure 3.2: (Color online) Behavior of the two-body trace distance-based discord of response Q_r (left panel) and two-body trace distance-based entanglement of response E_r (right panel) for symmetry-preserving ground states, in the thermodynamic limit, as functions of the external field h, in the case of $\gamma = 0.4$, for different inter-spin distances r. Solid blue curve: $r = 2$; dashed red curve: $r = 3$; dot-dashed green curve: $r = 8$; dotted black curve: $r = \infty$. In both panels, the two solid vertical lines correspond, respectively, to the factorizing field (left) and to the critical field (right).

Moreover, in Fig. (3.2) I plot the bahavior of E_r and Q_r for different inter-spins distances r, as a function of the external field and for a fixed value of $\gamma = 0.4$. Due to the monogamy of the squared concurrence [30, 98], E_r dramatically drops to zero as r increases, in agreement with Ref. [3]. On the contrary, while in the disordered and critical phases Q_r vanishes as r increases, in the ordered phase Q_r remains diferent from zero, even in the limit of infinite r. Indeed, in both the disordered and critical phases, the only non-vanishing spin correlation functions are $\langle \sigma_i^z \rangle$ and $\langle \sigma_i^z \sigma_{i+r}^z \rangle$, so that the two-body reduced state can be written as a classical mixture of eigenvectors of $\sigma_i^z \sigma_{i+r}^z$. In the ordered phase, also the two-body correlation function $\langle \sigma_i^x \sigma_{i+r}^x \rangle$ appears, thus preventing the two-body ground state from being a mixture of classical states.

3.1.2 Maximally symmetry-breaking ground states

In this section, I compare the two-body entanglement of response and discord of response for maximally symmetry-breaking ground states.

In Fig. (3.3), I plot E_1 and Q_1 for two neighboring spins, as a funtion of the external field and for different values of the anisotropy γ. It is evident that only the two-body discord of response is affected by the symmetry-breaking. In fact, according to Ref. [100], the concurrence and, consequently, the two-body entanglement of response, attains the same value for any $h \geq h_f$ both in the

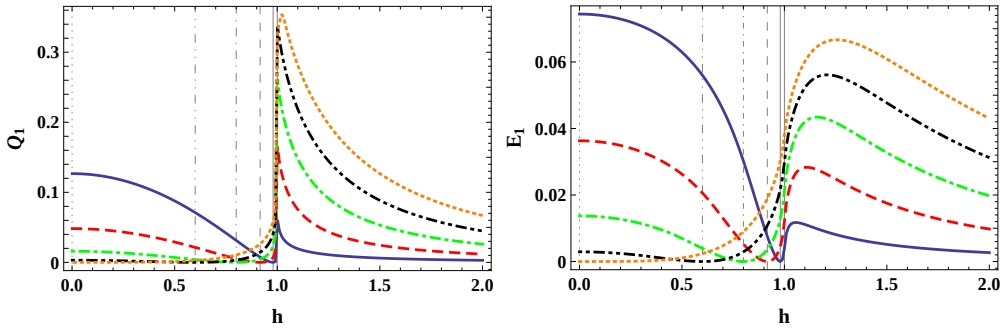

Figure 3.3: (Color online) Behavior of the nearest-neighbor trace distance-based discord of response Q_1 (left panel) and nearest-neighbor trace distance-based entanglement of response E_1 (right panel) for maximally symmetry-breaking ground states, as functions of the external field h and for different values of the anisotropy γ. Solid blue curve: $\gamma = 0.2$; dashed red curve: $\gamma = 0.4$; dot-dashed green curve: $\gamma = 0.6$; double-dot-dashed black curve: $\gamma = 0.8$; dotted orange curve: $\gamma = 1$. In both panels, to each curve there corresponds a vertical line denoting the associated factorizing field h_f. The rightmost vertical line denotes the critical field $h_c = 1$.

symmetry-preserving and the symmetry-breaking ground states. Otherwise, if $h < h_f$, there is a slight enhancement in the pairwise entanglement of response in the symmetry-breaking ground states compared to the corresponding symmetry-preserving ones. On the contrary, the two-body discord of response undergoes a dramatic suppression in the entire ordered phase $h < h_c$, when moving from symmetry-preserving to symmetry-breaking ground states.

Moreover, in Fig. (3.4), I plot the behavior of E_r and Q_r for different inter-spins distances r, as a function of the external field and for a fixed value of $\gamma = 0.4$. Moving from symmetry-preserving to maximally symmetry-breaking ground states, both the two-body entanglement of response and the two-body discord of response vanish asymptotically with increasing inter-spin distance r. The behavior of the two-body entanglement of response is again due to the monogamy of the squared concurrence [30, 98]. The bahavior of the two-body discord of response, instead, is due to the fact that also $\langle \sigma_i^x \rangle$ and $\langle \sigma_i^x \sigma_{i+r}^z \rangle$ are nonvanishing in the limit of infinite inter-spin distance r. This feature allows to write any two-spin reduced density matrix obtained from the symmetry-breaking ground states as a classical mixture of eigenvectors of $O_i O_{i+r}$, where O_i is an Hermitian operator defined on the i-th site as $O_i = \cos\beta\sigma_i^z + \sin\beta\sigma_i^x$, with $\tan\beta = \frac{\langle \sigma_i^x \rangle}{\langle \sigma_i^z \rangle}$.

It can be concluded that the pairwise quantum correlations between any two

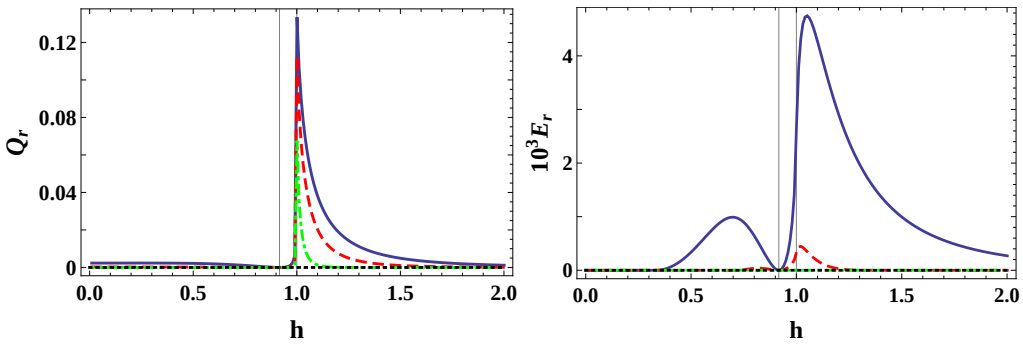

Figure 3.4: (Color online) Behavior of the two-body trace distance-based discord of response Q_r (left panel) and two-body trace distance-based entanglement of response E_r (right panel) for maximally symmetry-breaking ground states, as functions of the external field h, for $\gamma = 0.4$ and for different inter-spin distances r. Solid blue curve: $r = 2$; dashed red curve: $r = 3$; dot-dashed green curve: $r = 8$; dotted black curve: $r = \infty$. In both panels, the two solid vertical lines correspond, respectively, to the factorizing field (left) and to the critical field (right).

spins, as quantified by the two-body discord of response and two-body entanglement, decreases significantly in the entire ordered phase, when symmetry breaking is taken into account. In particular, these two-body correlations measures are minimized and disappear in the limit of infinite intra-pairs distance r only for maxymally symmetry-breaking ground states. Thus, the MSBGSs are the only ground states that satisfy the first criterion of classicality.

3.2 Global properties of quantum correlations

I now investigate the nature of quantum ground states in the ordered phase, with respect to the properties of local convertibility and entanglement distribution.

3.2.1 Local convertibility

In general, given two pure bipartite quantum states, $|\psi_1\rangle$ and $|\psi_2\rangle$, one says that $|\psi_1\rangle$ is locally convertible into $|\psi_2\rangle$, if $|\psi_1\rangle$ can be transformed into $|\psi_2\rangle$ by using only local quantum operations and classical communication (LOCC), and the aid of an ancillary entangled system [71, 72].

This concept of local convertibility can be formalized in terms of the entire hierarchy of the Rényi entanglement entropies $S_\alpha(\rho_A) = \frac{1}{1-\alpha}\log_2\left[Tr(\rho_A^\alpha)\right]$ of

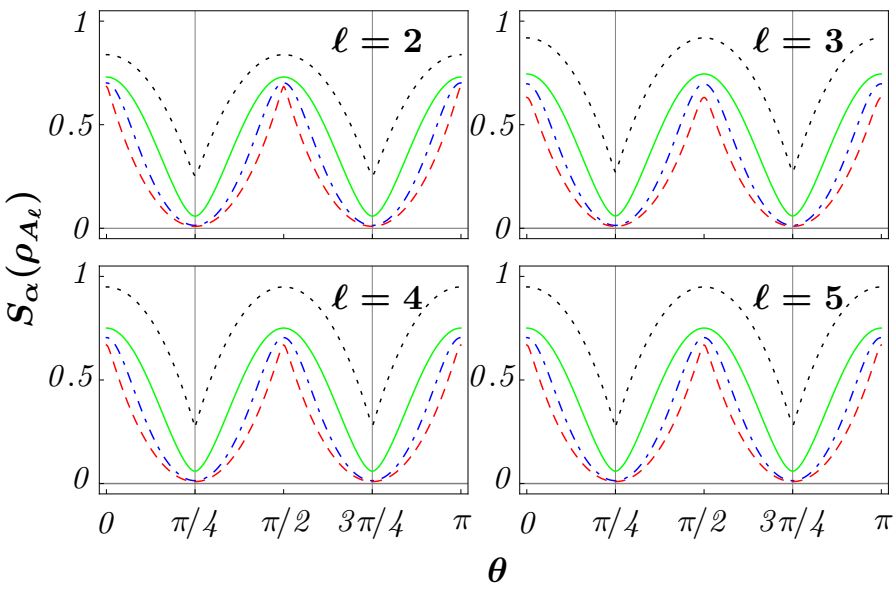

Figure 3.5: (Color online) Behavior of the Rényi entropies $S_\alpha(\rho_A)$ as functions of the different ground states in the ordered phase $h < h_c$, for a subsystem A_ℓ made of ℓ contiguous spins. Each line stands for a different value of α. Black dotted line: $\alpha = 0.5$. Green solid line: $\alpha \to 1^+$ (von Neumann entropy). Blue dot-dashed line: $\alpha = 3$. Red dashed line: $\alpha \to \infty$. The different ground states are parameterized by the superposition amplitudes $u = \cos(\theta)$ and $v = \sin(\theta)$. The two vertical lines correspond to the two MSBGSs, respectively obtained for $\theta = \pi/4$ and $\theta = 3\pi/4$. The Hamiltonian parameters are set at the intermediate values $\gamma = 0.5$ and $h = 0.5$.

the reduced density operator ρ_A of a subsystem A, which provides a complete characterization of the entanglement spectrum and its scaling behavior in different quantum phases [49]. The necessary and sufficient condition for a bipartite state $|\psi_1\rangle$ to be locally convertible into another state $|\psi_2\rangle$ is that the inequality $S_\alpha(\psi_1) \geq S_\alpha(\psi_2)$ holds for all bipartitions and for all $\alpha > 0$ [122]. Local convertibility has been recently applied to the characterization of topological ordered phases and to the computational power of different quantum phases [56, 33, 32].

It was previously shown that symmetric ground states are always locally convertible among themselves for $h_f < h < h_c$, and never for $h < h_f < h_c$ [49]. Here, I extend the results, by investigating the local convertibility property of *all* quantum ground states in the ordered phase. In Fig. (3.5), I report the behavior of the Rényi entropies S_α, as functions of the different ground states and for a subsystem A made of ℓ contiguous spins, while in Fig. (3.6) I report it for a

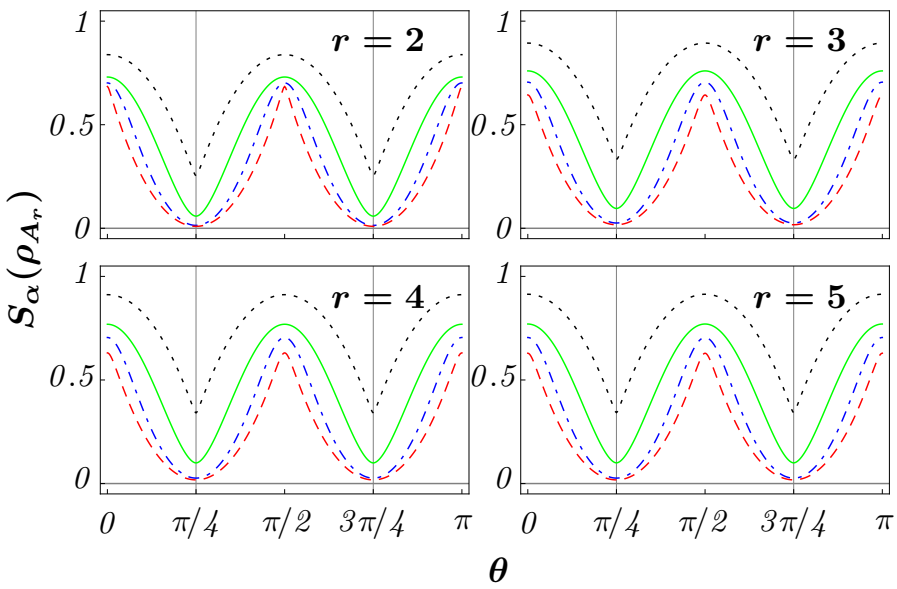

Figure 3.6: (Color online) Behavior of the Rényi entropies $S_\alpha(\rho_A)$ as functions of the different ground states in the ordered phase $h < h_c$, for a subsystem A_r made by two spins and for different inter-spin distances r. Each line stands for a different value of α. Black dotted line: $\alpha = 0.5$. Green solid line: $\alpha \to 1^+$ (von Neumann entropy). Blue dot-dashed line: $\alpha = 3$. Red dashed line: $\alpha \to \infty$. The different ground states are parameterized by the superposition amplitudes $u = \cos(\theta)$ and $v = \sin(\theta)$. The two vertical lines correspond to the two MSBGSs, respectively obtained for $\theta = \pi/4$ and $\theta = 3\pi/4$. The Hamiltonian parameters are set at the intermediate values $\gamma = 0.5$ and $h = 0.5$.

subsystem A made of two spins and for various inter-spin distances r.

It can be observed that the MSBGSs are characterized by the smallest value of all Rényi entropies, independently of the size ℓ of the subsystem A and of the inter-spin distance r. Therefore, all different ground states are always locally convertible to a MSBGS, while the opposite is impossible. Thus, the MSBGSs are the only ground states that satisfy the second quantitative criterion of classicality.

3.2.2 Entanglement distribution

I now compare symmetry-breaking and symmetry-preserving ground states with respect to entanglement distribution. The monogamy inequality imposes how bipartite entanglement may be distributed among many parties [30, 98].

For a given system of N spins-1/2 it reads:

$$\tau(i|N-1) \geq \sum_{j=1}^{N-1} \tau(i|j) \quad j \neq i, \quad \forall\, i\,. \tag{3.2}$$

In the above expression, $\tau = C^2$ is known as the tangle, where C is the concurrence [62, 128]. The l.h.s. quantifies the bipartite entanglement between one particular reference spin i, arbitrarily chosen in the system, and all the remaining $N-1$ spins. The r.h.s. is the sum of all the pairwise entanglements between the reference spin and each of the remaining $N-1$ spins. The inequality implies that entanglement cannot be freely distributed among multiple quantum parties $N \geq 3$.

The residual tangle $\tilde{\tau}$ is the positive semi-definite difference between the l.h.s and the r.h.s in Eq. (3.2). It measures the amount of entanglement not quantifiable as elementary bipartite spin-spin entanglement. Its minimum value, compatible with monogamy, provides yet another quantitative criterion for classicality.

In the XY models, since the expectation value of σ_i^y vanishes on each element of the ground space, the expressions of the tangle τ and the residual tangle $\tilde{\tau}$ for any arbitrarily chosen spin in the chain respectively read

$$\tau = 1 - m_z^2 - (u^* v + v^* u)^2 m_x^2\,, \tag{3.3}$$

$$\tilde{\tau} = \tau - 2\sum_{r=1}^{\infty} C_r^2(u,v) \geq 0\,, \tag{3.4}$$

where $m_z = \langle e|\sigma_i^z|e\rangle = \langle o|\sigma_i^z|o\rangle$ is the on-site magnetization along z, $m_x = \langle e|\sigma_i^x|o\rangle = \sqrt{\lim_{r\to\infty}\langle e|\sigma_i^x\sigma_{i+r}^x|e\rangle}$ is the order parameter, and $C_r(u,v)$ stands for the concurrence between two spins at a distance r, for an arbitrary ground state $|g(u,v)\rangle$, Eq. (2.36).

By comparing all ground states (symmetric, partially symmetry-breaking, maximally symmetry-breaking), if $h < h_f < h_c$ the spin-spin concurrences are maximum in the MSBGSs [100]. If $h_f < h < h_c$, they are equal on each ground state, because they do not depend on the superposition amplitudes u and v. It immediately follows that the sum in the r.h. of Eq. (3.4) is maximized by the MSBGSs, i.e. the residual tangle is minimized by the MSBGSs. Therefore, the MSBGSs are the only ones that satisfy the third quantitative criterion of classicality.

4
Quench of a symmetry-breaking ground state

In this chapter, I analyze how evolves the distinguishability between locally inequivalent ground states, i.e. ground states that differ for expectation values of some local physical observable defined on a finite subset, after a quench of the Hamiltonian parameters. It has been observed, in chapter (3), that, among locally distinguishable ground states, the MSBGSs are the most classical ones and thus the only ones selected in real-world situations. It is therefore natural to wonder if the image of an integrable system, that starts in one of its distinguishable ground states of a symmetry-breaking ordered phase, after a sudden change of the Hamiltonian parameters, still preserves any information about the particular initial ground state. I introduce a way to quantify the local distinguishability in terms of the trace distance between reduced density matrices, obtained projecting on the same subset different ground states, and I prove that, for several integrable models, with different classes of symmetry, the local distinguishability exponentially disappears in time [51].

4.1 A quantitative approach to the distinguishability

In this section, I provide a quantitative approach to the distinguishability between two different ground states, in a symmetry-breaking ordered phase. I consider the XY models in a transverse magnetic field and the N-cluster Ising models, one dimensional systems of spin-1/2, described by the translational invariant Hamiltonians $H^{XY}_{\{\gamma,h\}}$ and $H^{cI}_{\{\phi\}}$ of Eqs. (2.1) and (2.2) respectively, that satisfy the parity symmetry respect to a spin direction, regardless the values of the Hamiltonian parameters $\{\lambda\}$.

The reduced density matrix $\rho(u, v, S)$, obtained projecting a generic ground state in a generic finite subset S, according with Sec. (2.3), is the tool to deal with the problem of the local distinguishability. For a block S made by L spins

($S = \{i_1, \cdots, i_L\}$), it can be expressed as the sum of a symmetric part $\rho^{sym}(S)$, i.e. the reduced density matrix obtained from the even $|e_{\{\lambda\}}\rangle$ or the odd $|o_{\{\lambda\}}\rangle$ ground states, that commute with the parity operator, and a traceless matrix $\tilde{\chi}(S)$, that includes all the symmetry-breaking correlation functions, i.e. all the terms that are nonvanishing only in presence of a symmetry-breaking, as in Eq. (2.41)

$$\rho(u, v, S) = \rho^{sym}(S) + (u^* v + v^* u)\tilde{\chi}(S) \tag{4.1}$$

Two state are locally distinguishable if there exist a finite subset S for which the two reduced density matrices are different. Hence, a quantity measure of the distance between two reduced density matrices, it is also a measure of their distinguishability. For sake of simplicity, I work with the trace distance [94] that allows to simplify our analysis. From the definition, the maximum distance between two reduced density matrices is reached when the two states are the symmetric ground state and the maximally symmetry-breaking ground state respectively. Named $\rho^{max}(S)$ the reduced density matrix obtained projecting the maximally symmetry-breaking ground state on S ($u = v = 1/\sqrt{2}$)

$$\rho^{max}(S) = \rho^{sym}(S) + \tilde{\chi}(S) \tag{4.2}$$

and D_S the maximum of the local distinguishability

$$D_S = \|\rho^{max}(S) - \rho^{sym}(S)\| \tag{4.3}$$

it follows that

$$D_S = \frac{1}{2}\sum_{i=1}^{2^L} |\nu_i| \tag{4.4}$$

where the $\{\nu_i\}$ is the set of the eigenvalues of the traceless matrix $\tilde{\chi}(S)$, that are functions of the symmetry-breaking spin correlation functions with support in S.

In static conditions, for a system in a magnetically ordered phase, D_S is always different from zero, because there exist a magnetic order parameter, regardless the choice of S. For other kind of orders, as the nematic one [78, 47], in which the symmetry-breaking order parameter has a support greater than one single spin, D_S is different from zero or not depending on the fact that S has a dimension comparable with the order parameter or not.

What happens when one introduces the time dependence? The results can be easily generalized to the time dependent situations, for which the evolution is due to a sudden quench of the Hamiltonian parameters $\{\lambda\}$, from $\{\lambda_0\}$ to $\{\lambda_1\}$. In such cases $H_{\{\lambda_0\}}$, $H_{\{\lambda_1\}}$ and also the time-evolution unitary operator

$U_{\{\lambda_1\}} = \exp(-\imath H_{\{\lambda_1\}} t)$ will commute with the parity. This implies that the time evolution induced by $U_{\{\lambda_1\}}$ does not change the superposition coefficient in Eq. (2.36). Therefore, to evaluate the time dependent distance between the two reduced density matrices, it is enough to determine the set of the eigenvalues of time-dependent traceless matrix $\tilde{\chi}(S,t)$. Hence, one can generalized the maximum of the distinguishability of Eq. (4.4) to the dynamic case $D_S(t)$ as

$$D_S(t) = \frac{1}{2}\sum_{i=1}^{2^l} |\nu_i(t)| \tag{4.5}$$

where $\nu_i(t)$ are the time dependent eigenvalues of $\tilde{\chi}(S,t)$, defined as

$$\tilde{\chi}(S,t) = \rho^{max}(S,t) - \rho^{sym}(S,t) \tag{4.6}$$

In Eq. (4.6), $\rho^{\max}(S,t)$ and $\rho^{sym}(S,t)$ are the straightforward generalization to the dynamic case of the reduced density matrices $\rho^{max}(S)$ and $\rho^{sym}(S)$.

4.2 Numerical results for the XY model

In this section, I apply the quantitative approach to local distinguishability described in the previous section to the XY model in a transverse magnetic field, the well known one-dimensional spin-1/2 model described by the Hamiltonian $H^{XY}_{\{\gamma,h\}}$ of Eq. (2.1)

$$H^{XY}_{\{\gamma,h\}} = -\frac{1+\gamma}{2}\sum_j \sigma^x_j \sigma^x_{j+1} - \frac{1-\gamma}{2}\sum_j \sigma^y_j \sigma^y_{j+1} - h\sum_j \sigma^z_j \tag{4.7}$$

where the two Hamiltonian parameters are respectively the anisotropy γ and the transverse external field h.

The XY models satisfy the hypothesis considered in the previous section, i.e. the Hamiltonian in eq. (4.7) always commutes with the parity operator along z direction, $P_z = \bigotimes_i \sigma^z_i$, and it shows a magnetically ordered phase for $\gamma \in (0,1]$ and $h < h_c \equiv 1$ [113, 10], in which the parity symmetry is broken by an order parameter equal to

$$\langle \sigma^x_i \rangle = \frac{[\gamma^2(1-h^2)]^{1/8}}{[2(1+\gamma)]^{1/2}} \,. \tag{4.8}$$

The order parameter $\langle \sigma^x_i \rangle$ never vanishes in the magnetically ordered phase, regardless the choice of S. Consequently, the maximum of the distinguishability in the static condition D_S never vanishes. On the contrary, for the dynamic situation there is no closed formula. However, by applying the methods described

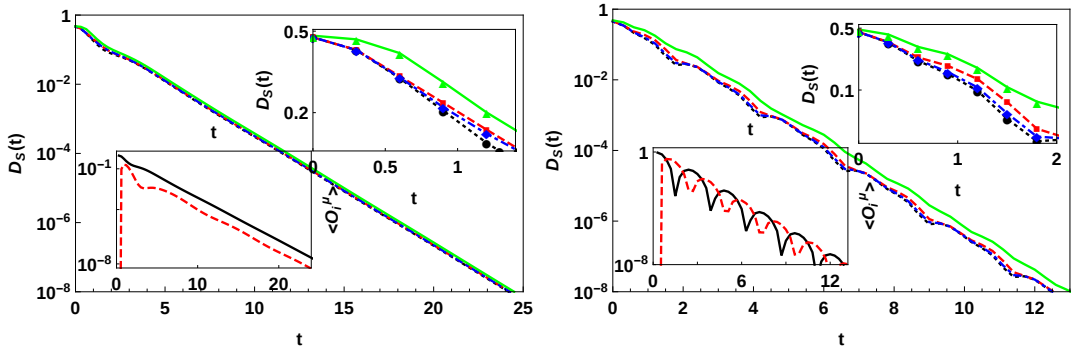

Figure 4.1: (Color online) Behavior of the time-dependent distinguishability for two different sudden quenches of the Hamiltonian parameter for the XY model. Fixing the anisotropy $\gamma = 0.5$, in the left panel I report the results for the external field quenched from $h_0 = 0.2$ to $h_1 = 0.8$, while in the right panel, the external field is quenched from $h_0 = 0.4$ to $h_1 = 1.2$. In both cases, in the main plot one can observe the behavior of the maximal distinguishability $D_S(t)$ as a function of the time t, for subsystem S made by one single spin (Black dotted line), two neighbors spins (Blue dot-dashed line), two next neighbor spins (Red dashed line) and three spins (Green lines). In the inset at the top right, it is plotted a zoom of the main inset for very short times, in which the transient is highlighted. In the inset at the bottom left, it is plotted the behavior of the absolute value of the magnetizations $\langle \sigma_i^x \rangle$ along the x (Black line) and $\langle \sigma_i^y \rangle$ along the y (Red line) axes respectively.

in the Sec. (2.4), it can be derived the behavior of $D_S(t)$, as a function of time, for several choice of initial and final Hamiltonian parameters. In Fig. (4.1) I plot $D_S(t)$ for a fixed value of the anisotropy γ and for two quenches of the external field $h_0 = 0.2$, $h_1 = 0.8$ and $h_0 = 0.4$, $h_1 = 1.2$ in the left and right panels respectively. After a short transient, in which the maximum of the time-dependent local distinguishability can increase with respect to the static case, $D_S(t)$ shows an exponential decay $e^{-t/\tau}$, which a common time scale τ. The presence, duration and relevance of the transient depend on the difference between the initial and final sets of the Hamiltonian parameters and on the choice of S: it becomes more and more relevant as the size of S increase and the distance between the initial and final Hamiltonian parameters decreases. The time scale τ, instead, does not depend on S but depends on the parameters of the system before and after the quench:it increases as the two sets become closer and closer. As en example, in Fig. (4.2) I report the behavior of the time scale τ as function of the external field h_1, in the XY model, for several sets of the initial parameters $\gamma_0 = \gamma_1$ and h_0.

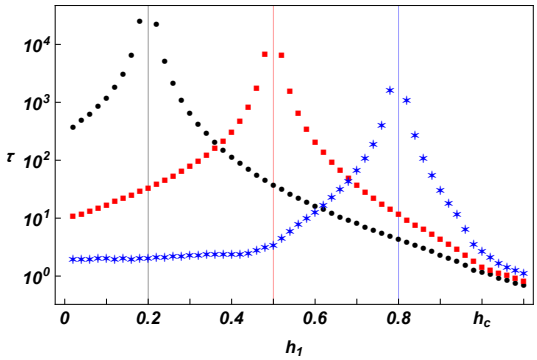

Figure 4.2: (Color online) Behavior of time scale τ, as a function of the final external field h_1, in the XY models, for several sets of the initial parameters and for different quenches that involve only the external field. Black circles represent the case in which $\gamma_0 = \gamma_1 = 0.8$ and the initial value of the external field is $h_0 = 0.2$; red squares stand for the case in which $\gamma_0 = \gamma_1 = 0.5$ and $h_0 = 0.5$; blue stars represent the case in which $\gamma_0 = \gamma_1 = 0.2$ and $h_0 = 0.8$.

The exponential decay of $D_S(t)$ is a consequence of the exponential decay that characterizes all the symmetry-breaking correlation functions with support included in S. In the bottom left insets of Fig. (4.1), I plotted some of these correlation functions, It is evident that the time evolution induced by a sudden quench of the Hamiltonian parameters forces a magnetization along y direction that in the static condition is equal to zero and that vanishes in the limit of large times. A similar behavior is also shared by all the other symmetry-breaking correlation functions, that in the static condition vanish, and also by the correlation functions which operators commute with the parity, that in static condition vanish and that in the steady state disappear with a behavior slower than an exponential one. This fact immediately implies that, regardless the choice of S, the steady state, realized in the limit of diverging time, has no memory about the superposition of the initial ground states, i.e. for any subset S, the reduced density matrix of the steady state $\rho(u, v, S, t \to \infty)$ holds the same symmetries of the reduced density matrix obtained from the symmetric ground state in the stationary condition $\rho^{sym}(S)$.

However, the two states show very different physical properties, due to the disappearance of the order parameter and the associated long range order. The most relevant example of such differences is the value of the mutual information between two macroscopically separated spins. In fact, it is known [57] that the symmetric ground states in a ferromagnetic phase are characterized by a non vanishing mutual information between two very far spins, associated to the presence of a non zero order parameter m_x

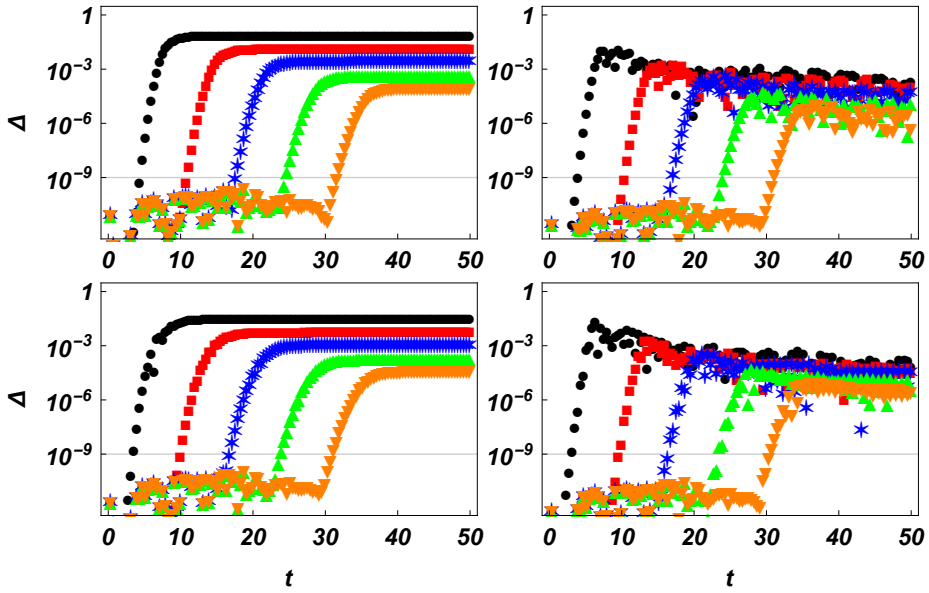

Figure 4.3: (Color online) Behavior of the absolute values of the differences Δ for four symmetry-breaking correlation functions, obtained choosing $R_{MAX} = R + \Delta R$ and $R_{MAX} = R$, as function of time, for a fixed set of the Hamiltonian parameters $\gamma = 0.8$, $h_0 = 0.2$ and $h_1 = 0.8$. I have arbitrarily chosen $\Delta R = 10$. The different curves stands for: black circles (left-most curve) $R = 20$; red squares $R = 40$; blue stars $R = 60$; green upward triangles $R = 80$; orange downward triangles (right-most curve) $R = 100$; From the top left ,in the clockwise order, I have plotted the difference for the following correlation functions $\langle \sigma_i^x \rangle$, $\langle \sigma_i^y \rangle$, $\langle \sigma_i^y \sigma_{i+1}^z \rangle$ and $\langle \sigma_i^x \sigma_{i+1}^z \rangle$. The lines at 10^{-9} indicate the computational noise upper limit at which the differences become significant.

$$\mathcal{I}_2(\infty) \;=\; \log_2 \left[1 + \frac{m_x^4 (1 - (uv^* + vu^*)^4)}{(1 + m_z^2 + m_x^2 (uv^* + vu^*)^2)^2} \right] \tag{4.9}$$

However, after the quench, all the correlation functions that break the parity symmetry, including also the order parameter m_x, go rapidly to zero, implying the disappearance of the mutual information. This represent a further proof of the fragility of the states with global entanglement, detected by the persistence of a non vanishing mutual information in the limit of large distance between the spins [57].

I want to point out that the expectation values of the operators that anti-commutes with P_z, i.e. $\langle \hat{O}_S^{\{\mu_i\}} \rangle_t = \sqrt{\lim_{R\to\infty} \langle W_{S\cup S+R}^{\{\mu_i\}} \rangle_t}$, cannot be evaluated

analytically, with the exception of some particular case at $t = 0$ or $t \to \infty$, in which one can use the Szegö [119] theorem, as pointed out in Sec. (2.4) This forces to make numerical evaluations, that limits the use of a value of R, named R_{MAX}, large but finite. In which limit this approximation is valid? In Fig. (4.3), I report the differences between evaluations of four symmetry-breaking correlation functions, made with two different R_{MAX} (R_{MAX} and $R_{MAX} + \Delta R$ with $\Delta R = 10$), for the XY models. If the difference is greater than the computational noise, set arbitrarly to 10^{-9}, the estimation of $\langle \hat{O}_A^{\{\mu_i\}} \rangle$ with that $R = R_{MAX}$ is not accurate. All the curves have a very similar pattern. Up to a certain time $t^*(R_{MAX})$, that grows with the increase of R_{MAX}, the difference is comparable with the computational noise. When t becomes greater than $t^*(R_{MAX})$, it can be observed a coherent increment of the difference, that saturates to a small threshold value, but nonetheless significant and not negligible with workable value of R_{MAX}. For this reason, all the results showed in the main text are obtained considering t always less that $t^*(R_{MAX})$.

4.3 Numerical results for the N-cluster Ising models

In the previous section, in the framework of the XY models, I proved that the maximum of the local distinguishability, after a sudden quench of the Hamiltonian parameters, goes to zero exponentially in time, regardless the particular choice of the initial and final set of Hamiltonian parameters, and of the subset S. As a consequence, in the limit of very large time, the system loses completely any information about the particular initial ground state. The question that naturally arises is: how general is this picture?

In the attempt to provide an answer to this question, I extend the analysis to different models with a symmetry-breaking ordered phase, the well known N-cluster Ising models [118, 46, 47], described by the Hamiltonian $H^{cI}_{\{\phi\}}$ of Eq. (2.2)

$$H^{cI}_{\{\phi\}} = -\cos(\phi) \sum_j \sigma^x_j Z^N_j \sigma^x_{j+N+1} + \sin(\phi) \sum_j \sigma^y_j \sigma^y_{j+1} \tag{4.10}$$

where ϕ is the phase parameter, that controls the relative weight of the cluster and Ising interaction terms and $Z^N_i = \bigotimes_{k=1}^N \sigma^z_{i+k}$

This family of models is relevant for the analysis, because it includes different Hamiltonians that fall into different classes of symmetry, that are not violated in the symmetry-breaking ground states, with the only exception of the parity along the z direction, with an order parameter for $\phi > \phi_c = \pi/4$ equal to

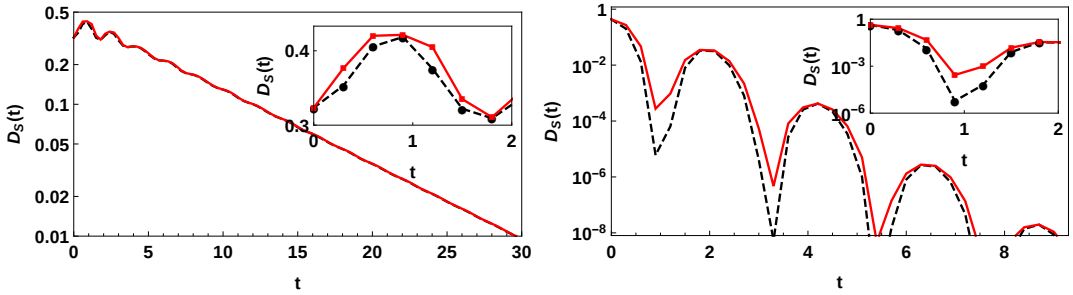

Figure 4.4: (Color online) Behavior of the time-dependent distinguishability for two different sudden quenches of the Hamiltonian parameters for the N-cluster Ising models, with $N = 1$. In the left panel, I report the results for the phase parameter ϕ quenched from $\phi_0 = \frac{5}{16}\pi$ to $\phi_1 = \frac{7}{16}\pi$, while in the right panel, ϕ is quenched from $\phi_0 = \frac{3}{8}\pi$ to $\phi_1 = \frac{1}{8}\pi$. In both cases, in the main plot one can see the behavior of the maximum of the distinguishability $D_S(t)$ as a function of the time t, for subsystem S made by one single spin, two neighbors spins and two next neighbor spins (Black dotted line), and three spins (Red solid line). In the inset, it is plotted a zoom of the main inset for very short times, in which the transient is highlighted.

$$(-1)^i \langle \sigma_i^y \rangle = \left(1 - \tan(\phi)^{-2}\right)^{\frac{N+2}{8}} \tag{4.11}$$

I extend to these models the same analysis made for the XY models in the previous section. In Fig. (4.4), I plot the numerical results for the maximum of the time-dependent distinguishability $D_S(t)$ as a function of the time t, for two different quenches of the parameter ϕ. Comparing the results for the N-cluster Ising models with the results for the XY models in Fig. (4.1), one can see several analogies and differences.

In completely analogy with the XY models, also for the N-cluster Ising models $D_S(t)$, after a transient in which it may increase, shows an exponential decay, which time scale does not depend on S but only on the values of ϕ before and after the quench. Therefore, the steady state, realized at a very large time, loses all the informations about the particular initial ground state.

On the contrary, the presence of other symmetries that are preserved in the symmetry-breaking ground states plays an extremely important role. In fact, if one takes a look at the two-body fermionic correlation functions $g_r(\phi_0, \phi_1, t)$, $f_r(\phi_0, \phi_1, t)$ and $h_r(\phi_0, \phi_1, t)$ of the N-cluster Ising models, one notes that, in the stationary case, $f_r(\phi_0) = -h_r(\phi_0) = \delta_{r,0}$, in completely analogy with the XY models, and $g_r(\phi_0) = 0 \ \forall r \neq a(N+2)+1$, whit a an integer [118, 47], differently from the XY models, where all the $g(\gamma, h_0, r) \neq 0$. Such a difference

implies that the only spin correlation functions, which support is included in a subsystem S with a size $L < N + 2$, different from zero in static conditions can be $\langle \sigma_i^y \rangle$. Consequently, $D_{S_1} = D_{S_2}$ if $L_{S_1}, L_{S_2} < N + 2$.

After the quench, instead, the two-body fermionic correlation functions depend on time. But, independently of the parameters before and after the quench, at any time $t > 0$, $g(\phi_0, \phi_1, r, t) = 0 \ \forall r \neq a(N + 2) + 1$ and $f(\phi_0, \phi_1, r, t) = -h(\phi_0, \phi_1, r, t)$ with $f(\phi_0, \phi_1, r, t) = 0 \ \forall r \neq a(N + 2)$. As a consequence, all the symmetry-breaking spin correlation functions, which operators have a support in a subsystem S with a size $L < N + 2$ remain zero also after the quench. In completely analogy with the stationary case, this results is due to the presence of residual symmetries of the system that are not violated by the ground states that break the parity symmetry. Consequently, $D_{S_1}(t) = D_{S_2}(t)$ if $L_{S_1}, L_{S_2} < N + 2$, as a generalization to the time dependence of the stationary results.

5
N-cluster models with a transverse magnetic field

In this chapter, following the great interest of the scientists towards systems with orders that do not have classical counterparts, I analyze a family of fully analytical solvable spin-1/2 models, named N-cluster models in a transverse magnetic field, in which a many-body cluster interaction competes with a uniform transverse magnetic field. These models, independently by the cluster size $N+2$, exhibit a quantum phase transition, that separates a paramagnetic phase from a cluster one, that corresponds to a nematic ordered phase or a symmetry protected topological ordered one for even or odd N respectively. I analytically solve the models and derive all the spin correlation functions, with which I reconstruct the reduced density matrix and different entanglement properties. In particular, I prove that, in contrast with the models analyzed in Ref. [47], for any value of N there is a region of the parameter ϕ for which the entanglement between a pair of spins, as quantified by the concurrence, does not vanish. Moreover, by analyzing the relation between conformal field theory [64] and the divergence of the block entanglement, at a quantum critical point $\phi = \phi_c = \pi/4$, I prove that all different models fall in different classes of symmetry, because the central charge turns out to be dependent on N.

5.1 Solution of the models

The Hamiltonian of equation (2.3) for the N-cluster models in a transverse magnetic field reads

$$H^{ch}_{\{\phi,N\}} = -\cos(\phi)\sum_j \sigma^x_j Z^N_j \sigma^x_{j+N+1} + \sin(\phi)\sum_j \sigma^z_j \tag{5.1}$$

where σ^α_j ($\alpha = 0, x, y, z$) are the Pauli matrices, $Z^N_j = \bigotimes_{k=1}^{N} \sigma^z_{j+k}$ and ϕ is the phase parameter that controls the relative weight of the interacting terms.

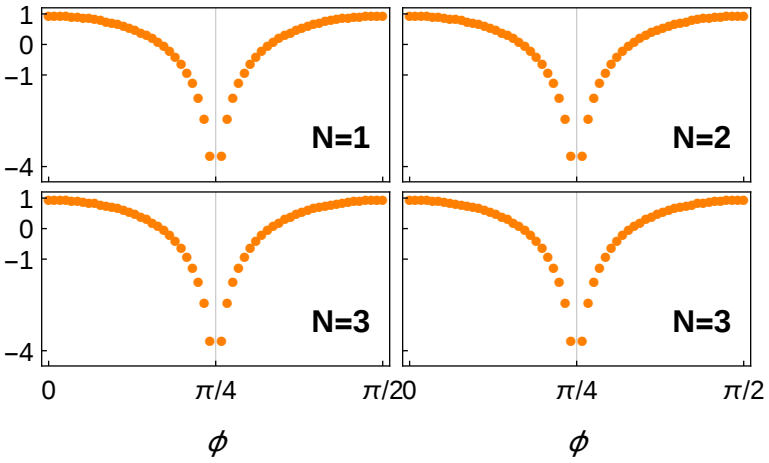

Figure 5.1: (Color online) Behavior of the second derivative of the energy density of the ground state $E_{\{\phi,N\}}$, as function of the phase parameter ϕ, for different cluster sizes $N+2$. The divergence is independent of N at the critical value $\phi_c = \frac{\pi}{4}$ and corresponds to a vanishing energy gap between the ground state and the first excited state.

In these models a many-body cluster interaction term competes with an external magnetic field that acts uniformly on all spins of the system. Independently by the cluster size $N+2$, these models exhibit a quantum phase transition at $\phi_c = \pi/4$, that separates a paramagnetic phase from a cluster phase, that corresponds to a nematic ordered phase or a symmetry protected topological ordered one for even or odd N respectively.

By following the well-known approach based on the Jordan-Wigner (JW) transformations [73] and illustrated in the Sec. (2.1), the one dimensional spin-1/2 Hamiltonian $H^{ch}_{\{\phi,N\}}$ can be mapped into a non-interacting spinless fermions Hamiltonian, freely moving along the chain [84, 9, 10, 118, 47], where, thanks the non locality of the JW, the cluster term, involving an interaction among $N+2$ spins, is mapped into a two body fermionic term, involving an interaction between sites at distance $N+1$. Thanks to a Fourier transform on the fermionic operators, one can solve the problem and derive the exact ground state $|\psi_{\{\phi,N\}}\rangle$ and the associated energy density $E_{\{\phi,N\}}$, in the thermodynamic limit, as in Eqs. (2.23) and (2.24) respectively.

Explicity, the expression of the energy density is given by

$$E_{\{\phi,N\}} = -\frac{2}{\pi}\int_0^{\pi}\sqrt{1+\cos((N+1)k)\,\sin(2\phi)}dk \tag{5.2}$$

According to the general theory of the continuous phase transitions at zero

temperature [113], the divergence of the second derivative of the energy density, with respect to the Hamiltonian parameters, signals the presence of a quantum critical point. In Fig. (5.1), I plot the second derivative of the energy density as a function of the phase parameter ϕ. It clearly shows a divergence at $\phi = \phi_c \equiv \pi/4$, independently by N. The singularity corresponds to the vanishing energy gap between the ground and the first excited state with modes $k = \frac{j\pi}{N+2}$, where j runs from 0 to $N+1$.

5.2 The spin correlations functions

With the analytic expression of the ground state $|\psi_{\{\phi,N\}}\rangle$ of the Hamiltonian $H^{ch}_{\{\phi,N\}}$, all the spin correlation functions can easily be derived. By following the method illustrated in Sec. (2.2), it immediately follows that

$$\begin{aligned} \langle A_i \rangle &= 0 \\ \langle B_i \rangle &= 0 \\ \langle A_i A_k \rangle &= \delta_{ik} \\ \langle B_i B_k \rangle &= -\delta_{ik} \\ \langle B_i A_k \rangle &= g_{i,k}(\phi, N) \equiv g_r(\phi, N) \end{aligned} \tag{5.3}$$

with $r = i - k$. The explicit expression of the non-trivially zero fermionic correlation function $g_r(\phi, N)$ can be obtained from the explicit expression of $\alpha_{\{\phi,N\},k}$ and $\beta_{\{\phi,N\},k}$ of Eq. (2.22), in terms of the $\epsilon_{\{\phi,N\},k}$ and $\delta_{\{\phi,N\},k}$ of Eq. (2.18)

$$g_r(\{\phi\}, N) = \frac{1}{\pi}\int_0^{\pi} \frac{\cos(k(N+1+r))\cos\phi + \cos(kr)\sin\phi}{\sqrt{1+\cos((N+1)k)\sin(2\phi)}} dk \, . \tag{5.4}$$

Solving this integral, one note that if $r \neq l(N+1)$, where l is an integer number that runs from $-\infty$ to ∞, then the $g_r(\phi, N)$ vanishes for all values of ϕ. This fact, plays a fundamental role in the behavior of the entanglement property among different spins.

From Eqs. (5.3) and (5.4), one can recover all the spin correlation functions of interest, and I point out some interesting results about some specific ones.

The presence of the external field along the z axis forces a magnetization along the z direction, i.e. $\langle \sigma^z_j \rangle$, that it equals to

$$\langle \sigma^z_j \rangle = -g_0(\phi, N) \tag{5.5}$$

and, therefore, it is always different from zero for all possible values of $\phi \neq 0$ and for all possible N.

The two-body spin correlation functions, instead, can be written as $\langle \sigma_i^\mu \sigma_{i+r}^\mu \rangle$ with $\mu = x, y, z$. If $\mu \equiv z$, the correlation function $\langle \sigma_i^z \sigma_{i+r}^z \rangle$ have a very simple expression in terms of $g_r(\phi, N)$

$$\langle \sigma_i^z \sigma_{i+r}^z \rangle = g_0(\phi, N)^2 - g_r(\phi, N) g_{-r}(\phi, N) \tag{5.6}$$

In the case of $r \neq l(N+1)$, $\forall l \in \mathcal{I}$, it follows that

$$\langle \sigma_i^z \sigma_{i+r}^z \rangle = g_0(\phi, N)^2 \equiv \langle \sigma_j^z \rangle^2 \tag{5.7}$$

Otherwise, if $\mu = x, y$, the spin correlation functions are given by the Slater determinant expressed in Eqs. (2.33) and (2.34). Taking into account that $g_r(\phi, N)$ vanishes for all $r \neq l(N+1)$, it follows that

$$\langle \sigma_i^x \sigma_{i+r}^x \rangle = \langle \sigma_i^y \sigma_{i+r}^y \rangle = 0 \quad \forall r \neq l(N+1) \tag{5.8}$$

In the very relevant case in which $r = N+1$, one can note that

$$\begin{aligned} \langle \sigma_i^x \sigma_{i+N+1}^x \rangle &= (-1)^N g_{-(N+1)}(\phi, N)\ g_0(\phi, N)^N \\ \langle \sigma_i^y \sigma_{i+N+1}^y \rangle &= (-1)^N g_{N+1}(\phi, N)\ g_0(\phi, N)^N \end{aligned} \tag{5.9}$$

5.3 The order parameters

As pointed out in Sec. (5.1), the behavior of the second derivative of the ground state energy density shows that the system undergoes a quantum phase transition at $\phi = \phi_c \equiv \pi/4$, regardless the value of N. However, the divergence of the free energy is not a detector of the kind of phases realized belove and above a quantum critical point. In this section, I determine the nature of the two phases, for all possible value of N, by studying the behavior of the order parameters that characterize them.

In the phase dominated by the many-body cluster interaction terms, i.e. when $\phi < \phi_c$, one can apply the results obtained in Ref. [47]. In fact, for $\phi = 0$ the two models coincide and hence also the order parameters are the same, for any N. When $\phi \geq 0$, until ϕ_c is reached, the same order parameters are different from zero, for the adiabatic deformation of the ground state [74].

Therefore, the many-body cluster phase is characterized by two different kind of orders, depending on N. For odd values of N, the system is in a symmetry protected topological ordered phase, characterized by a string order parameter while, for even values of N, the system is in a nematic phase, characterized

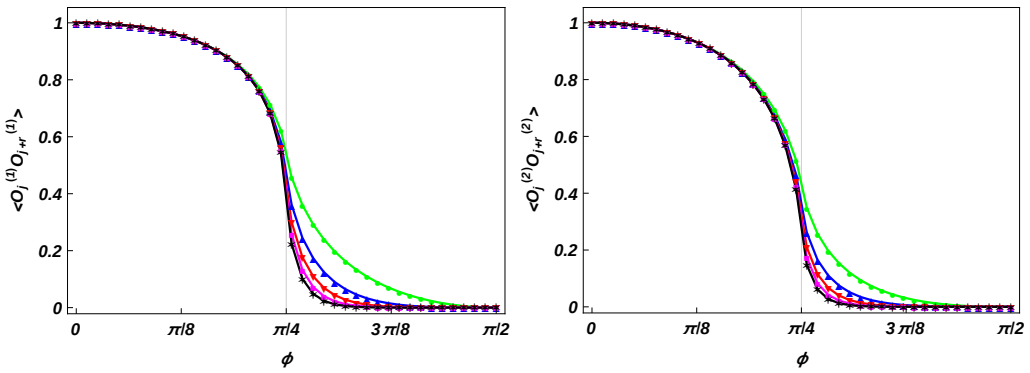

Figure 5.2: (Color online) Behavior of the expectation value $\left\langle \mathcal{O}_j^{(N)} \mathcal{O}_{j+r}^{(N)} \right\rangle$ for $N = 1$ (left panel) and $N = 2$ (right panel) and $r = 3, 6, 9, 12, 15$, as a function of the phase parameter ϕ. Green dots (upper curve) $r = 3$, blue up-triangles $r = 6$, red down-triangles $r = 9$, magenta squares $r = 12$ and black stars (lower curve) $r = 15$. As r increases, the expectation value tends to disappear in the paramagnetic phase while it remains finite in the cluster phase.

by an order parameter defined on a block of spins with dimension greater than one single spin. Hence, one can define two operators, for odd and even values of N respectively

$$\begin{aligned} \mathcal{O}_j^{(N)} &= \left(\bigotimes_{k=1}^{j-N-1} \sigma_k^z \right) \sigma_{j-N}^y \sigma_{j-N+1}^x \cdots \sigma_j^x \qquad \text{odd } N \\ \mathcal{O}_j^{(N)} &= \sigma_j^x \sigma_{j+1}^y \sigma_{j+2}^x \cdots \sigma_{j+N}^x \qquad \text{even } N \end{aligned} \tag{5.10}$$

in such a way to rewrite the Hamiltonian of Eq. (5.1) as follows

$$H_{\{\phi,N\}}^{ch} = -\cos(\phi) \sum_j \mathcal{O}_j^{(N)} \mathcal{O}_{j+1}^{(N)} + \sin(\phi) \sum_j \sigma_j^z \tag{5.11}$$

The the string order parameter $\mathcal{S}_j^{(N)}$ and the nematic order parameter $\mathcal{B}_j^{(N)}$ are defined as follows

$$\begin{aligned} \mathcal{S}_j^{(N)} &= \sqrt{\lim_{r\to\infty} \left\langle \mathcal{O}_j^{(N)} \mathcal{O}_{j+r}^{(N)} \right\rangle} \qquad \text{odd } N \\ \mathcal{B}_j^{(N)} &= \sqrt{\lim_{r\to\infty} \left\langle \mathcal{O}_j^{(N)} \mathcal{O}_{j+r}^{(N)} \right\rangle} \qquad \text{even } N \end{aligned} \tag{5.12}$$

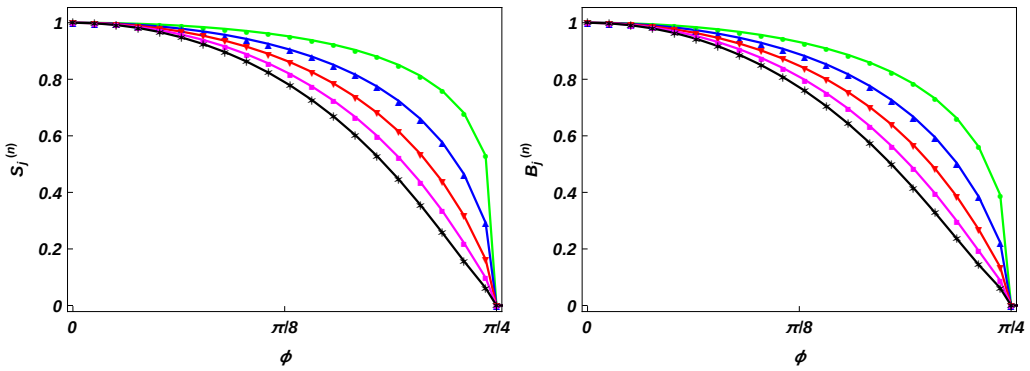

Figure 5.3: (Color online) In the left panel, I plot the behavior of the string order parameter $S_j^{(N)}$ for $N = 1, 3, 5, 7, 9$, as a function of the phase parameter $\phi < \phi_c$: green dots (upper curve) $N = 1$, blue up-triangles $N = 3$, red down-triangles $N = 5$, magenta squares $N = 7$ and black stars (lower curve) $N = 9$. In the right panel, I plot the behavior of the nematic order parameter $B_j^{(N)}$ for $N = 2, 4, 6, 8, 10$, as a funtion of the phase parameter $\phi < \phi_c$: green dots (upper curve) $N = 2$, blue up-triangles $N = 4$, red down-triangles $N = 6$, magenta squares $N = 8$ and black stars (lower curve) $N = 10$. The dots represent the numerical results of the order parameters $S_j^{(N)}$ and $B_j^{(N)}$ of Eqs. (5.12), whereas the curves correspond to analytical fits $S^{(N)}$ and $B^{(N)}$ defined in Eq. (5.13).

In Fig. (5.3), I plotted the expectation values $\langle \mathcal{O}_j^{(N)} \mathcal{O}_{j+r}^{(N)} \rangle$ for odd $N = 1$ (left panel) and even $N = 2$ (right panel) respectively, as a function of the phase parameter ϕ, by varying r. It is evident that, as r increases, these expectation values tend to disappear in the paramagnetic phase, while remain finite in the cluster phase, by making $\mathcal{O}_j^{(N)}$ a candidate for the order parameter. In Fig. (5.3), in fact, I plotted $\mathcal{S}_j^{(N)}$ (left panel) and $\mathcal{B}_j^{(N)}$ (right panel), for a sufficiently large value of r and for different values of N. It is evident that they capture perfectly the nature of the cluster phase, because they remain different from zero below the critical point and disappear above.

Analyzing the numerical data obtained for both defined order parameters, $\mathcal{S}_j^{(N)}$ and $\mathcal{B}_j^{(N)}$, I find finally the same dependence on N and ϕ, i.e.

$$\begin{aligned} \mathcal{S}^{(N)} &= \left(1 - \tan(\phi)^2\right)^{\frac{N+1}{8}} \\ \mathcal{B}^{(N)} &= \left(1 - \tan(\phi)^2\right)^{\frac{N+1}{8}} \end{aligned} \tag{5.13}$$

From the Eq. (5.13), it follows that critical exponent β depends on N

$$\beta(N) = \frac{N+1}{8} \tag{5.14}$$

Comparing these results to the equivalent expression in Ref. [47], it is evident that the critical exponents for two models are different: in the N-cluster models in a transverse magnetic field the critical exponent is $\frac{N+1}{8}$ while in the N-cluster Ising models it is equal to $\frac{N+2}{8}$. One can than conclude that, by fixing N, the two families of models fall in different classes of symmetry. Moreover, by fixing N and $\phi < \phi_c$, the order in the N-cluster models in a transverse magnetic field is stronger than the order in the N-cluster Ising models. It follows that an external uniform magnetic field affects the cluster phase less than a short range magnetic Ising-like interaction.

On the contrary, above the quantum critical point, i.e. for $\phi > \phi_c$, the models show a phase dominated by the external magnetic field. In such a phase, there is no order parameter and the system is in a typical paramagnetic phase.

5.4 The entanglement properties

In this section, I analyze the entanglement properties between spins in a block as well as between a block of spins and the rest of the chain. Despite the complexity of the class of models under investigation, I obtain general results showing the relevance of the entanglement features in these systems. To study the entanglement properties, I focus on the reduced density matrix of m spins, which is obtained by tracing out all the degrees of freedom of the remaining spins of the system, according with Sec. (2.3). The reduced density matrix of m adjacent spins can be expressed in terms of the m-points spin correlation functions as in Eq. (2.37)

$$\rho^{(m)} = \frac{1}{2^m} \sum_{\alpha_1,\ldots,\alpha_m} \langle \sigma_1^{\alpha_1} \sigma_2^{\alpha_2} \cdots \sigma_m^{\alpha_m} \rangle \, \sigma_1^{\alpha_1} \otimes \sigma_2^{\alpha_2} \otimes \cdots \otimes \sigma_m^{\alpha_m} \tag{5.15}$$

To obtain the expression of the m-point spin correlation functions, I used the results obtained in Sec. (5.2).

I focused the attention on three different entanglement measures: the concurrence [128], that quantifies the entanglement between two spins in the chain, the genuine multipartite entanglement [61, 58, 86] between spins in a block of the dimension of the cluster interaction and the von Neumann entanglement entropy between a block of adjacent spins and the rest of the chain, because of its relevant relation with the central charge at a quantum critical point [64].

5.4.1 Pairwise entanglement

Taking into account the properties of the spin correlation functions derived in Sec. (5.2), I prove the following theorem:

Theorem 1. *If the distance r between the two spins cannot be written as* $r = l(N+1)$, *with* $l \in \mathcal{I}$, *then the two spins are not entangled*

Proof: The proof is based on the results obtained in Sec. (5.2) for the spin correlation functions. In fact, in agreement with Eq. (5.15), the reduced density matrix of 2 spins can be written as a linear composition of single body and two body spin correlation functions. For what concern the single body spin correlation function, from the symmetry properties of the fermionic correlation function $g_r(\phi, N)$, it follows that

$$\begin{aligned} \langle \sigma_i^x \rangle &= 0 \\ \langle \sigma_i^y \rangle &= 0 \end{aligned} \tag{5.16}$$

because of $\langle A_i \rangle = \langle B_i \rangle = 0$ (see Eq. (5.3)). On the other hand, for what concern the two body spin correlation functions, all the functions that involve different spin operators vanish in agreement with the fact that $\langle A_i \rangle = \langle B_i \rangle = 0$ and $\langle A_i A_j \rangle = \langle B_i B_j \rangle = 0$ if $i \neq j$ (see Eq. (5.3)). Thus, the two spins reduced density matrix depends on four different correlation functions only: $\langle \sigma_i^z \rangle$, $\langle \sigma_i^x \sigma_{i+r}^x \rangle$, $\langle \sigma_i^y \sigma_{i+r}^y \rangle$ and $\langle \sigma_i^z \sigma_{i+r}^z \rangle$.

If $r \neq l(N+1)$, with $l \in \mathcal{I}$, it follows that

$$\begin{aligned} \langle \sigma_i^x \sigma_{i+r}^x \rangle &= 0 \\ \langle \sigma_i^y \sigma_{i+r}^y \rangle &= 0 \end{aligned} \tag{5.17}$$

The reduced density matrix depends only on $\langle \sigma_i^z \rangle$ and $\langle \sigma_i^z \sigma_{i+r}^z \rangle$ and, therefore, is diagonal in the basis of the eigenstate of σ_i^z and σ_{i+r}^z. This fact is the proof that the reduced density matrix is classical and no entanglement arises between i-th and $i+r$-th spins. Q.E.D.

On the contrary, when $r = l(N+1)$, $\langle \sigma_i^x \sigma_{i+r}^x \rangle \neq 0$ and $\langle \sigma_i^y \sigma_{i+r}^y \rangle \neq 0$. The reduced density matrix is not classical and it exists a region of the Hamiltonian parameters for which spins are entangled.

It is possible to quantify such entanglement in terms of the concurrence $\mathcal{C}(\rho)$ [128]. In Fig. (5.4), it is plotted the concurrence as a function of the phase parameter ϕ, for two spins at the endpoints of the cluster, i.e. $l = 1$ and $r = (N+1)$,

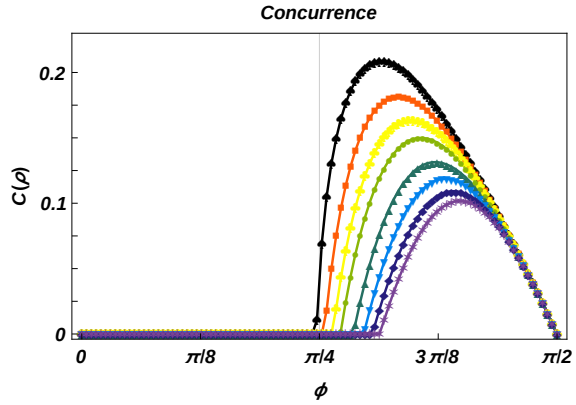

Figure 5.4: (Color online) Behavior of the concurrence $\mathcal{C}(\rho)$ between two spins at the endpoints of the cluster, as function of the phase parameter ϕ, for different N that runs from 1 (highest curve) to 12 (lowest curve). Note that only for $N = 1$ the concurrence is non-zero before and after the critical point and, generally, it decreases with increasing cluster size.

and for different values of N. It is evident that there exists a region of ϕ for which the concurrence does not vanish.

The concurrence shows a similar behavior with N: it is different from zero in a region confined in the paramagnetic phase, with the only exception of $N = 1$; by increasing N, the concurrence becomes smaller and smaller and the relative maximum goes towards higher value of ϕ. However, at $\phi = \pi/2$, regardless the value of N, the systems admit a factorization point [42, 43, 44], with a single factorized ground state, in which all entanglement quantities vanish.

On the other hand, for all $l > 1$ all the concurrences are identically zero. Therefore, the entanglement is always limited between spins at the endpoints of the clusters.

5.4.2 Genuine multipartite entanglement

For what concerne the genuine multipartite entanglement, I prove the following theorem

Theorem 2. *For each block made by m adjacent spins, with $m \leq N + 2$, there is no genuine multipartite entanglement*

Proof: The proof is based on the fact that, following the definition of the genuine multipartite entanglement for a mixed state, it must be impossible to find a decomposition of the reduced density matrix in states that show only entanglement between a couple of spins.

The reduced density matrix of a block made by $N+2$ adjacent spins can be written, as in Eq. (5.15), in terms of the spin correlation functions and, in turn, all the spin correlation functions can be written in terms of the $g_r(\phi, N)$ functions. Taking into account the results shown in Sec. (5.2) and the fact that the maximum distance between two spins in the block is $N+1$, the reduced density matrix depends only on three different functions: $g_0(\phi, N)$, $g_{N+1}(\phi, N)$ and $g_{-N-1}(\phi, N)$. Therefore the only spin correlation functions different from zero are that diagonal in the natural basis or that associated to an inversion of the two spins at the endpoints of the block. With this result, in the natural basis, the reduce density matrix can be written as a linear convex combination

$$\rho^{N+2} = \sum_i p_i \left(\bigotimes_{k=2,N+1} \chi_i^{(k)} \right) \otimes \chi_i^{(1,N+2)} \tag{5.18}$$

where $\chi_i^{(k)}$ is a state defined on the k-th spin (k runs from 2 to $N+1$) of the block and $\chi_i^{(1,N+2)}$ is a state (entangled or not) defined on the two endpoints spins of the block. In other words, the reduced density matrix can be written as a sum of states that, with the only exception of a possible bipartite entanglement between the two endpoints spins, are fully factorized. In such state, it comes immediately that any multipartite entanglement vanishes.

If now one considers a block made by $m = N+1$ adjacent spins, it follows that the reduced density matrix can be obtain by Eq. (5.18), tracing out one of the two endpoints spin. Thus, the reduced density matrix becomes a linear convex combination of fully disentangled states. Hence, also any subsystem cannot show any multipartite entanglement. Q.E.D.

It is interesting to make a comparison with the results reported in Ref. [47] where, on the contrary, there is no bipartite entanglement but a significant value of genuine multipartite entanglement, confined in the anti-ferromagnetic phase, with the only exception of $N = 1$. Comparing these two results, and taking into account the proof of the presence of the genuine multipartite entanglement in the XY-models [45, 63], it can counter-intuitively be concluded that a fundamental requirement to have genuine multipartite entanglement is the presence, in the Hamiltonian, of a simple Ising-like interaction.

5.4.3 Block entanglement

Another important entanglement property in multipartite systems concerns the entanglement between a block of m spins and the rest of the chain and how it relates to the holomorphic and anti-holomorphic sectors in conformal field

theory [64].

For this purpose, I compute the Von Neumann entropy of the reduced density matrix of m spins

$$S^{(m)} = -\mathrm{Tr}\left(\rho^{(m)} \log_2(\rho^{(m)})\right) \tag{5.19}$$

Using the methods developed in Ref. [125, 80], it follows that

$$S^{(m)} = \sum_{i=1}^{m} H_{\mathrm{Shannon}}\left(\frac{1+\nu_i}{2}\right) \tag{5.20}$$

where $H_{\mathrm{Shannon}}(x)$ is the Shannon entropy

$$H_{\mathrm{Shannon}}(x) = -x\log_2(x) - (1-x)\log_2(1-x) \tag{5.21}$$

and ν_i are the imaginary part of the eigenvalues of the matrix Γ' given by

$$\left(\Gamma'\right)_{ij} = \delta_{ij} - i\left(\Gamma^{(m)}\right)_{ij} \tag{5.22}$$

with

$$\Gamma^{(m)} = \begin{pmatrix} \Pi_0 & \Pi_{-1} & \cdots & \Pi_{-m+1} \\ \Pi_1 & \Pi_0 & \cdots & \Pi_{-m+2} \\ \vdots & \vdots & \ddots & \vdots \\ \Pi_{m-1} & \Pi_{m-2} & \cdots & \Pi_0 \end{pmatrix} \tag{5.23}$$

and

$$\Pi_r = \begin{pmatrix} 0 & g_r(\phi, N) \\ -g_{-r}(\phi, N) & 0 \end{pmatrix} \tag{5.24}$$

I evaluate numerically the von Neumann entropy for blocks of length ranging from 1 to 200 spins, at the critical point $\phi_c = \pi/4$, for N that runs from 1 to 8 and plot the results in Fig. (5.5).

Analyzing the numerical data, it can be deduced that

$$S^{(m)} \simeq 0.17(1+N)\ \log_2 m + \mathrm{const}(N) \tag{5.25}$$

The multiplicative constant in front of the logarithmic term is known to be related to the central charge of the $1+1$ dimensional conformal field theory, that describes the critical behavior of the chain via the relation [64]

$$S_m = \frac{\mathsf{c}+\bar{\mathsf{c}}}{6}\ \log_2 m \tag{5.26}$$

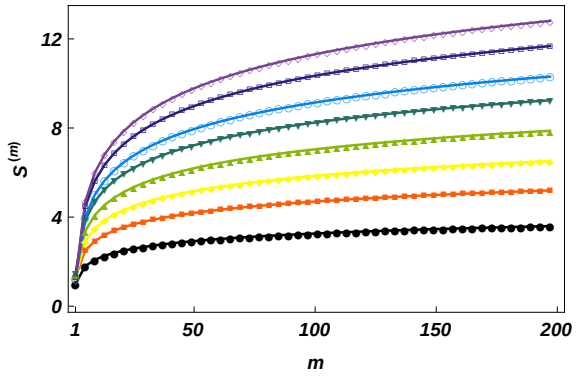

Figure 5.5: (Color online) Behavior of the von Neumann entropy $S^{(m)}$ as a funtion of the block size m, for different cluster sizes N, at the critical point $\phi_c = \pi/4$. The value of N runs from 1 lowest (black) curve to 8 the highest (violet) curve.

where c and $\bar{\mathsf{c}}$ are the central charges of the so-called holomorphic and anti-holomorphic sectors of the conformal field theory. Due to the existence of a duality in the system under investigation, it follows that $\mathsf{c} = \bar{\mathsf{c}}$ and hence

$$\mathsf{c} = \mathsf{c}(N) \simeq 0.51(1 + N) \tag{5.27}$$

Two quantum one-dimensional systems belong to the same universality class if they have the same central charge. In this case, the central charge, as well as the critical exponent β of Eq. (5.14), depends on N. This implies that the N-cluster models in a transverse magnetic field fall into different classes, with respect to their symmetries.

6
Minimal set of nonlinear ground-states functionals to detect 1-D quantum orders

Traditionally, the characterization of phase transitions in strongly correlated systems has been based on the "standard" Gizburg-Landau scenario of second order phase transitions. The order, associated to the breaking of some symmetry of the Hamiltonian, is characterized by local order parameters $\mathcal{O}$, whose expectation values are different from zero in the whole ordered phase. However, there are important cases where an order parameter is not available, as in presence of topological phases, or more simply where a local parameter is intrinsically difficult to construct or measure, as in presence of nematic phases. A similarly challenging situation realizes whenever the phase diagram of the material under investigation is not known at all. In all these cases a major problem is to identify a quantity able to detect a certain phase or phase transition. The question spontaneously arises is: could one find an alternative approach to complete characterize all the phases for which the Gizburg-Landau paradigm fails?

In this chapter, I provide an answer to this question, by proving that the von Neumann entropy, the Schmidt gap and the mutual information identify the minimal set of nonlinear ground-states functionals that completely characterize all kind of orders in 1-D quantum systems of spin-1/2 and fermions.

6.1 Models

In this section, I breefly review both the 1-D spin-1/2 models, i.e. the XY models in a transverse magnetic field, the N-cluster Ising model and the N-cluster models in a tranverse magnetic field, and the 1-D fermionic models, i.e. the Kitaev chain, that I have considered.

The Hamiltonian of the XY models in Eq. (2.1) reads

$$H^{XY}_{\{\gamma,h\}} = -\frac{1+\gamma}{2}\sum_j \sigma^x_j \sigma^x_{j+1} - \frac{1-\gamma}{2}\sum_j \sigma^y_j \sigma^y_{j+1} - h\sum_j \sigma^z_j \tag{6.1}$$

where γ is the anisotropy parameter and h the external uniform magnetic field, that control the relative weight of the interacting terms. Regardless of the value of γ, in the thermodynamic limit, these models feature a quantum phase transition at $h = h_c = 1$. For $h > h_c$ and for any value of γ, the ground state space is non-degenerate and there is a finite gap in the energy spectrum between the ground state and the first excited state. On the other hand, for $h < h_c$, two different cases arise: for $\gamma = 0$, the ground state space remains non-degenerate while the energy spectrum becomes gapless and this corresponds to the isotropic, gapless XX model, whereas for $\gamma > 0$ the ground state space becomes two-fold degenerate, the energy spectrum is gapped, and the system can be characterized by a non vanishing local order parameter.

The Hamiltonian of the N-cluster Ising models in Eq. (2.2) reads

$$H^{cI}_{\{\phi,N\}} = -\cos(\phi)\sum_j \sigma^x_j Z^N_j \sigma^x_{j+N+1} + \sin(\phi)\sum_j \sigma^y_j \sigma^y_{j+1} \tag{6.2}$$

where ϕ is the phase parameter that controls the relative weight of the interacting terms and $Z^N_j = \bigotimes_{k=1}^N \sigma^z_{j+k}$. Regardless the value of N, in the thermodinamic limit, these models feature a quantum phase transition at $\phi = \phi_c = \pi/4$. For $\phi > \phi_c$, the ground state space is two-fold degenerate, the energy spectrum is gapped, and the system can be characterized by a non vanishing local order parameter. On the other hand, for $\phi < \phi_c$, the systems exibit a cluster phase, the ground space becomes 2^{N+1} degenerate, the energy spectrum is gapped, and the system can be characterized by a non vanishing block order parameter (nematic phase) or a non vanishing string order parameter (topological phase) for even or odd N respectively.

The Hamiltonian of the N-cluster models in a transverse magnetic field in Eq. (2.3) reads

$$H^{ch}_{\{\phi,N\}} = -\cos(\phi)\sum_j \sigma^x_j Z^N_j \sigma^x_{j+N+1} + \sin(\phi)\sum_j \sigma^z_j \tag{6.3}$$

where ϕ is the phase parameter that controls the relative weight of the interacting terms and $Z^N_j = \bigotimes_{k=1}^N \sigma^z_{j+k}$. Regardless the value of N, in the thermodinamic limit, these models feature a quantum phase transition at $\phi = \phi_c = \pi/4$. For $\phi > \phi_c$, the ground state space is non-degenerate and there is a finite gap in the energy spectrum between the ground state and the first excited state. On

the other hand, for $\phi < \phi_c$, the systems exibit a cluster phase, the ground space becomes 2^{N+1} degenerate, the energy spectrum is gapped, and the system can be characterized by a non vanishing block order parameter (nematic phase) or a non vanishing string order parameter (topological phase) for even or odd N respectively.

The Hamiltonian of the Kitaev chain [75] reads

$$H^K_{\{\phi\}} = \sin(\phi) \sum_j (c_j c_{j+1} - c_j^+ c_{j+1} + \text{h.c.}) - \cos(\phi) \sum_j (c_j^+ c_j - \frac{1}{2}) \tag{6.4}$$

where ϕ is the phase parameter that controls the relative weight of the interacting terms and c_j^+, c_j are the creation and annihilation fermionic operators. In the thermodinamic limit, this model feature a quantum phase transition at $\phi = \phi_c = \pi/4$. For $\phi < \phi_c$, the ground state space is non-degenerate and there is a finite gap in the energy spectrum between the ground state and the first excited state. On the other hand, for $\phi > \phi_c$, the ground state space is two-fold degenerate, the energy spectrum is gapped, and the system can be characterized by a non vanishing string order parameter, defined on the whole system.

These 1-D models are useful for the analysis, because, despite their complexity, they can be exactly diagonalized by following the method illustrated in Sec. (2.1) and they span, by varying the Hamiltonian parameters, all possible kind of orders in 1-D quantum systems.

6.2 Von Neumann entropy

First attempts within an alternative approach to understanding quantum many-body systems and their simulatability [116], focused on the study of quantum phase transitions (QPT) in spin chains [97, 99], by exploiting the entanglement content of the ground states of such systems. A good figure of merit to measure the bipartite correlations embedded in the ground state of a spin chain, is the von Neumann entropy S. For a bipartite quantum system $(A|B)$ in a pure state, the von Neumann entropy is calculated from the reduced density matrix ρ_A or ρ_B according to the formula (1.21)

$$S(\rho_A) = -\text{Tr}(\rho_A \log \rho_A) = -\sum_{i=1}^{L} \lambda_i \log \lambda_i \tag{6.5}$$

where L is the number of spins in the subsystem A and λ_i are the eigenvalues of the reduced density matrix ρ_A. Its finite size scaling, i.e., the dependence of S with the size of the subsystem L, shows remarkable properties [125]. At

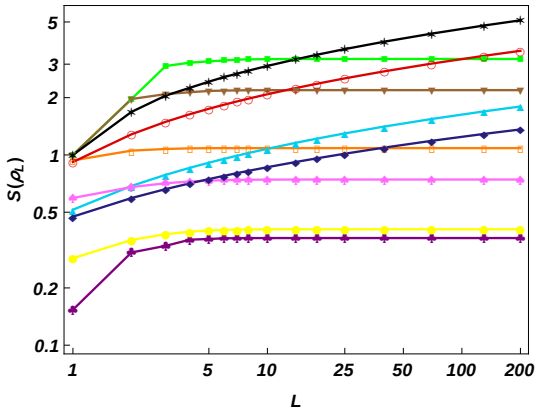

Figure 6.1: (Color online) Behavior of the von Neumann entropy $S(\rho_L)$, as a function of the size L of the subsystem. Purple club refer to 1-cluster model in a transverse magnetic field with $\phi = 3\pi/8$ (paramagnetic phase); yellow dots refer to Kitaev chain with $\phi = \arctan(0.5) - 0.1$ (paramagnetic phase); pink spade refer to Kitaev chain with $\phi = \arctan(0.5) + 0.1$ (topological phase); orange empty squares refer to XY model with $h = 0.5$ and $\gamma = 0.5$ (ferromagnetic phase); brown triangles refer to 1-cluster Ising model with $\phi = \pi/8$ (topological phase); green squares refer to 2-cluster Ising model with $\phi = \pi/8$ (nematic phase); blue diamonds refer to Kitaev chain with $\phi = \arctan(0.5)$ (critical point); light-blue triangles refer to XY model with $h = 1$ and $\gamma = 0.5$ (critical point); red empty circles refer to XY model with $h = 0.5$ and $\gamma = 0$ (critical phase); black stars refer to 1-cluster Ising model with $\phi = \pi/4$ (critical point).

criticality, where the system is gapless, the von Neumann entropy S diverges logarithmically as $S \sim \mathsf{c} \log L$ [125, 59, 64, 77, 18], where c is the so-called central charge of the corresponding QPT as provided by the conformal field theory (CFT). This universal logarithmic behavior of the entanglement entropy at criticality underpins the conformal invariance of QPT in 1-D, and leads also to a universal - depending asymptotically only on c - distribution of the eigenvalues of the reduced density matrix [23]. On the other hand, outside but close to criticality, when the system is gapped, the von Neumann entropy S scales as $S \sim \mathsf{c} \log \xi$ [18], being ξ the correlation length that sets the relevant scale for long-distances physics.

The logarithmic divergence of S, with the size L of the system, can be explained because when a system approaches a critical point a fundamental change in the ground state and in the structure of entanglement in the ground state occurs: the transition is governed by a change in the spatial extent of the entanglement. The entanglement between a block of spins and the rest of the lattice away from the critical point is bounded in a finite region because the correla-

tions are damped exponentially in the separation. At the critical point, the correlations, and hence entanglement, develop on all length scales. In some sense, at the critical point the state is delocalized, compared to the local nature of the entanglement away from the criticality.

In fig. (6.1), I report the behavior of the von Neumann entropy S as a funtion of the size L of the subsystem, for all the models considered in Sec. (6.1) and for a certain values of the Hamiltonian parameters that span all possible phases for these quantum systems. It is evident that, at a quantum critical point, where the system is gapless and the correlations develop at all length scale, S diverges logarithmically as L increases, according to $S \sim \mathsf{c} \log L$, while, away from the critical point, where the system is gapped and the correlation length ξ is bounded in a finite region, S saturates a constant value very quickly, according to $S \sim \mathsf{c} \log \xi$.

Therefore, the von Neumann entropy S can be unambiguously used to distinguish a critical system from a non critical one.

6.3 Schmidt gap

Away from criticality, when a system is gapped, the von Neumann entropy is not suitable to characterize quantum phases, because it saturates to a constant value, independently of the size L, for all 1-D gapped systems.

It is in this away-from-criticality regime that further informations, not included in the entanglement entropy, can be obtained from the entanglement spectrum, i.e. the set of eigenvalues $\{\lambda_i\}$ of the reduced density matrix ρ_A. Indeed, it is known that the (topological) Haldane phases, appearing for integer spin chains [104], and non-Abelian fractional quantum hall effect states [83] are characterized by a double (or higher) degeneracy of the entire entanglement spectrum. Moreover, for several 1-D spin systems [34, 82], the finite-size scaling (FFS) argument shows a complete characterization of the critical points and mass scaling exponents in terms of the scaling properties of the Schmidt gap $\Delta\lambda(\rho)$, i.e. the difference between the the two largest non trivially degenerated eigenvalues of the reduced density matrix ρ. Recent studies in 2D systems also show the scaling of the entanglement spectrum near phase transitions [2, 70].

The question spontaneously arises is then: could entanglement spectrum provide a complete characterization of quantum matter phases away from criticality? I provide an answer to this question, by proving that the Schmidt gap $\Delta\lambda(\rho)$ completely identifies paramagnetic phases. Indeed, in the paramagnetic phases, characterized by a non-degenerate state space and a finite gap in the energy spectrum between the ground state and the first excited state, the Schmidt gap $\Delta\lambda(\rho)$ saturates at a finite value, while otherwise it goes rapidly to zero, as

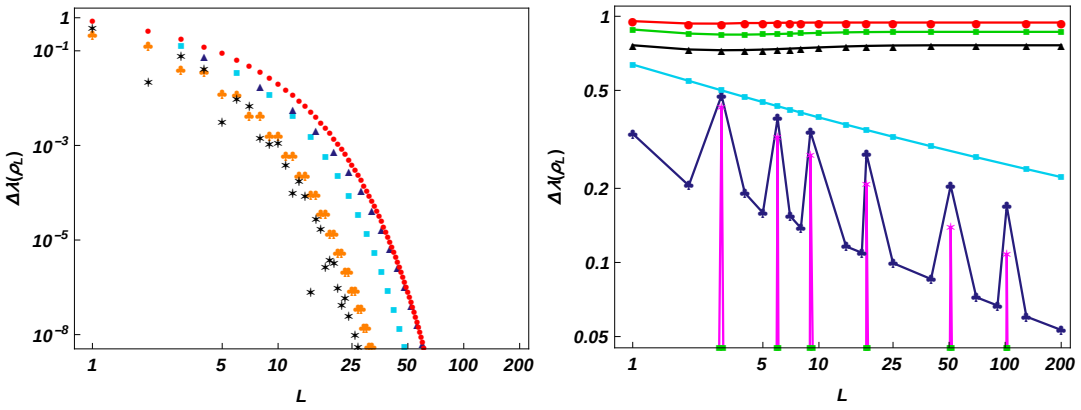

Figure 6.2: (Color online) Behavior of the Schmidt gap $\Delta\lambda(\rho_L)$, as a function of the size L of the subsystem. In the left panel, I plot the results for both topological and symmetry-breaking ordered phases. Red dots refer to Kitaev chain with $\phi = \arctan(0.5) + 0.1$ (topological phase); blue triangles refer to 2-cluster Ising model with $\phi = \pi/8$ (nematic phase); light-blue squares refer to 1-cluster Ising model with $\phi = \pi/8$ (topological phase); orange club refer to 1-cluster model in a transverse magnetic field with $\phi = \pi/8$ (topological phase); black strars refer to XY model with $h = \gamma = 0.5$(ferromagnetic phase). In the right panel, I plot the results for paramagnetic phases and criticality. Red dots refer to 1-cluster model in a transverse magnetic field with $\phi = 3\pi/8$ (paramagnetic phase); green squares refer to XY model with $h = 1.1$ and $\gamma = 0.5$ (paramagnetic phase); black triangles refer to Kitaev chain with $\phi = \arctan(0.5) - 0.1$ (paramagnetic phase); light-blue squares refer to Kitaev chain with $\phi = \arctan(0.5)$ (critical point); blue club refer to XX model with $h = 0.5$ (critical phase); magenta strars refer to 1-cluster Ising model with $\phi = \pi/4$ (critical point).

the size L of the subsystem increases.

An arbitrary vector $|\psi\rangle$, for a bipartite quantum system AB, can be written in the Schmidt decomposition $|\psi\rangle = \sum_k \lambda_k |\psi_k^A\rangle \otimes |\psi_k^B\rangle$ as in Eq. (1.10), where $|\psi_k^A\rangle$ ($|\psi_k^B\rangle$) is the kth eigenvector of the reduced density matrix ρ_A (ρ_B) of the subsystem A (B) and λ_k, the kth eigenvalue of the reduced density matrix, represents the entanglement spectrum that satisfies $\lambda_k \geq 0$ and $\sum_k \lambda_k^2 = 1$. By assuming that λ_k is arranged in a descending order with k, the Schmidt gap is defined as [34, 82]

$$\Delta\lambda(\rho_A) = \lambda_1 - \lambda_2 \tag{6.6}$$

with λ_1 and λ_2 the two largest non-trivially degenerate eigenvalues.

By following the results obtained in Ref. [34, 82], I extended the analysis to a

wide range of exactly-solvable models of spin-1/2 and fermions, that show exotic phases, such as nematic and topological ones, in addition to the traditionally symmetry-breaking ordered paramagnetic ones, and that fall in different classes of symmetry.

In fig. (6.2), I report the behavior of the Schmidt gap $\Delta\lambda$ as a function of the size L of the subsystem, for all the models considered in Sec. (6.1) and for a certain values of the Hamiltonian parameters that span all possible phases for these quantum systems. It is evident that, in the paramagnetic phases, where the ground state is unique and there is a finite gap with the first excited state, the Schmidt gap saturates very quickly to a constant value, as the size L of the system increases. Otherwise, it goes rapidly to zero. At a criticality, the entanglement spectrum tends to a continuum distribution, in the thermodynamic limit, that implies the closure of the Schmidt gap as the size L of the system increases. In the ordered phases, characterized by degenerate ground states in the thermodynamic limit, the Schmidt gap tends to disappears as the size L of the system increases.

According with Ref. [34, 82], it follows that the Schmidt gap $\Delta\lambda$ can be identified as a non-local parameter, that unambiguously capture the nature of paramagnetic phases.

6.4 Mutual information

The von Neumann entropy and the Schmidt gap unambiguously detect the criticality and the disorder of 1-D quantum systems, but are not suitable to provide a complete characterization of the ordered ones. In this scenario, further informations can be obtained from the mutual information, a *bona fide* measure of total correlations (classical plus quantum) [96]. I prove, indeed, that the mutual information, between two macroscopically separated subsystems A and B, completely identifies symmetry-breaking ordered phases, because it saturates to a finite value when it is possible to define a finite order parameter and goes rapidly to zero otherwise.

For a bipartite quantum system $(A|B)$, made by two subsystems A and B at a distance r, the mutual information is defined as [94]

$$\mathcal{I}_r(A|B) = \mathcal{S}(\rho_A) + \mathcal{S}(\rho_B) - \mathcal{S}(\rho_{AB}) \tag{6.7}$$

where $\mathcal{S}(\rho_X)$ is the von Neumann entropy of the density matrix pertaining to subsystem X. If for two arbitrary subsystems A and B, spatially separated by arbitrarily large distances r, the mutual information $\mathcal{I}(A|B)$ is vanishing, it is assured that there are no macroscopic correlations and, in particular, no

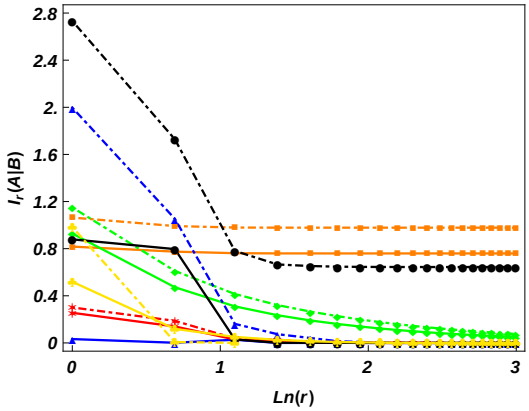

Figure 6.3: (Color online) Behavior of the mutual information $I_r(A|B)$, as a function of the distance r between the two subsystems A and B. Orange dot-dashed lines refer to XY chain with $h = \gamma = 0.5$ (ferromagnetic phase) and A=B=3 spin; orange dotted lines to XY chain with $h = \gamma = 0.5$ (ferromagnetic phase) and A=B=1 spin; green dot-dashed lines to XY chain with $\gamma = 0$, $h = 0.5$ (critical phase) and A=B=3 spin; green dotted lines to XY chain with $\gamma = 0$, $h = 0.5$ (critical phase) and A=B=2 spin; blue dot-dashed lines to 1-cluster Ising chain with $\phi = \pi/8$ (topological phase) and A=B=3 spin; blue dotted lines to 1-cluster Ising chain with $\phi = \pi/8$ (topological phase) and A=B=1 spin; red dot-dashed lines to 1-cluster + h chain with $\phi = 3\pi/8$ (paramagnetic phase) and A=B=3 spin; red dotted lines to 1-cluster + h chain with $\phi = 3\pi/8$ (paramagnetic phase) and A=B=2 spin; black dot-dashed lines to 2-cluster Ising chain with $\phi = \pi/8$ (nematic phase) and A=B=3 spin; black dotted lines to 2-cluster Ising chain with $\phi = \pi/8$ (nematic phase) and A=B=2 spin; yellow dot-dashed lines to Kitaev chain with $\phi = \arctan(0.5) - 0.1$ (paramagnetic phase) and A=B=2 spin; yellow dotted lines to Kitaev chain with $\phi = \arctan(0.5) + 0.1$ (topological phase) and A=B=2 spin.

macroscopic entanglement and no macroscopic quantum correlations. Otherwise, taking into account that the total system is in a global pure state, the two subsystems must be macroscopically entangled and quantum correlated.

In the XY model in a transverse magnetic field, that shows a quantum phase transition between a magnetically ordered phase and a paramagnetic one, it has been demonstrated that, in the entire phase with symmetry-breaking, the maximally symmetry-breaking states have vanishing long-distance mutual information $\mathcal{I}_\infty(A|B)$, while the latter remains finite for any non maximally symmetry-breaking superposition, attaining a maximum for the totally symmetric states. On the contrary, in the paramagnetic phase, $\mathcal{I}_\infty(A|B)$ identically vanishes for any state [57]. These results can be extended to the N-cluster models, that

exhibit non-trivially ordered phases, such as nematic and topological ones. I proved that, for dimensions of the subsystems A and B comparable with the size of the order parameters, the mutual information vanishes for the maximally symmetry-breaking states, while attains the maximum value for the totally symmetric ones, in completely agreement with Ref. [57]. In particular, it is possible to derive an analytical expression for the maximum (totally symmetric states) 2-Rényi based mutual information $\mathcal{I}_\infty(A|B)$, that is a functional of the order parameter

$$\mathcal{I}_\infty(A|B) \sim \log_2 \left(1 - \mathrm{C} \cdot {\mathcal{O}_\mathcal{P}}^\alpha\right) \tag{6.8}$$

where C is a constant that depends on certain correlation functions, α is a certain power law and $\mathcal{O}_\mathcal{P}$ is the order parameter. For the 2-cluster Ising model of Ref. [47] and for the 2-cluster models in a transverse magnetic field of chapter (5), that exibit a nematic phase ($N = 2$, odd) for $\phi < \phi_c = \pi/4$, the corresponding expression of the 2-Rènyi based mutual information $\mathcal{I}_\infty(A|B)$ is given by

$$\begin{aligned}
\mathcal{I}_\infty(3|3) &= \log_2 \left[1 + \frac{\mathcal{G}_{xyx}^4 (1 - (uv^* + vu^*)^4)}{(1 + \mathcal{G}_{xyx}^2 (uv^* + vu^*)^2)^2}\right] && \text{2-cluster Ising} \\
\mathcal{I}_\infty(3|3) &= \log_2 \left[1 + \frac{\mathcal{G}_{xyx}^4 (1 - (uv^* + vu^*)^4)}{((1 + m_z^2)^3 + \mathcal{G}_{xyx}^2 (uv^* + vu^*)^2)^2}\right] && \text{2-cluster field}
\end{aligned} \tag{6.9}$$

where $\mathcal{G}_{xyx} = \langle \sigma_x \sigma_y \sigma_x \rangle$ is the nematic order parameter and u, v the superposition amplitudes, according with Sec. (2.3). The only non-vanishing 2-Rènyi based mutual information $\mathcal{I}_\infty(A|B)$ is obtained for subsystems A and B made by 3 or more spins, i.e. subsystems on which the order parameter $\mathcal{G}_{xyx}$ is different from zero. Due to the normalization constraint, $|u|^2 + |v|^2 = 1$, the fractions in Eq. (6.9) are semi-definite positive and vanish only either at $\mathcal{G}_{xyx} = 0$, i.e.. away from the cluster ordered phase, or when $(uv^* + u^*v) = 1$. Therefore, in the cluster phase, the only ground states with vanishing long-range mutual information are the maximally symmetry-breaking ground states ($u = v = 1/\sqrt{2}$) and the maximum is achieved in the totally symmetric ($u = 1$, $v = 0$) or anti-symmetric ($u = 0$, $v = 1$) ones.

Therefore, I applied these results, for the symmetric ground states, to all models considered in Sec. (6.1), for certain values of the Hamiltonian parameters, that span all possible phases for these quantum systems, and for different sizes of the subsystems A and B, and reported in Fig. (6.3) the scaling of the mutual information $\mathcal{I}_\infty(A|B)$ as the distance r between A and B increases. It is evident that the mutual information saturates to a finite constant value very

	Disordered	Critical	Ordered		Topological
			Nematic	On site	
$\Delta\lambda(\rho_L)$	$\xrightarrow[L\to\infty]{} \neq 0$	$\xrightarrow[L\to\infty]{} 0$	$\xrightarrow[L\to\infty]{} 0$	$\xrightarrow[L\to\infty]{} 0$	$\xrightarrow[L\to\infty]{} 0$
$S(\rho_L)$	$\xrightarrow[L\to\infty]{} \neq 0$	$\sim \log(L)$	$\xrightarrow[L\to\infty]{} \neq 0$	$\xrightarrow[L\to\infty]{} \neq 0$	$\xrightarrow[L\to\infty]{} \neq 0$
$I_r(A\|B)$	$\xrightarrow[r\to\infty]{} 0$	$\xrightarrow[r\to\infty]{} 0$	$\xrightarrow[r\to\infty]{} \neq 0$	$\xrightarrow[r\to\infty]{} \neq 0$	$\xrightarrow[r\to\infty]{} 0$

Table 6.1: Behavior of the Schmidt gap, the von Neumann entropy, and the mutual information for all possible 1-D quantum phases. The Schmidt gap $\Delta\lambda(\rho_L)$ detects the disorder of a system, because it saturates a finite constant value in a disordered phase and goes rapidly to zero otherwise, as L increases; the von Neumann entropy $S(\rho_L)$ distinguishes a critical system from a non critical one, because of the logarithmic scale with the size L of the system at a critical point; the symmetry-breaking ordered systems, instead, is characterized by the mutual information $I_r(A|B)$, because it saturate a constant value in the ordered phases and disappears otherwise, as the distance between two subsystems A and B increases. Topological ordered phases, moreover, can be detected by analyzing all three nonlinear ground-states functionals.

quickly for models that exhibit quantum symmetry-breaking ordered phases, if the dimensions of the subsystems A and B are comparable with the size of the order parameters, and goes rapidly to zero otherwise.

Therefore, it follows that the mutual information can be unambiguously used to distinguish symmetry-breaking ordered phases from other ones.

How about the topological ordered phases? The topological ordered phases, via their deeply non-local quantum order, need all three functionals to be completely characterized. In fact, whenever the von Neumann entropy saturates to a constant value and the Schmidt gap and the mutual information disappear, in the limit of increasing size L and distance r, the system unambiguously shows topological order.

In Tab. (6.4), I summarized the results.

7
Conclusions and outlook

The aim of this thesis focused on the investigation of two open problems of complex quantum systems: the "real-world" selection of the maximally symmetry-breaking ground states and the classification of all 1-D quantum orders in systems for which the Gizburg-Landau approach fails.

In the first direction, I investigated the classical nature of local inequivalent, i.e. distinguishable for the expectation value of some symmetry operators, quantum ground states associated to a symmetry-breaking ordered phase, by introducing three independent quantitative criteria of classicality. According to these three criteria, I found that the maximally symmetry-breaking ground states are the most classical ones, i.e the only ones that: i) minimize pairwise quantum correlations, as measured by the quantum discord; ii) are always local convertible, by only applying LOCC transformations; iii) minimize the residual tangle, satisfying at its minimum the monogamy of entanglement. This result strongly supports the intuitive idea that the physical mechanism which selects the maximally symmetry-breaking ground states is due to the unavoidable presence of environmental perturbations, such as local fields, which in real-world experiments necessarily drive the system into the most classical among all possible ground states.

Furthermore, I analyzed how evolves the local distinguishability between these inequivalent ground states, after a quench of the Hamiltonian parameters, in the framework of two integrable models that fall into different classes of symmetry, i.e. the XY models in a transverse magnetic field and the N-cluster Ising models. Despite the integrability that avoids the thermalization, I demonstrated that the local distinguishability disappears exponentially in time, independently of the models and the parameters before and after the quench. Hence, in the steady state, all the informations about the particular initial ground state are completely erased by the time evolution. Moreover, I proved that an unitary time evolution induced by a sudden quench, for models with only magnetic order, forces the rise of long-range correlation functions also in the direction of minimum asymmetry. These long-range correlation functions may

induce interesting phenomena, such as the amplification of the entanglement between two neighbors spins, with relevant applications for the quantum information and computation [12]. I also provided further evidence of the fragility of the states that show a nonzero global entanglement. It follows that these states are unstable, not only from a point of view of interactions with an external environment, as shown by the behavior of the local convertibility or of the mutual information [57], but also in a presence of a unitary evolution, typical of a closed system.

In this sense, the work can be seen as a generalization of some previous results, concerning the analysis of the time evolution of the order parameter, obtained, in the framework of the XY model, by the group leaded by P. Calabrese [20, 21, 22], providing a more general approach based on all the correlation functions that break the symmetry. It is important to remember that these results concerned short-range one-dimensional models, which not allow phase transitions at temperatures different from zero [90]. In a future work, the aim is to generalize these results to models that show ordered phases even at temperatures different from zero and to other types of time evolution, that could preserve the quantumness of a state.

In the second direction, I deeply analyzed the properties of a family of fully analytical solvable models, named the N-cluster models in transverse magnetic field. These models are characterized by a $N+2$ body cluster interaction term, competing with a spatially uniform transverse magnetic field. Using the Jordan-Wigner transformations, I diagonalized the models and proved that their classes of symmetry depend on N. However, in these models a phase transition always occurs exactly when both terms are equally weighted, regardless the value of N. The paramagnetic phase, realized for $\phi > \phi_c$, shows a very similar aspect, for all N. On the contrary, the cluster phase, realized for $\phi < \phi_c$, exhibits two different orders, depending on N. For odd or even cluster size $N+2$, the models exhibit a symmetry protected topological order or a nematic order respectively, in agreement with the results obtained in Ref. [47]. I also investigated how the apparent complexity of the orders translates to the amount of entanglement shared among spins in a block or among a block of spins and the rest of the system. Surprisingly, in completely contrast with the results obtained for the N-cluster Ising models [47], any possible multipartite entanglement vanishes, while the bipartite entanglement, as quantified by the concurrence, between two spins at distance $N+1$ has a non-vanishing value in a region confined in the paramagnetic phase, with the only exception of the $N=1$. The remarkable importance of this family of fully analytical solvable models is the presence of exotic phases, such as nematic and topological phases. Hence, they may become a good testing ground for non-trivial spin orderings and serve as a prototype

for studying the possible applications of quantum information tasks.

Furthermore, I investigated the quantum phase transitions of a wide range of one dimensional models of spin-1/2 and fermions and I provided the minimal set of nonlinear ground-states functionals to detect all kind of orders in 1-D. This approach is particularly useful in systems for which the Gizburg-Landau approach fails, because an order parameter is not available, as in presence of topological phases, or more simply because it is difficult to construct or measure, as in presence of nematic phases. In particular, I considered the XY models in a transverse magnetic field, the N-cluster Ising models, the N-cluster models in a transverse magnetic field and the Kitaev chain, all exactly-solvable models that span, by varying the Hamiltonian parameter, all 1-D quantum orders. By studying the scaling with the size L of the system, I proved that the von Neumann entropy unambiguously characterize the criticality of a system, the mutual information unambiguously detect the ordered phases and the Schmidt gap unambiguously identify the disordered ones. The topological ordered phases, instead, via their deeply non-local quantum order, need all three functionals to be completely characterized. In fact, whenever the von Neumann entropy saturates to a constant value and the Schmidt gap and the mutual information disappear, in the limit of increasing size L and distance r, the system unambiguously shows topological order.

In this sense, the work can be seen as a generalization of results also known in the framework of some 1-D systems [34, 82], to a wide range of exactly-solvable models of spin-1/2 and fermions, that show exotic phases, such as nematic and topological ones, in addition to the traditionally symmetry-breaking ordered and paramagnetic ones, and that fall in different classes of symmetry. In a future work, the aim is to make this picture more general, by extending the analysis to the case of higher dimensional systems (both in space and degrees of freedom).

Bibliography

[1] A. Acín, D. Bruss, M. Lewenstein, and A. Sanpera, *Classification of mixed three-qubit states*, Phys. Rev. Lett., 87 (2001), p. 040401.

[2] V. Alba, M. Haque, and A. M. Läuchli, *Entanglement spectrum of the two-dimensional bose-hubbard model*, Phys. Rev. Lett., 110 (2013), p. 260403.

[3] L. Amico, F. Baroni, A. Fubini, D. Patanè, V. Tognetti, and P. Verrucchi, *Divergence of the entanglement range in low-dimensional quantum systems*, Phys. Rev. A, 74 (2006), p. 022322.

[4] L. Amico, R. Fazio, A. Osterloh, and V. Vedral, *Entanglement in many-body systems*, Rev. Mod. Phys., 80 (2008), pp. 517–576.

[5] P. W. Anderson, *Resonating valence bonds: A new kind of insulator?*, Materials Research Bulletin, 8 (1973), pp. 153 – 160.

[6] ——, *The resonating valence bond state in la2cuo4 and superconductivity*, Science, 235 (1987), pp. 1196–1198.

[7] A. F. Andreev and I. Grishchuk, *Spin nematic*, Sov. Phys. JETP, 60 (1984), p. 267.

[8] H. Arodz, J. Dziarmaga, and W. H. Zurek, *Patterns of symmetry breaking*, vol. 127, Springer Science & Business Media, 2012.

[9] E. Barouch and B. M. McCoy, *Statistical mechanics of the xy model. ii. spin-correlation functions*, Phys. Rev. A, 3 (1971), pp. 786–804.

[10] E. Barouch, B. M. McCoy, and M. Dresden, *Statistical mechanics of the XY model. i*, Phys. Rev. A, 2 (1970), pp. 1075–1092.

[11] T. Barthel and U. Schollwöck, *Dephasing and the steady state in quantum many-particle systems*, Phys. Rev. Lett., 100 (2008), p. 100601.

[12] A. Bayat, S. M. Giampaolo, F. Illuminati, and M. B. Plenio, *Entanglement amplification in the nonperturbative dynamics of modular quantum systems*, Phys. Rev. A, 88 (2013), p. 022319.

[13] I. BENGTSSON AND K. ŹYCZKOWSKI, *Geometry of Quantum States: An Introduction to Quantum Entanglement*, Cambridge University Press, 2008.

[14] B. A. BERNEVIG, D. GIULIANO, AND R. B. LAUGHLIN, *Spectroscopy of matter near criticality*, Ann. Phys., 311 (2004), pp. 182–190.

[15] M. BLASONE, F. DELL'ANNO, S. D. SIENA, S. M. GIAMPAOLO, AND F. ILLUMINATI, *Geometric measures of multipartite entanglement in finite-size spin chains*, Physica Scripta, 2010 (2010), p. 014016.

[16] O. BRATTELI AND D. W. ROBINSON, *Operator Algebras and Quantum Statistical Mechanics 1*, Springer Science & Business Media, 1987.

[17] D. BRUSS, *Characterizing entanglement*, Journal of Mathematical Physics, 43 (2002), pp. 4237–4251.

[18] P. CALABRESE AND J. CARDY, *Entanglement entropy and quantum field theory*, Journal of Statistical Mechanics: Theory and Experiment, 2004 (2004), p. P06002.

[19] P. CALABRESE AND J. CARDY, *Time dependence of correlation functions following a quantum quench*, Phys. Rev. Lett., 96 (2006), p. 136801.

[20] P. CALABRESE, F. H. L. ESSLER, AND M. FAGOTTI, *Quantum quench in the transverse-field ising chain*, Phys. Rev. Lett., 106 (2011), p. 227203.

[21] P. CALABRESE, F. H. L. ESSLER, AND M. FAGOTTI, *Quantum quench in the transverse field ising chain: I. time evolution of order parameter correlators*, Journal of Statistical Mechanics: Theory and Experiment, 2012 (2012), p. P07016.

[22] ——, *Quantum quenches in the transverse field ising chain: Ii. stationary state properties*, Journal of Statistical Mechanics: Theory and Experiment, 2012 (2012), p. P07022.

[23] P. CALABRESE AND A. LEFEVRE, *Entanglement spectrum in one-dimensional systems*, Phys. Rev. A, 78 (2008), p. 032329.

[24] E. CANOVI, E. ERCOLESSI, P. NALDESI, L. TADDIA, AND D. VODOLA, *Dynamics of entanglement entropy and entanglement spectrum crossing a quantum phase transition*, Phys. Rev. B, 89 (2014), p. 104303.

[25] M. A. CAZALILLA, *Effect of suddenly turning on interactions in the luttinger model*, Phys. Rev. Lett., 97 (2006), p. 156403.

[26] X. CHEN, Z.-C. GU, AND X.-G. WEN, *Local unitary transformation, long-range quantum entanglement, wave function renormalization, and topological order*, Phys. Rev. B, 82 (2010), p. 155138.

[27] D. CHRUŚCIŃSKI, J. PYTEL, AND G. SARBICKI, *Constructing optimal entanglement witnesses*, Phys. Rev. A, 80 (2009), p. 062314.

[28] A. V. CHUBUKOV, *Chiral, nematic, and dimer states in quantum spin chains*, Phys. Rev. B, 44 (1991), pp. 4693–4696.

[29] F. CICCARELLO, T. TUFARELLI, AND V. GIOVANNETTI, *Toward computability of trace distance discord*, New Journal of Physics, 16 (2014), p. 013038.

[30] V. COFFMAN, J. KUNDU, AND W. K. WOOTTERS, *Distributed entanglement*, Phys. Rev. A, 61 (2000), p. 052306.

[31] T. M. COVER AND J. A. THOMAS, *Elements of Information Theory*, Wiley, 1991.

[32] J. CUI, L. AMICO, H. FAN, M. GU, A. HAMMA, AND V. VEDRAL, *Local characterization of one-dimensional topologically ordered states*, Phys. Rev. B., 88 (2013), p. 125117.

[33] J. CUI, M. GU, L. C. KWEK, M. F. SANTOS, AND V. VEDRAL, *Quantum phases with differing computational power*, Nature Communication, 3 (2012), p. 818.

[34] G. DE CHIARA, L. LEPORI, M. LEWENSTEIN, AND A. SANPERA, *Entanglement spectrum, critical exponents, and order parameters in quantum spin chains*, Phys. Rev. Lett., 109 (2012), p. 237208.

[35] K. DUIVENVOORDEN AND T. QUELLA, *Discriminating string order parameter for topological phases of gapped $su(n)$ spin chains*, Phys. Rev. B, 86 (2012), p. 235142.

[36] W. DÜR AND J. I. CIRAC, *Classification of multiqubit mixed states: Separability and distillability properties*, Phys. Rev. A, 61 (2000), p. 042314.

[37] W. DÜR, J. I. CIRAC, AND R. TARRACH, *Separability and distillability of multiparticle quantum systems*, Phys. Rev. Lett., 83 (1999), pp. 3562–3565.

[38] M. ECKSTEIN AND M. KOLLAR, *Nonthermal steady states after an interaction quench in the falicov-kimball model*, Phys. Rev. Lett., 100 (2008), p. 120404.

[39] A. EINSTEIN, B. PODOLSKY, AND N. ROSEN, *Can quantum-mechanical description of physical reality be considered complete?*, Phys. Rev., 47 (1935), pp. 777–780.

[40] A. EKERT AND P. L. KNIGHT, *Entangled quantum systems and the schmidt decomposition*, American Journal of Physics, 63 (1998).

[41] S. GHARIBIAN, *Quantifying nonclassicality with local unitary operations*, Phys. Rev. A, 86 (2012), p. 042106.

[42] S. M. GIAMPAOLO, G. ADESSO, AND F. ILLUMINATI, *Theory of ground state factorization in quantum cooperative systems*, Phys. Rev. Lett., 100 (2008), p. 197201.

[43] ——, *Theory of ground state factorization in quantum cooperative systems*, Phys. Rev. Lett., 100 (2008), p. 197201.

[44] ——, *Probing quantum frustrated systems via factorization of the ground state*, Phys. Rev. Lett., 104 (2010), p. 207202.

[45] S. M. GIAMPAOLO AND B. C. HIESMAYR, *Genuine multipartite entanglement in the xy model*, Phys. Rev. A, 88 (2013), p. 052305.

[46] S. M. GIAMPAOLO AND B. C. HIESMAYR, *Genuine multipartite entanglement in the cluster-ising model*, New Journal of Physics, 16 (2014), p. 093033.

[47] S. M. GIAMPAOLO AND B. C. HIESMAYR, *Topological and nematic ordered phases in many-body cluster-ising models*, Phys. Rev. A, 92 (2015), p. 012306.

[48] S. M. GIAMPAOLO AND F. ILLUMINATI, *Characterization of separability and entanglement in $(2 \times d)$- and $(3 \times d)$-dimensional systems by single-qubit and single-qutrit unitary transformations*, Phys. Rev. A, 76 (2007), p. 042301.

[49] S. M. GIAMPAOLO, S. MONTANGERO, F. DELL'ANNO, S. DE SIENA, AND F. ILLUMINATI, *Universal aspects in the behavior of the entanglement spectrum in one dimension: Scaling transition at the factorization point and ordered entangled structures*, Phys. Rev. B, 88 (2013), p. 125142.

[50] S. M. GIAMPAOLO, A. STRELTSOV, W. ROGA, D. BRUSS, AND F. ILLUMINATI, *Quantifying nonclassicality: Global impact of local unitary evolutions*, Phys. Rev. A, 87 (2013), p. 012313.

[51] S. M. GIAMPAOLO AND G. ZONZO, *Quench of a symmetry-broken ground state*, Phys. Rev. A, 95 (2017), p. 012121.

[52] C. GOGOLIN AND J. EISERT, *Equilibration, thermalisation, and the emergence of statistical mechanics in closed quantum systems*, Reports on Progress in Physics, 79 (2016), p. 056001.

[53] J. GOLDSTONE, A. SALAM, AND S. WEINBERG, *Broken symmetries*, Phys. Rev., 127 (1962), pp. 965–970.

[54] V. GRITSEV, E. DEMLER, M. LUKIN, AND A. POLKOVNIKOV, *Spectroscopy of collective excitations in interacting low-dimensional many-body systems using quench dynamics*, Phys. Rev. Lett., 99 (2007), p. 200404.

[55] L. GURVITS, *Classical deterministic complexity of edmonds' problem and quantum entanglement*, Proceedings of the 35th ACM Symposium on the Theory of Computing, (2003), pp. 10–19.

[56] A. HAMMA, L. CINCIO, S. SANTRA, P. ZANARDI, AND L. AMICO, *Local response of topological order to an external perturbation*, Phys. Rev. Lett., 110 (2013), p. 210602.

[57] A. HAMMA, S. M. GIAMPAOLO, AND F. ILLUMINATI, *Mutual information and spontaneous symmetry breaking*, Phys. Rev. A, 93 (2016), p. 012303.

[58] S. M. HASHEMI RAFSANJANI, M. HUBER, C. J. BROADBENT, AND J. H. EBERLY, *Genuinely multipartite concurrence of n-qubit x matrices*, Phys. Rev. A, 86 (2012), p. 062303.

[59] M. B. HASTINGS, *An area law for one-dimensional quantum systems*, Journal of Statistical Mechanics: Theory and Experiment, 2007 (2007), p. P08024.

[60] F. HEIDRICH-MEISNER, A. HONECKER, AND T. VEKUA, *Frustrated ferromagnetic spin-$\frac{1}{2}$ chain in a magnetic field: The phase diagram and thermodynamic properties*, Phys. Rev. B, 74 (2006), p. 020403.

[61] B. C. HIESMAYR AND M. HUBER, *Multipartite entanglement measure for all discrete systems*, Phys. Rev. A, 78 (2008), p. 012342.

[62] S. HILL AND W. K. WOOTTERS, *Entanglement of a pair of quantum bits*, Phys. Rev. Lett., 78 (1997), pp. 5022–5025.

[63] M. HOFMANN, A. OSTERLOH, AND O. GÜHNE, *Scaling of genuine multiparticle entanglement close to a quantum phase transition*, Phys. Rev. B, 89 (2014), p. 134101.

[64] C. HOLZHEY, F. LARSEN, AND F. WILCZEK, *Geometric and renormalized entropy in conformal field theory*, Nuclear Physics B, 424 (1994), pp. 443 – 467.

[65] M. HORODECKI, P. HORODECKI, AND R. HORODECKI, *Mixed-state entanglement and distillation: Is there a "bound" entanglement in nature?*, Phys. Rev. Lett., 80 (1998), pp. 5239–5242.

[66] R. HORODECKI, P. HORODECKI, M. HORODECKI, AND K. HORODECKI, *Quantum entanglement*, Rev. Mod. Phys., 81 (2009), pp. 865–942.

[67] S. HORTIKAR AND M. SREDNICKI, *Random matrix elements and eigenfunctions in chaotic systems*, Phys. Rev. E, 57 (1998), pp. 7313–7316.

[68] F. IGLÓI AND H. RIEGER, *Long-range correlations in the nonequilibrium quantum relaxation of a spin chain*, Phys. Rev. Lett., 85 (2000), pp. 3233–3236.

[69] S. V. ISAKOV, M. B. HASTINGS, AND R. G. MELKO, *Topological entanglement entropy of a bose–hubbard spin liquid*, Nature Physics, 7 (2011), pp. 772–775.

[70] A. J. A. JAMES AND R. M. KONIK, *Understanding the entanglement entropy and spectra of 2d quantum systems through arrays of coupled 1d chains*, Phys. Rev. B, 87 (2013), p. 241103.

[71] D. JONATHAN AND M. B. PLENIO, *Entanglement-assisted local manipulation of pure quantum states*, Phys. Rev. Lett., 83 (1999), pp. 3566–3569.

[72] ——, *Minimal conditions for local pure-state entanglement manipulation*, Phys. Rev. Lett., 83 (1999), pp. 1455–1458.

[73] P. JORDAN AND E. WIGNER, *Über das paulische äquivalenzverbot*, Zeitschrift für Physik, 47 (1928), pp. 631–651.

[74] T. KATO, *On the adiabatic theorem of quantum mechanics*, Journal of the Physical Society of Japan, 5 (1950), pp. 435–439.

[75] A. Y. KITAEV, *Unpaired majorana fermions in quantum wires*, Physics-Uspekhi, 44 (2001), p. 131.

[76] A. Y. KITAEV, *Fault-tolerant quantum computation by anyons*, Annals of Physics, 303 (2003), p. 2.

[77] V. E. KOREPIN, *Universality of entropy scaling in one dimensional gapless models*, Phys. Rev. Lett., 92 (2004), p. 096402.

[78] C. LACROIX, P. MENDELS, AND F. MILA, *Introduction to Frustrated Magnetism*, Springer Series in Solid-State Sciences, 2011.

[79] A. LAMACRAFT, *Quantum quenches in a spinor condensate*, Phys. Rev. Lett., 98 (2007), p. 160404.

[80] J. I. LATORRE, E. RICO, AND G. VIDAL, *Ground state entanglement in quantum spin chains*, Quant. Inf. Comput., 4 (2004), p. 48.

[81] T. E. LEE, Y. N. JOGLEKAR, AND P. RICHERME, *String order via floquet interactions in atomic systems*, Phys. Rev. A, 94 (2016), p. 023610.

[82] L. LEPORI, G. DE CHIARA, AND A. SANPERA, *Scaling of the entanglement spectrum near quantum phase transitions*, Phys. Rev. B, 87 (2013), p. 235107.

[83] H. LI AND F. D. M. HALDANE, *Entanglement spectrum as a generalization of entanglement entropy: Identification of topological order in non-abelian fractional quantum hall effect states*, Phys. Rev. Lett., 101 (2008), p. 010504.

[84] E. LIEB, T. SCHULTZ, AND D. MATTIS, *Two soluble models of an antiferromagnetic chain*, Annals of Physics, 16 (1961), pp. 407 – 466.

[85] N. LINDEN, S. POPESCU, A. J. SHORT, AND A. WINTER, *Quantum mechanical evolution towards thermal equilibrium*, Phys. Rev. E, 79 (2009), p. 061103.

[86] Z.-H. MA, Z.-H. CHEN, J.-L. CHEN, C. SPENGLER, A. GABRIEL, AND M. HUBER, *Measure of genuine multipartite entanglement with computable lower bounds*, Phys. Rev. A, 83 (2011), p. 062325.

[87] S. R. MANMANA, E. M. STOUDENMIRE, K. R. A. HAZZARD, A. M. REY, AND A. V. GORSHKOV, *Topological phases in ultracold polar-molecule quantum magnets*, Phys. Rev. B, 87 (2013), p. 081106.

[88] M. A. MARTÍN-DELGADO, R. SHANKAR, AND G. SIERRA, *Phase transitions in staggered spin ladders*, Phys. Rev. Lett., 77 (1996), pp. 3443–3446.

[89] Z. Y. MENG, T. C. LANG, S. WESSEL, F. F. ASSAAD, AND A. MURAMATSU, *Quantum spin liquid emerging in two-dimensional correlated dirac fermions*, Nature, 464 (2010), pp. 847–851.

[90] N. D. MERMIN AND H. WAGNER, *Absence of ferromagnetism or antiferromagnetism in one- or two-dimensional isotropic heisenberg models*, Phys. Rev. Lett., 17 (1966), pp. 1133–1136.

[91] A. MONRAS, G. ADESSO, S. M. GIAMPAOLO, G. GUALDI, G. B. DAVIES, AND F. ILLUMINATI, *Entanglement quantification by local unitary operations*, Phys. Rev. A, 84 (2011), p. 012301.

[92] S. MONTES AND A. HAMMA, *Phase diagram and quench dynamics of the cluster-xy spin chain*, Phys. Rev. E, 86 (2012), p. 021101.

[93] T. NAKANO, M. PIANI, AND G. ADESSO, *Negativity of quantumness and its interpretations*, Phys. Rev. A, 88 (2013), p. 012117.

[94] M. A. NIELSEN AND I. L. CHUANG, *Quantum Computation and Quantum Information*, Cambridge University Press, 2000.

[95] M. A. NIELSEN AND J. KEMPE, *Separable states are more disordered globally than locally*, Phys. Rev. Lett., 86 (2001), pp. 5184–5187.

[96] H. OLLIVIER AND W. H. ZUREK, *Quantum discord: A measure of the quantumness of correlations*, Phys. Rev. Lett., 88 (2001), p. 017901.

[97] T. J. OSBORNE AND M. A. NIELSEN, *Entanglement in a simple quantum phase transition*, Phys. Rev. A, 66 (2002), p. 032110.

[98] T. J. OSBORNE AND F. VERSTRAETE, *General monogamy inequality for bipartite qubit entanglement*, Phys. Rev. Lett., 96 (2006), p. 220503.

[99] A. OSTERLOH, L. AMICO, G. FALCI, AND R. FAZIO, *Scaling of entanglement close to a quantum phase transitions*, Nature (London), 416 (2002), pp. 608–610.

[100] A. OSTERLOH, G. PALACIOS, AND S. MONTANGERO, *Enhancement of pairwise entanglement via $_2$ symmetry breaking*, Phys. Rev. Lett., 97 (2006), p. 257201.

[101] A. PERES, *Separability criterion for density matrices*, Phys. Rev. Lett., 77 (1996), pp. 1413–1415.

[102] M. B. PLENIO AND S. VIRMANI, *An introduction to entanglement measures*, Quant. Inf. Comput., 7 (2007), pp. 1–51.

[103] A. POLKOVNIKOV, K. SENGUPTA, A. SILVA, AND M. VENGALATTORE, *Colloquium*, Rev. Mod. Phys., 83 (2011), pp. 863–883.

[104] F. POLLMANN, A. M. TURNER, E. BERG, AND M. OSHIKAWA, *Entanglement spectrum of a topological phase in one dimension*, Phys. Rev. B, 81 (2010), p. 064439.

[105] S. POPESCU, A. J. SHORT, AND A. WINTER, *Entanglement and the foundations of statistical mechanics*, Nature Physics, 2 (2006), pp. 754–758.

[106] M. RIGOL, V. DUNJKO, AND M. OLSHANII, *Thermalization and its mechanism for generic isolated quantum systems*, Nature, 452 (2008), pp. 854–858.

[107] M. RIGOL, V. DUNJKO, V. YUROVSKY, AND M. OLSHANII, *Relaxation in a completely integrable many-body quantum system: An ab initio study of the dynamics of the highly excited states of 1d lattice hard-core bosons*, Phys. Rev. Lett., 98 (2007), p. 050405.

[108] M. RIGOL AND M. SREDNICKI, *Alternatives to eigenstate thermalization*, Phys. Rev. Lett., 108 (2012), p. 110601.

[109] W. ROGA, S. M. GIAMPAOLO, AND F. ILLUMINATI, *Discord of response*, Journal of Physics A: Mathematical and Theoretical, 47 (2014), p. 365301.

[110] R. ROSSIGNOLI, N. CANOSA, AND J. M. MATERA, *Entanglement of finite cyclic chains at factorizing fields*, Phys. Rev. A, 77 (2008), p. 052322.

[111] D. ROSSINI, A. SILVA, G. MUSSARDO, AND G. E. SANTORO, *Effective thermal dynamics following a quantum quench in a spin chain*, Phys. Rev. Lett., 102 (2009), p. 127204.

[112] D. ROSSINI, S. SUZUKI, G. MUSSARDO, G. E. SANTORO, AND A. SILVA, *Long time dynamics following a quench in an integrable quantum spin chain: Local versus nonlocal operators and effective thermal behavior*, Phys. Rev. B, 82 (2010), p. 144302.

[113] S. SACHDEV, *Quantum Phase Transitions*, Cambridge University Press, 2000.

[114] E. SANTOS, *Entropy inequalities and bell inequalities for two-qubit systems*, Phys. Rev. A, 69 (2004), p. 022305.

[115] E. SCHMIDT, *Zur theorie der linearen und nichtlinearen integralgleichungen. i. teil: Entwicklung willkürlicher funktionen nach systemen vorgeschriebener*, Mathematische Annalen, 63 (1907), pp. 433–476.

[116] N. SCHUCH, M. M. WOLF, F. VERSTRAETE, AND J. I. CIRAC, *Computational complexity of projected entangled pair states*, Phys. Rev. Lett., 98 (2007), p. 140506.

[117] T. SENTHIL, A. VISHWANATH, L. BALENTS, S. SACHDEV, AND M. P. A. FISHER, *Deconfined quantum critical points*, Science, 303 (2004), pp. 1490–1494.

[118] P. SMACCHIA, L. AMICO, P. FACCHI, R. FAZIO, G. FLORIO, S. PASCAZIO, AND V. VEDRAL, *Statistical mechanics of the cluster ising model*, Phys. Rev. A, 84 (2011), p. 022304.

[119] G. SZEGÖ, *Ein grenzwertsatz über die toeplitzschen determinanten einer reellen positiven funktion*, Math. Ann., 76 (1915), p. 490.

[120] H. TAKEZOE, E. GORECKA, AND M. ČEPIČ, *Antiferroelectric liquid crystals: Interplay of simplicity and complexity*, Rev. Mod. Phys., 82 (2010), pp. 897–937.

[121] B. M. TERHAL, *Detecting quantum entanglement*, Theoretical Computer Science, 287 (2002), pp. 313 – 335.

[122] S. TURGUT, *Catalytic transformations for bipartite pure states*, Journal of Physics A: Mathematical and Theoretical, 40 (2007), p. 12185.

[123] V. VEDRAL, *Introduction to Quantum Information Theory*, Oxford University Press, USA, 2007.

[124] F. VERSTRAETE, V. MURG, AND J. CIRAC, *Matrix product states, projected entangled pair states, and variational renormalization group methods for quantum spin systems*, Advances in Physics, 57 (2008), pp. 143–224.

[125] G. VIDAL, J. I. LATORRE, E. RICO, AND A. Y. KITAEV, *Entanglement in quantum critical phenomena*, Phys. Rev. Lett., 90 (2003).

[126] X. G. WEN, *Topological orders in rigid states*, International Journal of Modern Physics B, 04 (1990), pp. 239–271.

[127] X. G. WEN AND Q. NIU, *Ground-state degeneracy of the fractional quantum hall states in the presence of a random potential and on high-genus riemann surfaces*, Phys. Rev. B, 41 (1990), pp. 9377–9396.

[128] W. K. WOOTTERS, *Entanglement of formation of an arbitrary state of two qubits*, Phys. Rev. Lett., 80 (1998), pp. 2245–2248.

[129] Y. ZENG, A. HAMMA, AND H. FAN, *Thermalization of topological entropy after a quantum quench*, Phys. Rev. B, 94 (2016), p. 125104.

[130] Y. ZHANG, T. GROVER, AND A. VISHWANATH, *Entanglement entropy of critical spin liquids*, Phys. Rev. Lett., 107 (2011), p. 067202.

Thanks to my supervisors F. Illuminati and F. Corberi, to my collaborators S. M. Giampaolo, M. Blasone, W. Roga, M. Dalmonte, L. Ferro, M. Cianciaruso, D. Buono, G. Torre, to my family and to everyone who made suitable the way.